
Entanglement through Interfaces and Toy Models of Holography

Enrico Mohandas Brehm



München 2017

Entanglement through Interfaces and Toy Models of Holography

Enrico Mohandas Brehm

Dissertation
an der Fakultät für Physik
der Ludwig-Maximilians-Universität
München

vorgelegt von
Enrico Mohandas Brehm
aus Stuttgart

München, den 3. August 2017

Erstgutachter: Prof. Dr. Ilka Brunner

Zweitgutachter: Prof. Dr. Peter Mayr

Tag der mündlichen Prüfung: 27. September 2017

Abstract

This thesis is dedicated to the analysis of correlation structure in two quite different examples.

In the first one we investigate the entanglement entropy (EE) through conformal interfaces in two-dimensional conformal field theories. The EE is a measure for the strength of entanglement between two subsystems of a system in a pure state. Interfaces are one-dimensional objects on a two-dimensional surface along which two conformal field theories are glued together. They are called conformal if their gluing conditions is invariant under conformal transformations that preserve the shape of the interface. Special interfaces are topological ones. They are called topological because the partition function does not change when the interface is continuously deformed. We in particular show that in a vast class of conformal field theories the presence of a topological interface at the boundary between two subregions makes the EE get dressed with an additional sub-leading but universal contribution that solely depends on the interface data. This sub-leading contribution can be interpreted as a relative entropy measuring the relative loss of entanglement compared to no interface insertion. We also compute the EE through general conformal interfaces in the critical Ising model and find that its leading order is affected by the interfaces if and only if it is not topological. Any conformal defect can be characterized by its transmissivity. As physically expected, the EE through conformal interfaces in the Ising model decreases for lower transmissivities.

The second example is what we call classical holographic codes. They are classical probabilistic codes defined by a network on a uniform tiling of a constant time slice of AdS_3 -spacetime. They share some remarkable properties with certain quantum error correcting codes that are designed to mimic particular properties of the AdS/CFT correspondence. Under these features are the Ryu-Takayanagi formula and bulk reconstruction properties that both reflect deep connections between the correlation structure of a theory and the geometry of its dual description. Our classical codes can be seen as toy models for holography that show that the latter features do not necessarily originate from a quantum description.

Zusammenfassung

In dieser Arbeit analysieren wir Korrelationsstrukturen in zwei unterschiedlichen Beispielen.

Im ersten behandeln wir die “Entanglement Entropie” (EE) durch Defekte in zweidimensionalen konformen Feldtheorien. Die EE ist ein Maß für die Quantenverschränkung zwischen zwei Untersystemen eines Systems, das durch einen reinen Zustand beschrieben wird. Defekte sind eindimensionale Objekte auf einer zweidimensionalen Fläche entlang derer konforme Feldtheorien verklebt werden können. Sie werden konform genannt, wenn ihre Eigenschaften invariant unter jenen konformen Transformationen sind, die die Form des Defektes nicht verändern. Topologische Defekte bilden eine besondere Klasse. Sie sind dadurch definiert, dass kontinuierlichen Deformationen keinen Effekt auf die Zustandssumme des Systems haben. Wir zeigen in dieser Arbeit, dass in einer großen Klasse von konformen Feldtheorien die EE durch topologischen Defekt das Ergebnis ohne Defekt um einen universellen Term nicht führender Ordnung ergänzt. Dieser hängt nur von den Defektdate ab und kann als relative Entropie interpretiert werden, die den Verlust an Verschränkung relativ zur Situation ohne Defekt misst. Wir berechnen zudem die EE durch beliebige konforme Defekte des kritischen Isingmodells. Diese können insbesondere durch ihre Transmissivität charakterisiert werden. Wir können zeigen, dass nicht-topologische Defekte auch die führende Ordnung der EE beeinflussen und dass sie, wie es physikalisch zu erwarten ist, für niedrigere Werte der Transmissivität sinkt.

Beim zweiten Beispiel handelt es sich um spezielle Systeme, die wir klassische holografische Codes nennen. Man kann sie als probabilistische klassische Codes realisieren, die durch ein Netzwerk auf einer uniformen Abdeckung eines Schnitts entlang konstanter Zeit durch einen AdS_3 -Raum definiert sind. Erstaunlicherweise teilen sie einige Eigenschaften mit speziellen Quantencodes zur Fehlerkorrektur, die wiederum spezielle Eigenschaften holographischer Theorien und im besonderen der AdS/CFT Korrespondenz mimen. Unsere klassischen Codes zeigen, dass Eigenschaften wie die Ryu-Takayanagi-Formel und Rekonstruktionseigenschaften, die beide eine Verbindung zwischen der Korrelationsstruktur einer Theorie und der Geometrie ihrer dualen Beschreibung aufzeigen, nicht notwendigerweise von einer Quantenbeschreibung herrühren.

Contents

Abstract	v
Zusammenfassung	vii
Introduction	1
1 About Conformal Field Theory	9
1.1 Conformal transformation	10
1.2 Conformal anomaly: the Virasoro algebra	11
1.3 Basic ingredients of conformal field theories	11
1.3.1 Some special classes of local fields	12
1.4 Noether's theorem and the Ward identities	13
1.4.1 The energy-momentum tensor	13
1.5 Operator product expansion	14
1.5.1 Some special OPEs	15
1.6 The space of states	16
1.6.1 Highest weight representations	17
1.6.2 Fusion algebra	17
1.7 Correlations of (quasi-)primary fields	18
1.8 Conformal field theory on the torus	19
1.8.1 The torus and modular transformations	19
1.8.2 The partition function	20
1.8.3 The Verlinde formula	22
1.9 Boundaries in conformal field theory	22
1.9.1 Boundary fields and the Cardy condition	24
1.10 Interfaces in conformal field theory	25
1.10.1 Defect junction fields and Cardy condition	27
1.10.2 Factorizing and topological defects	27

Contents

1.10.3	The folding trick	31
1.10.4	On the fusion of interfaces	32
1.10.5	Reflection and transmission of interfaces	33
2	About Entanglement Measures	35
2.1	Measures of entanglement	37
2.1.1	Entanglement measures in experiment	41
2.2	Entanglement entropy in two-dimensional CFT	42
3	Entanglement Entropy through Interfaces	47
3.1	Entanglement entropy through topological interfaces	51
3.1.1	Left/Right entanglement entropy	61
3.1.2	Results for bosonic tori	67
3.2	Entanglement entropy through Ising interfaces	73
3.2.1	Conformal interfaces of the Ising model	74
3.2.2	Derivation of the partition functions	77
3.2.3	Derivation of the entanglement entropy	83
3.2.4	Explicit derivation of E^{NS}	84
3.2.5	Comments on the result and special cases	86
3.2.6	Supersymmetric interfaces	88
4	Classical Holographic Codes	93
4.1	Holography and the AdS/CFT correspondence	94
4.1.1	Geometrizing the renormalization group flow	94
4.1.2	The large- N_c expansion	96
4.1.3	The reason for AdS	97
4.1.4	Some properties of the duality	98
4.2	Holographic quantum error-correcting codes	101
4.2.1	Qutrit example	101
4.2.2	Holographic pentagon code	103
4.3	Classical holographic codes	105
4.3.1	Classical trit example	105
4.3.2	Classical codes on hyperbolic space	108
4.4	Features of classical holographic codes	112
4.4.1	Ryu-Takayanagi formula	113

4.4.2	Bulk and operator reconstruction	115
4.4.3	Secret sharing	117
4.5	On a possible physical interpretation	118
Conclusion and Outlook		123
Danksagung		129
A Special Objects		131
A.1	Important functions in CFT	131
A.2	Bernoulli polynomials and numbers	133
B Entanglement through Interfaces		135
B.1	Entanglement entropy of a fusion product	135
B.2	Odd is enough	136
C Classical Holographic Codes		139
C.1	Some properties of \mathfrak{S}	139
C.2	Proof of a version of the RT formula for classical holographic codes	141

*Es wird das Jetzt gezeigt, dieses Jetzt. Jetzt;
es hat schon aufgehört zu sein, indem es gezeigt wird;
das Jetzt, das ist, ist ein anderes als das gezeigte,
und wir sehen, daß das Jetzt eben dieses ist, indem es ist, schon nicht mehr zu sein.
Das Jetzt, wie es uns gezeigt wird, ist es ein gewesenes, und dies ist seine Wahrheit;
es hat nicht die Wahrheit des Seins.*

aus "Phänomenologie des Geistes" von G. F. W. Hegel

Introduction

Modern physics is strongly entangled with the concept of correlation. Let it be a classical statistical system where correlation is the dependence between random variables, or a quantum system where quantum correlations dictate how observables and in particular their outcome in measurements depend on each other. In general, correlation quantifies how much one can predict about one part of a system from the knowledge about another part compared to how much one can predict without this knowledge.

Any quantum system is a statistical system, but there is a fundamental difference between classical and quantum correlations which originates from the different origin of the respective probabilities. Classical probabilities emerge from the absence of knowledge. For example, one doesn't know about the exact microscopic realization of a macroscopic situation, or the knowledge about initial values is not precise enough. In the quantum case the probabilities originate from genuine, intrinsic, and fundamental uncertainties which are related to the fact that particular preparations or measurements do not commute. This also leads to the non-local features of quantum mechanics that led to a lot confusion especially at the early stages of quantum theory [1].

The conceptual differences in the general origin and treatment of correlations leads to the fact that in quantum physics one can reach degrees of correlation that are not possible in a classical statistical system [2]. Those correlations violate a bound that follows from the so-called Bell's inequalities, and can be seen as purely quantum. They are often the interesting types of correlations because they can tell us if a system can in principle not be described by classical physics, which in particular means that the randomness that appears in the statistical description of the measurable quantities of the system cannot originate from some sort of noise and/or lack of knowledge. They in particular teach us that we actually must bother quantum physics to describe it accurately.¹

¹This is true under the assumption of no-signalling in the system, *i.e.* there is no instantaneous information transfer possible between distant sub-systems. See *e.g.* [3, 4] for deeper treatment of the subject. It is even possible to mathematically construct systems with degrees of correlations that cannot be achieved by any quantum theory but still are no-signalling. We can also recommend the lecture notes

Introduction

The most prominent type of quantum correlation is called entanglement. Strongly entangled quantum system can in fact violate Bell's inequalities. Especially in recent years its popularity grew because of the broad field of quantum information science [6]. Entanglement can for example be used to easily perform classically very hard computational tasks [7]. Understanding the general entanglement structure of quantum systems can simplify its numerical treatment significantly too [8, 9]. A deeper understanding of entanglement in various quantum systems is hence of great benefit – from the purely theoretical viewpoint, for their numerical treatment, and also for practical uses and in experiment – especially when we consider quantum information technology.

Both classical statistical systems and quantum systems can have a field theoretical description. In the first case the field theory describes kinematics in equilibrium, for example the statistical average of a random variable. Field theories as effective descriptions of statistical systems do not describe dynamics and, hence, have no time dependence – in other words they are euclidean. In the quantum case the field theory normally describe both the kinematics and dynamics of the quantum system. It depends on time and is Lorentzian. However, euclidean and Lorentzian field theories are very often related by so-called Wick rotations – one analytically continues the “time”-direction on the complex plane and declares the euclidean theory to be restricted to the real axis and the Lorentzian one to the imaginary axis. If there is no obstruction in the Wick rotation then the two descriptions are equivalent. A prominent example is the critical Ising model: the field theoretical description of the 2D Ising lattice at equilibrium and the Ising chain evolved in time are related by a Wick rotation and, hence, are equivalent.

Especially in the field theoretical description the concept of renormalization plays a crucial role. At fixed points of renormalization group (RG) flows [10], field theories must become scale invariant and very often are conformal field theories. Phase transitions and the corresponding critical phenomena which lie at RG fixed points can, hence, be described by conformal field theories [11]. They can provide us with a universal description of in general microscopically very different physical systems that show a uniform behavior around a critical point.

Two-dimensional conformal field theories are even more special because the symmetry of conformal transformations is much larger. In fact, the algebra of local conformal transformations is infinite dimensional, which is not the case in higher dimensions. This large amount of symmetry renders these theories comparably accessible and has resulted in very

[5] for more on the subject.

deep understanding of their general structure. Besides the description of critical behavior in statistical systems, two-dimensional conformal field theories also play a crucial role in the perturbative description of string theory, which is a possible candidate for a unified description of all forces appearing in nature [12, 13, 14]. All fields in nature and space-time itself emerge in string theory from a conformal field theory on the worldsheet of the string.² We see that two-dimensional conformal field theories appear in both high-energy physics – mainly through string theory – and low-energy physics – mainly in the context of critical phenomena of condensed matter systems.

A natural question to ask in two-dimensional conformal field theory is that about their correlation structure. The correlation of local excitations is governed by correlation functions, that are vacuum expectation values of insertions of local operators. The conformal symmetry gives huge constraints on their specific form and especially for theories defined on the plane with less than four operator insertions the results are remarkably easy. We will see this in chapter 1, where we give a review of the subject of two-dimensional conformal field theory. The investigation of correlation structure of states is yet another subject of investigation. Assume that a physical system at its critical point on some manifold is specified by a (pure) state from its conformal field theory description. Then one can ask about the entanglement in this state between two subsystems. One can for example define the subsystems by a spatial bipartition of that manifold. A suitable measure of entanglement in the situation of bipartitions of pure states is the entanglement entropy [15]. We will talk about measures of entanglement and in particular about the entanglement entropy, which plays a huge role in the present work, in section 2. In case of the vacuum/groundstate on the plane with a bipartition into two intervals the results are known for arbitrary conformal field theories, and again they are remarkably easy. For example, the entanglement entropy between a large interval and its complement is a universal quantity and given by [16]

$$E_L = \frac{c}{3} \log \left(\frac{L}{\epsilon} \right) + \tilde{d}, \quad (0.1)$$

where L is the large size of the interval, c is the central charge of the conformal field theory³, ϵ is some high energy length scale/UV cutoff, and \tilde{d} is a sub-leading contribution. We will review this result and its computation in section 2.2.

One can also consider situations where the physical separation of the full system is given

²The description is perturbative because in the full string theory one has to sum over all possible world sheets.

³See section 1.2 for a definition of the central charge.

Introduction

by a conformal interface (to which we also refer as “defect”). This is a one-dimensional submanifold, which in the present work is localized in the spatial direction, separating two-dimensional space-time into two parts [17]. An interface conformal field theory naturally consists of two sub-systems – the two theories that are joined by the defect line. The domain wall can be fully or partially transmissive, such that the quantum field theories living on the two sides are related non-trivially across the defect line [18]. Interfaces appear naturally in conformal field theory, especially when we see them as critical points in the continuum limit of condensed matter/statistical systems. Consider for example impurities in quantum wires or even the junction of two wires. In the conformal field theory limit the physical description has to include defects to describe them [19, 20]. However, they can also be motivated from more abstract considerations. Defects can implement symmetries or dualities [21, 22], they can encode the information of renormalization group flows [23, 24], can be regarded as brane spectrum generating objects in string theory [25] and more. We see that they are of great importance in a complete description of conformal field theories. Investigating the entanglement entropy through interfaces/defects is one step to understand these objects better, and a big part of the present work is dedicated to this investigation.

The first main result is the derivation of the ground state entanglement entropy through so-called topological defects in a big class of conformal field theories, and in particular in rational models. It is worked out in section 3.1 and was originally published in [26]. Topological defects are the class of defects that do not change the partition function when they are smoothly deformed on the manifold the conformal field theory is defined on [27].⁴ As one can expect, they do not change the leading order behavior of the entanglement entropy. However, they give a universal sub-leading contribution to the entanglement entropy that has a very nice physical interpretation. It is given by a relative entropy that tells you how much correlation is lost compared to no defect insertion. We apply the result to special examples and in particular can show that the derivation of the entanglement entropy between left- and right-moving degrees of freedom at a boundary of a conformal field theory can be computed in an analogous fashion and reproduces results from [28].

Generally, the derivation of the entanglement entropy through non-topological interfaces is much more involved. A first main obstacle is that the non-topological interfaces are not known in most cases. One rare example where all defects are known is the conformal field theory describing the critical point of the two-dimensional Ising model [20]. There,

⁴A detailed discussion on topological defects can be found in section 1.10.2.

the interfaces are separated in three classes corresponding to the three topological defects present in the Ising model and can be specified by their transmission coefficient \mathcal{T} , which can take any value between zero for two separated boundary conditions and one – *i.e.* full transmission – for topological defects. The next main result is the entanglement entropy through general conformal defects of the two-dimensional Ising model. This is worked out in section 3.2 and was originally done in [29]. The leading order contribution to the entanglement entropy now depends on the transmission and is given by

$$\frac{\sigma(\mathcal{T})}{2} \log \left(\frac{L}{\epsilon} \right), \quad (0.2)$$

where $\sigma(\mathcal{T})$ is a monotonous function increasing from zero for separated boundary conditions to familiar result $c/3$ for topological defects. The sub-leading contribution due to the interface is the one obtained from the topological defect and does not change within the respective class. We also consider defects of the supersymmetric combination of a free boson and a free fermion. The derivation of the entanglement entropy through these interfaces is basically a combination of the results for the free boson derived in [30] and the one we obtain in this work. The result simplifies remarkably as shown in section 3.2.6.

The correlation structure of a physical system must be present in all its descriptions. Two descriptions that capture one and the same system, which means that they characterize the same degrees of freedom with the same kinematics and dynamics, are called dual to each other. A very famous duality is conjectured by the holographic principle which states that a gravitational theory describing a region of space (the bulk) is equivalent to a (non-gravitational) theory confined to the boundary of that region [31, 32]. This means that intrinsically non-geometric features can be equivalently described geometrically. An explicit and very well understood example for holography is the AdS/CFT correspondence [33]. It relates (quantum) gravity on $(d+1)$ -dimensional asymptotically Anti-de Sitter (AdS) space to a d -dimensional conformal field theory on the boundary. One remarkable aspect of this duality is the interplay of bulk geometry and entanglement in the conformal field theory. This is most evident in the proposal that entanglement entropy in the CFT is equivalently given by the area of a minimal surface in the AdS space [34, 35], which is known as the Ryu-Takayanagi (RT) formula. A huge part of the correlation structure of a systems in a state with a gravitational dual seems to be encoded in the geometric structure of that dual space.

Since then, many connections between geometry and entanglement have been proposed

Introduction

[36, 37, 38, 39, 40, 41, 42]. Also, more generally, concepts of quantum information theory were beneficially applied to (quantum) gravity and, in particular, to black holes [43, 44, 45, 46, 47, 48, 49]. Recently, a tool called tensor networks, which originates from condensed matter physics to efficiently represent quantum many-body states and especially their entanglement structure [50], was employed to describe holography [51] and AdS/CFT [36, 52]. Furthermore, similarities between bulk operator reconstruction properties in AdS/CFT and properties of certain quantum error-correcting codes (QECC) were found [53]. The interesting question to ask there is, how local excitations in the bulk are non-locally represented on the boundary, or, how is the information about operators in the gravity theory represented on the boundary and how do they change entanglement? AdS/CFT and certain QECC behave alike in this perspective.

An interesting family of toy models for holography was proposed in [54]. There, the authors combine tensor networks and quantum error-correcting codes. AdS space is uniformly tiled to define a tensor network from so-called perfect tensors that establishes an isometric map from the bulk to the boundary. This is what they call a holographic quantum error-correcting code, and it reproduces some of the key features of the AdS/CFT correspondence, as *e.g.* the RT formula and bulk reconstruction properties. Later, it was pointed out that a version of the Ryu-Takayanagi formula holds quite generically in quantum error-correcting codes [55]. Furthermore, networks of random tensors [56] and almost-perfect tensors [57] were considered. Also, issues like sub-AdS locality [58] and the relation to gauge invariance [59] were addressed. All these constructions are intrinsically quantum and focus on the structure of entanglement.

In the last third of the present work, which is an adaption of the work [60], we pose the question how far one can get without quantum correlations, like entanglement. Or to put it differently, which features can be reproduced in classical codes for classical degrees of freedom? In a sense, this question is related to the one about general correlation in quantum systems. As we mentioned earlier, there are degrees of correlation in quantum theories that can not be achieved by classical statistical systems. The above examples for toy models for holography all take advantage from these degrees of entanglement. However, are they necessary to describe the wanted features? Do they need a full quantum-mechanical description to work?

Interestingly, we are able to produce features similar to those mentioned above in a completely classical theory. This is first shown in a very straightforward example in section 4.3.1, where we consider a classical probabilistic encoding of one logical (bulk) trit into three

physical boundary trits.⁵ The code satisfies a version of the RT formula for the mutual information, and operations on the logical trits can be represented on the boundary as expected from a toy model for the AdS/CFT correspondence. We then construct more involved codes that we like to call Classical Holographic Codes (CHC) in section 4.3.⁶ Therefore, we consider a network defined by a uniform tiling of hyperbolic space. We provide a general way to construct probabilistic mappings from bulk bits located at the vertices of the network to boundary bits at the open edges at the boundary of the network. The code produces entropy and strong classical correlation. The latter is bound to the RT formula, which in our case states that the mutual information between subregions on the boundary is equivalently given by the length of a minimal cut through the network. This points to the fact that the structure of all sufficiently strong correlations, classical and quantum, can be encoded in a geometric structure. With our examples, we can also answer the question of the latter paragraph and announce that features like the RT-formula, bulk reconstruction properties, and subregion duality do not need a quantum description to work – simply because we constructed fully classical statistical systems that have these properties.

The remainder of this thesis is organized as follows. In the first chapter, we give an overview on two-dimensional conformal field theory and in particular review the basics about conformal interfaces. We only quote well-known results from established literature, and approach the subject rather traditionally. The second chapter is concerned with the review about important concepts for entanglement measures. We briefly discuss the general mathematical structure of entanglement and its measures, followed by explicit constructions in two-dimensional field theories. Again the quotes are established results from literature. The purpose of the first two chapters is to introduce the reader who has not yet worked with conformal field theory, interfaces and/or entanglement measures to the concepts that we will need later on.

The third chapter contains all our results on the entanglement entropy through conformal interfaces. We first develop the rough ideas and formulas to compute the entanglement entropy through general conformal defects. We then show the computation for the entanglement entropy through general topological defects in rational conformal field theories with some explicit examples. We also reproduce results for the left/right entanglement entropy with our methods and in particular apply our results to torodial compactified bosons.

⁵It is strongly motivated by the qutrit example provided in [53] which is reviewed in section 4.2.1.

⁶These codes are motivated by the holographic quantum error correcting codes in [54].

Introduction

All the latter results were published for the first time in [26]. In the remainder of the third chapter, we compute the entanglement entropy through general conformal defects in the critical Ising model and combine our results with results from the free boson to obtain the EE through supersymmetric interfaces. The results here originate from the publication [29].

In the fourth chapter we switch the subject to investigate toy models that capture information-theoretical features of the AdS/CFT correspondence. It begins with a motivation on the correspondence and a review of the features we later focus on. The aim of this first section is to introduce the reader not familiar with holography to the subject. After that we shortly review quantum toy models of AdS/CFT that motivated us to finally introduce our classical holographic codes. We give a rather general construction of these classical toy models for holography and prove the features that justify to call them that way. Originally, the idea of classical holographic codes was published in [60].

Finally, in the last chapter, we give a conclusion and outlook to the present thesis.

Chapter 1

About Conformal Field Theory

We here want to give a brief overview over the basics of conformal field theory in two dimensions from our point of view. It is a very evolved subject and there exists a huge number of texts that can be recommended to read and learn from. We here only give a small selection. A standard reference and very complete introduction is [61] which itself contains many references. Other nice reviews that give an introduction to the subject are [62, 63, 64, 65, 66].

There exist different but mostly equivalent definitions of what a conformal field theory is. They mainly take a different view on how to specify the basic ingredients of the theory and how to describe them mathematically. A very widely spread definition is that of [67], which focused on the field theory aspects. An equivalent but more geometrical definition can be found in [68]. A very mathematical definition in the language of category theory was given in [69]. These approaches to define two-dimensional conformal field theories led to the discovery of the deep relation between their chiral structure and three-dimensional topological field theories [70, 71]. A whole series with a category theoretical approach to conformal field theory which highlights a similar connection to topological field theory in three dimensions is the one initiated by [72]¹. Another mathematically very precise definition is in terms of so-called vertex operator algebras [73]. They led to more insight into several other mathematical concepts like quantum groups and Hopf algebras, too.

Our approach is based on the definitions in [67] and, thus, for us the most basic definition of a two-dimensional conformal field theory is that of a quantum field theory that is defined on a two-dimensional manifold and is invariant under local conformal transformations on that manifold.

¹This goes even further and shows that full correlators rather than just conformal blocks have a description in three-dimensional conformal

1.1 Conformal transformation

Conformal transformations between manifolds of arbitrary dimensions are differential maps that locally preserve the angle between two lines. If the two manifolds are the same this means that the metric is invariant under the map up to a position dependent positive scale factor. In flat space of signature (m, n) the (globally defined) conformal transformations form a finite dimensional group that is isomorphic to $SO(m+1, n+1)$. The conformal group in particular includes the Poincare group as a subgroup which consists of all transformations that leave the metric invariant, i.e. the scale factor is one. Another class of important conformal transformations are dilations. They in particular imply that a theory that is invariant under conformal transformations looks the same at every length scale.

In two-dimensional Euclidean space the condition for a transformation to be conformal implies that the map satisfies locally the Cauchy-Riemann equations. It hence follows that it can be written as a locally (anti-)holomorphic function on complex rather than real coordinates. Conversely it is also true that every locally (anti-)holomorphic function on the complex plane gives rise to a conformal transformation in two dimensions. In general, conformal transformations in two-dimensional Euclidean space can be seen as (anti-)meromorphic functions with isolated singularities. Hence, they can be written as Laurent series which shows that a possible set of generators for conformal transformations in two dimensions consists of

$$l_n = -z^{n+1}\partial_z, \quad \bar{l}_n = -\bar{z}^{n+1}\partial_{\bar{z}}, \quad n \in \mathbb{Z}, \quad (1.1)$$

with commutation relations

$$[l_m, l_n] = (m - n)l_{m+n} \quad (1.2)$$

$$[\bar{l}_m, \bar{l}_n] = (m - n)\bar{l}_{m+n} \quad (1.3)$$

$$[\bar{l}_m, l_n] = 0. \quad (1.4)$$

The algebra of local conformal transformations in two-dimensional Euclidean space is hence given by two commuting copies of the so-called *Witt algebra* and it is in particular *infinite* dimensional.

1.2 Conformal anomaly: the Virasoro algebra

In quantum theories one often has to deal with the “soft” breaking of symmetries which can lead to an *anomaly*. This can mean that the theory is organised in projective rather than proper representations of the symmetry, or equivalently that one has to consider the proper representations of a central extension of the symmetry algebra. We then call the extended algebra quantum where the original one is called classical.

In case of two-dimensional CFTs the classical symmetry algebra is the Witt algebra. Its central extension can be shown to be unique up to a single anomaly factor $c \in \mathbb{R}$ which is called the *central charge*. On the level of the quantum theory, it belongs to the Casimir that can be built from the operators of the classical symmetry algebra. The central charge then is an eigenvalue of the Casimir operator. For a fixed value c the central extension of the Witt algebra is called the Virasoro algebra Vir_c . Its commutation relations are given by

$$[L_m, L_n] = (m - n)L_{m+n} + \frac{c}{12}(m^3 - m)\delta_{m+n,0}, \quad (1.5)$$

where we now use capital letters for the generators. The relations for the still commuting second copy are the same.²

Physically, the soft breaking of conformal symmetry is related to the introduction of a macroscopic scale. The central charge describes the way how a specific system responds to macroscopic length scales. It for example quantifies how the system reacts on boundary conditions, finite size³ or curvature (*trace anomaly* of the energy momentum tensor). In CFTs that describe statistical systems on a cylinder the central charge is directly related to the free energy per unit length.

1.3 Basic ingredients of conformal field theories

In the present description, the two most important constituents of a conformal field theories are a set of *fields* $\Phi(z, \bar{z})$ and *correlation functions* of such fields written as

$$\langle \Phi_1(z_1, \bar{z}_1) \Phi_2(z_2, \bar{z}_2) \dots \Phi_n(z_n, \bar{z}_n) \rangle. \quad (1.6)$$

The fields are (distributional) operators acting on some space of states. When the theory

²However, it can in general have a different central charge \bar{c} !

³Here, the connection of the central charge to the *Casimir energy* is most evident.

exhibits an action the fields are the fundamental constituents appearing therein and “composite fields” built out of them. In a statistical system they describe local fluctuations of scaling fields.

The correlation functions are expectation values – i.e. measurable quantities – of scattering amplitudes. They can be defined with respect to some distinguished state, or by a path integral expression if there is an action. In statistical systems they measure correlation of local fluctuations in the fields involving a statistical average.

On the plane, the correlator of n fields is in particular a function of the n insertion points and, hence, defined on \mathbb{C}^n . Typically it is singular on the diagonals, i.e. when two or more fields are inserted at the same point. The investigation of this singular structure is one of the key routes in the understanding of quantum field theories in general.

The fields we are most interested in are local ones, i.e. fields that are only influenced by their immediate surroundings. The measurable quantities are correlation functions, so that the definition of a physically local field should involve correlators. We, hence, call fields *local* with respect to each other if the order in which they appear in a correlator does not change the result up to sign if they are inserted at distinguished points.

Another condition on the local fields of a CFT is that of covariance under conformal transformation. This means that their transformation property is implemented by a representation of the local conformal group.

1.3.1 Some special classes of local fields

Every conformal field theory contains a special class of conformally covariant fields, the so-called primary fields $\phi(z, \bar{z})$. They transform as components of a conformally covariant tensor with h “ z ” and \bar{h} “ \bar{z} ” indices. More explicitly, under any conformal map $z \mapsto f(z)$, $\bar{z} \mapsto \bar{f}(\bar{z})$ their transformation is given by

$$\phi(z, \bar{z}) \mapsto (\partial f)^h (\bar{\partial} \bar{f})^{\bar{h}} \phi(f(z), \bar{f}(\bar{z})). \quad (1.7)$$

The real numbers h and \bar{h} are called the *conformal weights* of the primary field ϕ . For an infinitesimal local conformal transformation $z \mapsto z + \epsilon(z)$ and $\bar{z} \mapsto \bar{z} + \bar{\epsilon}(\bar{z})$ the variation of primary fields is given by

$$\delta_{\epsilon, \bar{\epsilon}} \phi = (h\partial\epsilon + \epsilon\partial + \bar{h}\bar{\partial}\bar{\epsilon} + \bar{\epsilon}\bar{\partial}) \phi. \quad (1.8)$$

If the transformation property (1.7) only holds for the subgroup of proper conformal transformations⁴ the corresponding field is called *quasi-primary*. Fields that are neither primary nor quasi-primary are called *secondary*.

1.4 Noether's theorem and the Ward identities

In field theories a continuous symmetry always implies the existence of a conserved current J^a , where a is a spacetime index and conserved means that it is divergence free, i.e.

$$\nabla_a J^a = 0. \quad (1.9)$$

This statement, which is most evident in a path integral formalism, is an easy formulation of *Noether's theorem*. A more quantum version of this (classical) theorem is encoded in the so called *Ward identities*. They relate specific correlation functions when there is a continuous symmetry, where the relations stay unchanged even under renormalisation. We here only want to state the Ward identity for two-dimensional conformal field theories defined on the complex plane. There the variation of some local field Φ with respect to the symmetry corresponding to the conserved current $J^a = (J, \bar{J})$ at some position (z_0, \bar{z}_0) is given by

$$\delta\Phi(z_0, \bar{z}_0) \propto \oint_{\partial B(z_0, \bar{z}_0)} (Jdz - \bar{J}d\bar{z}) \Phi(z_0, \bar{z}_0), \quad (1.10)$$

where B is some neighborhood of (z_0, \bar{z}_0) , *e.g.* a ball shaped region. The equation holds within correlators, *i.e.* it is not necessarily an operator equation.

1.4.1 The energy-momentum tensor

Many field theories exhibit translation invariance, which means that they are invariant under coordinate transformations with $\delta\sigma^a \propto v^a$, where σ^a are coordinates of the space the theory is defined on and v^a is some translation vector. The fields Φ of the theory transform as $\delta\Phi \propto v^a \partial_a \Phi$ and the conserved (Noether) current is given by

$$J_a \propto v^b T_{ab}, \quad (1.11)$$

⁴This means that $f \in SL(2\mathbb{C})/\mathbb{Z}_2$ that are the conformal transformations globally defined on the complex plane.

where T_{ab} is called the *energy-momentum tensor*. As the current also the energy-momentum tensor is conserved.

In particular, any conformally invariant theory is translation invariant. So any CFT possesses a conserved energy-momentum tensor. However, it is constrained even further. One can show that the energy-momentum tensor is traceless when the theory is invariant under dilations, so that

$$T^a_a = 0 \tag{1.12}$$

in any conformal field theory. In two dimensions and on the complex plane conservation and tracelessness of the energy-momentum tensor imply that it possesses only two non-vanishing components that are locally holomorphic and antiholomorphic, respectively. We hence define

$$T(z) := T_{zz}(z), \quad \tilde{T}(\bar{z}) = T_{\bar{z}\bar{z}}(\bar{z}). \tag{1.13}$$

As any (anti-)holomorphic function, $T(z)$ and $\tilde{T}(\bar{z})$ can be expressed in Laurent series with modes L_n and \tilde{L}_n , $n \in \mathbb{Z}$. As we discussed in section 1.1 they are the generators of the full conformal symmetry and in particular every mode itself is a conserved quantity in the sense of Noether's theorem. The energy-momentum tensor is hence not only the conserved quantity for translations but for the full conformal symmetry. The latter also shows that a two-dimensional field theory is automatically conformally invariant if it possesses translation and dilation symmetry.⁵ This is not generally true in higher dimensions.

1.5 Operator product expansion

Previously, we shortly mentioned that the understanding of singularities appearing in quantum field theories is of great importance. One possibility to understand or even resolve these is to claim the existence of a convergent expansion of the product of two fields (operators) as a (possibly infinite) sum of fields out of a given set. Usually, one considers the set of all local fields. This is then called an *operator product expansion* (OPE). More precisely, if we have a point σ_1 in Euclidean space and two local fields Φ_i, Φ_j , then there exists a neighbourhood of σ_1 in which we can write for every point $\sigma_2 \neq \sigma_1$

$$\Phi_i(\sigma_1)\Phi_j(\sigma_2) = \sum_k c_{ij}^k(\sigma_1 - \sigma_2) \phi_k(\sigma_2), \tag{1.14}$$

⁵This is not necessarily true on quantum level. There this is only true for unitary theories and one can construct non-unitary counter examples.

where k runs over a (possibly countable infinite) index set, Φ_k are local fields, and c_{ij}^k are analytic functions in the neighbourhood. This operator equation holds inside general correlators as long as the separation between the two points is small compared to the distance to any other operator insertion.

In two-dimensional conformal field theory OPEs of local fields are actually computable. There, one usually uses them as asymptotic expansion where only the first few terms give the dominant behavior for small separations. Very often one “forgets” about the non-singular terms and does not even write them down. This is the case because – as in the Ward identity (1.10) – one derives correlators by closed contour integrals in which only singular terms contribute due to Cauchy’s integral theorem.

1.5.1 Some special OPEs

Using the Ward identity, the transformation property of primaries under infinitesimal conformal transformations and the insight that the energy-momentum tensor is the conserved current of these one can derive the OPEs

$$\begin{aligned} T(z)\phi(w, \bar{w}) &= \frac{h}{(z-w)^2}\phi(w, \bar{w}) + \frac{1}{z-w}\partial_w\phi(w, \bar{w}), \\ \bar{T}(\bar{z})\phi(w, \bar{w}) &= \frac{\bar{h}}{(\bar{z}-\bar{w})^2}\phi(w, \bar{w}) + \frac{1}{\bar{z}-\bar{w}}\partial_{\bar{w}}\phi(w, \bar{w}). \end{aligned} \tag{1.15}$$

These equations may also serve as the defining properties for primary fields of conformal weight (h, \bar{h}) .

Another important OPE is that of the energy-momentum tensor with itself which is given by

$$T(z)T(w) = \frac{c/2}{(z-w)^4} + \frac{2T(w)}{(z-w)^2} + \frac{\partial_w T(w)}{z-w}, \tag{1.16}$$

and likewise for the anti-holomorphic component. It in particular shows that the energy-momentum tensor itself is not a primary field. It is, however, a quasi-primary field. This is also visible in its transformation property under a conformal mapping $f(z)$ which can be computed to be

$$T'(z) = \left(\frac{\partial f}{\partial z}\right)^2 T(f(z)) + \frac{c}{12}S(f(z), z), \tag{1.17}$$

where $S(w, z)$ is the Schwarzian derivative

$$S(w, z) = \frac{1}{(\partial_z w)^2} \left((\partial_z w)(\partial_z^3 w) - \frac{3}{2}(\partial_z^2 w)^2 \right), \quad (1.18)$$

that only vanishes for proper conformal transformations.

1.6 The space of states

A quantum field theory whose physical quantities are invariant under a given (quantum) symmetry must be organised in representations of that symmetry. This in particular means that the space of states, *i.e.* the Hilbert space of the theory, decomposes in (irreducible) representations. It can be written as a direct sum

$$\mathcal{H} = \bigoplus_{i \in \mathcal{I}} \mathcal{H}_i \quad (1.19)$$

where the \mathcal{H}_i 's are (irreducible) representations specified by the label i .⁶

The symmetry of two-dimensional conformal field theory are two copies of the Virasoro algebra – a chiral and a anti-chiral one. Because the two copies commute, we can simultaneously decompose the space of states in chiral and anti-chiral representations, *i.e.* it is of the form

$$\mathcal{H} = \bigoplus_{i,j} M_{ij} (\mathcal{H}_i \otimes \bar{\mathcal{H}}_j), \quad (1.20)$$

where here \mathcal{H}_i are chiral irreducible representations and $\bar{\mathcal{H}}_j$ the anti-chiral ones. M_{ij} are positive integers and describe the multiplicity of the tensor product $\mathcal{H}_i \otimes \bar{\mathcal{H}}_j$ in the space of states. If the sum over i and j is finite then the theory is called *rational*.

Not every combination of multiplicities M_{ij} corresponds to a consistent theory. In principle one needs to check all the amplitudes for states in \mathcal{H} which have to satisfy several conditions – especially locality. In general, it is very hard to obtain all the information about the structure of all correlation functions. An approach to construct local amplitudes out of the chiral and anti-chiral data of the theory is the *conformal bootstrap*. Another opportunity to find at least necessary conditions on M_{ij} is to consider the theory on the

⁶The index set \mathcal{I} can in principle be infinite and does not even have to be countable, s.t. the sum must be seen as a generalized direct sum. However, in what comes we only want to consider finite or countable index sets.

torus. The vacuum amplitude (or partition function) on the torus should be invariant under so called modular transformations which highly constraints the possible combinations of M_{ij} . We will talk about this in more detail in section 1.8.

Let us again think of CFTs defined on the plane. There, states can be defined *asymptotically* that may be interpreted as a field insertion in the infinite past: The fields act at a specific point (infinity) as operators on a (unique) vacuum. However, due to conformal symmetry the specific point can be chosen arbitrarily. In this way we can relate every field to a corresponding state, where the relation is one-to-one and onto. This is called the *state-operator correspondence*. Hence, the above structure of the space of states also exactly determines the structure of the space of local operators.

1.6.1 Highest weight representations

Very important states are those corresponding to primary fields. Let us write $|\phi\rangle$ for the unique state that corresponds to the primary ϕ . One can show that it satisfies defining properties of so called highest weight representation of the Virasoro algebra: It is a eigenstate to L_0, \bar{L}_0 and is annihilated by half of the algebra namely by all L_n, \bar{L}_n with $n > 0$. The action of L_n and \bar{L}_n with $n < 0$ on the state $|\phi\rangle$ creates new states, where one calls the corresponding fields *descendant*. The highest weight state together with the states created in this way is called *Verma module* and the set of all the corresponding fields, *i.e.* the primary and all its descendents, is called the conformal family denoted by $[\phi]$.

The Verma module can contain states of vanishing or even negative norm depending on the combination of the primary's conformal weights and the theory's central charge. In a unitary theory negative norm states should be absent which happens iff all conformal weights are non-negative. Vanishing norm states can be removed from the Verma module and generate themselves an independent Verma module that is in a sense orthogonal to the parent one. After the removal of these sub-modules, the leftover is irreducible. It is then called a *highest weight representation*.

1.6.2 Fusion algebra

The idea of an operator product expansion of two fields can be generalized to that of two Verma modules. Taking the product of two Verma modules is then like taking the tensor product of two representations of the symmetry algebra of the theory. The tensor product of two irreducible representations is typically reducible and can be decomposed again in

irreducible representations. Hence the product, which is also called a fusion, of two Verma modules can be written as a sum of Verma module, *i.e.*

$$[\phi_i] \times [\phi_j] = \sum_k N_{ij}^k [\phi_k] \quad (1.21)$$

where k runs over all possible irreducible representations. The N_{ij}^k are called fusion coefficient and tell how often representation k appears in the tensor product of representations i and j . They are hence natural numbers. The set of Verma modules of a conformal field theory together with the above product and the natural understanding of a sum defines the (associative) *fusion algebra* of that conformal field theory.

1.7 Correlations of (quasi-)primary fields

A remarkable result of conformal field theory is that the structure of correlators with up to three insertions of (quasi-)primary fields on the complex plane is fully determined by the proper conformal transformations. More precisely, one can show that any one-point correlator has to vanish unless both conformal weights of the field vanish. This follows directly from translation invariance and from the transformation properties of (quasi-)primaries under dilations. The special conformal transformation then force the two- and three-point correlators to be of the form

$$\langle \phi_i(z, \bar{z}) \phi_j(w, \bar{w}) \rangle = \frac{d_{ij} \delta_{h_i, h_j} \delta_{\bar{h}_i, \bar{h}_j}}{(z-w)^{2h_i} (\bar{z}-\bar{w})^{2\bar{h}_i}}, \quad (1.22)$$

and

$$\langle \phi_i(z_1, \bar{z}_1) \phi_j(z_2, \bar{z}_2) \phi_k(z_3, \bar{z}_3) \rangle = \frac{C_{ijk}}{z_{12}^{(ijk)} z_{23}^{(jki)} z_{13}^{(ikj)} \bar{z}_{12}^{\overline{(ijk)}} \bar{z}_{23}^{\overline{(jki)}} \bar{z}_{13}^{\overline{(ikj)}}}, \quad (1.23)$$

where $(ijk) = h_i + h_j - h_k$ and $\overline{(ijk)} = \bar{h}_i + \bar{h}_j - \bar{h}_k$ with (h_i, \bar{h}_i) the conformal weights of the respective (quasi-)primaries, $z_{ij} = z_i - z_j$, and $\bar{z}_{ij} = \bar{z}_i - \bar{z}_j$. The numerical coefficients d_{ij} are normalization constants that can always be normalized to $d_{ij} = \delta_{i,j}$ by a suitable choice of basis for primary fields. The coefficients C_{ijk} are strongly entangled with the coefficients appearing in the operator product expansion of ϕ_i with ϕ_j and in particular are only non-zero if the fusion coefficient N_{ij}^k is non-zero, too.

Correlators containing more than three (quasi-)primary fields have more complicated dependencies for which we refer to the relevant literature.

1.8 Conformal field theory on the torus

So far we only considered two dimensional conformal field theories to be defined on the complex plane. There the holomorphic and antiholomorphic sectors of the theory completely decouple. This property, however, is very unique to the fixed points in parameter space and in general only occurs in the infinite-plane geometry. It is, however, not very physical because as we move away from the critical point the spectrum is continuously deformed and the generic coupling between the left and right sectors of physically reasonable theories should also give rise to constraints on the respective sectors of the conformal field theory.

To impose these physical constraints without leaving the critical point one has to couple the holomorphic and antiholomorphic sectors of the theory through the geometry of the space on which it is defined. The simplest case to do so is to consider the theory on the torus – the Riemann surface of genus 1. In context of critical phenomena, one normally does not consider Riemann surfaces of higher genus. In string theory, however, higher genus Riemann surfaces are the basis of calculating loop scattering amplitudes and thus play a crucial role in its perturbative description.

1.8.1 The torus and modular transformations

The torus can be described as a cylinder of finite length with the boundaries glued together, where one has the possibility of twisting the ends of the cylinder. Equivalently, it can be defined by a lattice on the complex plane. All points on \mathbb{C} are identified whose difference is a lattice vector. The fundamental domain of the lattice, which is the parallelogram spanned by the two smallest lattice vectors (w_1, w_2) , can be identified with the torus. In a geometric picture, one obtains the torus by identifying opposite edges of that domain. The properties of a conformal field theory on a torus should depend neither on the overall scale nor on the orientation of the lattice. Hence, the relevant parameter is $\tau \equiv w_2/w_1$, the *modular parameter* of the torus.

For a conformal field theory that is consistently defined on a torus the interactions of the left and right sectors originate from *modular invariance*: The properties of the theory must not depend on the choice of vectors that define the same lattice in \mathbb{C} . The group that transforms all these vectors into each other is $SL(2, \mathbb{Z})$ under which the relevant parameter

τ transforms as

$$\tau \mapsto \frac{a\tau + b}{c\tau + d}, \quad \begin{pmatrix} a & b \\ c & d \end{pmatrix} \in SL(2, \mathbb{Z}). \quad (1.24)$$

For this transformation an overall sign change in the matrix plays no role and, hence, the symmetry of interest is the *modular group* $SL(2, \mathbb{Z})/\mathbb{Z}_2$, or $PSL(2, \mathbb{Z})$. Two favorably chosen generators of this group are the so-called modular T and S transformations given by

$$T : \tau \mapsto \tau + 1, \quad (1.25)$$

$$S : \tau \mapsto -\frac{1}{\tau}. \quad (1.26)$$

1.8.2 The partition function

On the infinitely long cylinder we can impose the interpretation of time along the cylinder with asymptotic states being defined at the infinite past and future. The time evolution of these states – organized in representations of the symmetries of the theory – is generated by the Hamiltonian of the conformal field theory on the cylinder, $H_{cyl.} = \frac{2\pi}{L}(L_0 + \bar{L}_0 - \frac{c+\bar{c}}{24})$, where L is its circumference. An evolution in spatial direction is generated by the momentum operator $P_{cyl.} = \frac{2\pi}{L}(L_0 - \bar{L}_0)$. On the torus we want to stick to this interpretation, where we choose $L \equiv w_1 \in \mathbb{R}^+$. The operator that translates states along the torus parallel to w_2 is then $\exp(-\text{Im}(w_2)H_{cyl.} + i\text{Re}(w_2)P_{cyl.})$. The partition function, which corresponds to the generating functional in general quantum field theories, is then given by a sum over all possible states transported along w_2 and hence reads

$$\begin{aligned} \mathcal{Z}(\tau, \bar{\tau}) &= \text{Tr}_{\mathcal{H}} \left(e^{-\text{Im}(w_2)H_{cyl.} + i\text{Re}(w_2)P_{cyl.}} \right) \\ &= \text{Tr}_{\mathcal{H}} \left(q^{L_0 - \frac{c}{24}} \bar{q}^{\bar{L}_0 - \frac{\bar{c}}{24}} \right), \end{aligned} \quad (1.27)$$

where $q = e^{2\pi i\tau}$. The partition function has to be invariant under the action of the modular group which is in particular the case if it is invariant under modular T and modular S transformations. This highly constrains the possible spectrum of a conformal field theory living on a torus as we will see by the following considerations.

Recall from section 1.6 that the space of states is of the form

$$\mathcal{H} = \bigoplus_{i,j} M_{ij} \mathcal{H}_i \otimes \bar{\mathcal{H}}_j \quad (1.28)$$

and that there exists a correspondence to the operator content of the theory. With this, the partition function is given by

$$\mathcal{Z}(\tau, \bar{\tau}) = \sum_{i,j} M_{ij} \chi_i(\tau) \bar{\chi}_j(\bar{\tau}) \quad (1.29)$$

$$\equiv \vec{\chi}^T M \vec{\chi}, \quad (1.30)$$

with the definition of the Virasoro characters

$$\chi_i(\tau) = \text{Tr}_{\mathcal{H}_i}(q^{L_0 - \frac{c}{24}}). \quad (1.31)$$

The characters transform in a very specific way under modular transformations. In particular, for the two favoured generators – the modular T and the modular S transformation – they transform as

$$S : \chi_i(\tau) \mapsto \chi_i(-\frac{1}{\tau}) = S_{ij} \chi_j(\tau), \quad (1.32)$$

$$T : \chi_i(\tau) \mapsto \chi_i(\tau + 1) = T_{ij} \chi_j(\tau). \quad (1.33)$$

In non-pathological cases $T_{ij} = \delta_{ij} e^{2\pi i \varphi_i}$, so that the modular T transformation simply multiplies a character with a phase factor, where the phase in minimal models is *e.g.* given by $\varphi_i = (h_i - c/24)$. The modular S transformation shows in general a more complicated structure.

Now, the condition of invariance of the partition function under modular S transformation reads

$$\begin{aligned} \mathcal{Z}(\tau, \bar{\tau}) = \sum_{ij} M_{ij} \chi_i(\tau) \bar{\chi}_j(\bar{\tau}) &\stackrel{!}{=} \sum_{ij,kl} M_{ij} S_{ik} S_{jl}^* \chi_k(\tau) \bar{\chi}_l(\bar{\tau}) = \mathcal{Z}(-\frac{1}{\tau}, -\frac{1}{\bar{\tau}}), \quad \text{or} \\ S^T M S^* &\stackrel{!}{=} M \end{aligned} \quad (1.34)$$

and equivalently for the modular T transformation.⁷ These constraints highly restrict the possible spectra, which are given by the matrix M , of a possible modular invariant conformal field theory. Especially in the case of unitary rational theories, i.e. when the index set of (i, j) is finite and all primaries have positive weight, invariance under modular invariance is enough to completely classify all of these.

⁷We want to mention that the S -matrix defined in this way is – at least in all known cases – unitary and symmetric, such that the second equation can also be written as $SMS^\dagger \stackrel{!}{=} M$.

1.8.3 The Verlinde formula

The study of conformal field theory on the torus reveals a deep connection between the modular properties of a conformal field theory and the fusion coefficients appearing in its fusion algebra. It can be shown that the fusion coefficients $N_{ij}^k \in \mathbb{N}$ can be computed from S -matrix elements by the so called Verlinde formula

$$N_{ij}^k = \sum_m \frac{S_{im} S_{jm} S_{mk}^*}{S_{0m}}. \quad (1.35)$$

It is actual remarkable that the above quite simple combination of in general complex S -matrix elements always gives a natural number.

1.9 Boundaries in conformal field theory

The relevance of models defined on a region with boundaries is big. They can for example bound a region to finite size, which plays an important role for statistical models or one-dimensional quantum models. Especially for simulations, that are always done in a finite region, finite size effects have to be considered. The properties of the infinite-sized models, *i.e.* the model in the thermodynamic limit, then have to be extracted from the finite-size properties.

The study of conformal field theories with boundaries also tells us a lot about critical systems near an actual physical boundary. In particular one is interested in the effect of boundaries on correlation functions. One of the most prominent examples where the concept of CFTs with a boundary plays an important role is the Kondo effect. There a cloud of free fermions surrounds a fermionic impurity. Due to rotational symmetry around the impurity, the problem can be reduced to (1+1) dimensions, where the spatial direction is given by the distance from the impurity which then can be described as a boundary to the system. In the process of understanding the Kondo model, Wilson developed the basic ideas of renormalization [10]. At the critical point of RG flow the Kondo model is naturally given by a (1+1) d CFT with a boundary.

They also play a fundamental role in string theory, where they are needed to describe open strings. In the target space of the strings the world sheet boundary has the interpretation of a defect where open strings can end. Such objects are called D-branes and reveal a very rich variety of important properties. They for example play an important role when

it comes to compactification in string theory. Superstring theory can only be formulated consistently in ten dimensions. It is, however, necessary to regard six of these dimensions compact and small because the physics we measure around us at our low energies (compared to string theory scale) is effectively four-dimensional. The D-branes *e.g.* come into play when we talk about gauge theories. The effective theory on a D-brane is a gauge theory [74]. Different D-brane configurations that are filling four dimensional spacetime and some part of the compact space give rise to different effective gauge theories and can also reproduce the gauge sector of the Standard Model of particle physics. Another use of D-branes is in the context of black holes. One can construct yet other D-brane configurations that give rise to an entropy that is expected from black holes. Especially for supersymmetric black holes (in five dimensions) there exist nice constructions of D-branes that reproduce their entropy exactly [75].

Boundaries are very often part of the definition of the theory and are not seen as a limitation. We then talk of boundary conformal field theories (BCFTs). At a boundary of the manifold one imposes local boundary conditions on the fields of the theory. These conditions are in general not compatible with the full conformal symmetry – at least all transformations that change the boundary’s shape are broken. A boundary condition is called conformal if it is compatible with all conformal transformations that keep the shape of the boundary invariant. Since the energy momentum tensor generates conformal transformations, its boundary conditions tell if a boundary is conformal or not.

An easy exemplary manifold with boundary is the complex upper half plane. There the conformal boundary condition is

$$\lim_{y \rightarrow 0} \left(T(x + iy) - \tilde{T}(x - iy) \right) = 0, \quad x \in \mathbb{R}. \quad (1.36)$$

It becomes $T_{xy} = 0$ when expressed in Cartesian coordinates, which shows that no energy or momentum flows through the real axis. For time evolution τ along the imaginary axis, one introduces a boundary state $|\mathcal{B}\rangle$ which is a state in the Hilbert space of the theory that respects the boundary condition – now written in terms of the Virasoro generators

$$(L_n - \bar{L}_n) |\mathcal{B}\rangle = 0. \quad (1.37)$$

This means that the boundary state breaks one half of the conformal charges. Such a boundary state is coherent, *i.e.* it belongs to an extension of the Hilbert space, and it is in particular not normalisable. As before, we decompose the Hilbert space as in (1.20). If the

boundary state preserves the full chiral algebra, the gluing condition (1.37) is supplemented by similar conditions for the additional generators. Together these gluing conditions can only be solved in a sector $\mathcal{H}_i \otimes \mathcal{H}_{\bar{i}}$ where the two representations in the product are isomorphic. In this way one obtains the Ishibashi states $|i\rangle\rangle = \sum_N |i, N\rangle \otimes U|\bar{i}, \bar{N}\rangle \in \mathcal{H}_i \otimes \bar{\mathcal{H}}_i$ [76], where U is a unitary transformations that commutes with all anti-chiral symmetry generators. A boundary state then is a linear combination of those

$$|\mathcal{B}\rangle = \sum_i b_{\mathcal{B}i} |i\rangle\rangle, \quad (1.38)$$

where so far the coefficients $b_{\mathcal{B}i}$ are arbitrary but will become constrained by the so called *Cardy condition*. The sum only runs over representations of the bulk space with $i = \sigma(\bar{i})$, where σ is an automorphism of the symmetry algebra.

A convenient trick to deal with correlation functions on the upper half plane is to introduce a mirror image of the system on the lower half-plane by a parity transformation. This means that fields change their holomorphic indices into antiholomorphic indices when going from the upper to the lower half plane. This is compatible with the above boundary condition for T . One effectively replaces antiholomorphic degrees of freedom on the upper half-plane by holomorphic degrees of freedom on the lower half-plane. In this way one can regard an N -point correlator of a theory defined on the upper half-plane as a holomorphic $2N$ -point correlator in the full plane as follows

$$\langle \prod_{i=1}^N \Phi_{h_i, \bar{h}_i}(z, \bar{z}) \rangle = \langle \prod_{i=1}^N \phi_{h_i}(z) \prod_{i=1}^N \bar{\phi}_{\bar{h}_i}(z_i^*) \rangle, \quad (1.39)$$

where $\phi_h(z)$ is the holomorphic part of $\Phi_{h, \bar{h}}(z, \bar{z})$ and $\bar{\phi}_{\bar{h}}(z_i^*)$ is its antiholomorphic part after a parity transformation on the lower half-plane which renders it holomorphic.

It can be understood as unfolding the theory “CFT \otimes $\overline{\text{CFT}}$ ” on the upper half-plane to a chiral theory on the full plane with an interface at $z \in \mathbb{R}$ that glues together “CFT” and “ $\overline{\text{CFT}}$ ”.

1.9.1 Boundary fields and the Cardy condition

With the above method of unfolding (or imaging), the existence of local fields on the boundary appears rather naturally. Consider a primary field $\Phi(z, \bar{z})$ on the upper half plane. Very near to the boundary it can be replaced by the OPE of its chiral part with its

mirrored antichiral part, i.e.

$$\phi(z)\phi(z^*) \approx \sum_i (z - z^*)^{h_i - 2h} \phi_B^{(i)}(x), \quad (1.40)$$

where $x = (z + z^*)/2 \in \mathbb{R}$ and hence the fields $\phi_B^{(i)}$ live on the boundary. They are called boundary fields and can change the boundary condition when inserted at a point on the boundary. This can be justified by looking at a conformal field theory defined on a cylinder of length L and circumference T . In the limit of large T it is conformally equivalent to the upper half-plane via the exponential map. One now demands that the theory defined on this cylinder is equivalent for two quantization schemes – the one where time is periodic and flows around the cylinder, the other where it flows along the cylinder from boundary to boundary.⁸ In the first scheme the partition function is determined by the spectrum of those fields that can change one boundary to the respective other with the corresponding Hamiltonian. In the second scheme the partition function can be derived by time evolving one boundary state into the other, where time evolution is given by the Hamiltonian of the theory without boundaries. The results are related by an S -transformation and should hence be the same. This condition is called the *Cardy condition* – or in string theory also often the open closed string duality. It is the tool to construct consistent boundary conditions, *i.e.* it gives high constraints on the possible values of the coefficients $b_{\mathcal{B}_i}$ in the linear combination of Ishibashi states (1.38) and reduces the linear space of solutions of the local gluing conditions to a positive cone of a lattice. In addition, if the boundary conditions are given it can be used to derive the spectrum of boundary changing fields.

1.10 Interfaces in conformal field theory

Interfaces and defects can be regarded as natural generalizations of boundaries. Consider a Riemannian manifold that is divided into subregions where one can define an potential different theory in each part. The defects then sit at the boundaries of these regions and glue the theories together. They are one-dimensional submanifolds that set local gluing condition on the fields of the two theories that they connect. The easiest example is the complex plane with one theory defined on the upper half-plane and the other one in the lower half-plane. The interface then sits on the real axis.

⁸This is very much like the condition of invariance under modular transformation on the torus which can be regarded as a finite cylinder with twisted periodic boundary conditions at the two ends.

In physics they can appear in various scenarios with very different effects and interpretations. They appear very naturally in two-dimensional statistical systems and one-dimensional quantum systems. Consider for example a two-dimensional lattice model where the couplings are altered from their normal values along a line. In the continuum limit this gives rise to a defect. Another physical situation that gives rise to interfaces is the junction of two (or even more) quantum wires when one again considers the continuum limit. Interfaces can also be used to describe tunneling in the quantum Hall effect [77].

In string theory, defects also play a growingly important role. As already mentioned and as will become clear soon, interfaces can be regarded as generalizations of boundaries. Since boundaries give rise to D-branes in string theory, one might ask if defects give rise to a generalization of those in the target space. The answer to this question is tough. There are defects that have a localized interpretation in spacetime. However, other defects have no target space interpretation at all. Another interesting application of defects in string theory is that a class of them can be regarded as brane spectrum generating. They can be moved on the world sheet and even onto a boundary and in this way change the boundary condition and the respective D-brane [25].

One can also interpret defects as “symmetries” that relate the features of the two theories they connect. They can reflect group symmetries or dualities of a theory [22], there is a preferred defect that connects the endpoints of renormalization group flows encoding the information of the flow [23], and can reflect a spectrum generating symmetry in string theory [21].

Similar to boundaries, a defect is dubbed *conformal* if its gluing conditions are compatible with all conformal transformations that leave the shape of the defect invariant. For the example of a defect along the real axis in the complex plane, the necessary gluing condition then is

$$\lim_{y \rightarrow 0^+} \left(T^{(1)}(x + iy) - \tilde{T}^{(1)}(x - iy) \right) = \lim_{y \rightarrow 0^-} \left(T^{(2)}(x + iy) - \tilde{T}^{(2)}(x - iy) \right), \quad (1.41)$$

where $T^{(1)}$ ($T^{(2)}$) is the energy momentum tensor of the theory defined on the upper (lower) half-plane. When time evolution is defined orthogonal to the defect – in the above example along the imaginary axis – then it can be realized as an operator \mathcal{I} mapping states from the Hilbert space of one theory to the other. The above gluing condition then tells that this operator has to commute with all the generators of conformal transformations along

the defect. For a defect along the real line this reads

$$(L_n^{(1)} - \bar{L}_n^{(1)}) \mathcal{I} = \mathcal{I} (L_n^{(2)} - \bar{L}_n^{(2)}) . \quad (1.42)$$

1.10.1 Defect junction fields and Cardy condition

As in the case of boundaries, there exist fields on interfaces that may or may not change the gluing condition. Consequently, interfaces have to satisfy a Cardy condition which tells that quantization parallel and quantization orthogonal to the interface are equivalent. Quantization parallel to the interface gives rise to the spectrum of defect (changing) fields. Consistent spectra of defect fields and defect changing fields give high constraints on possible interfaces.

In the case of defects, the situation can be generalized. Consider the junction of several interfaces at a point on the Riemann surface. At this point one has to introduce a defect junction field. However, their treatment is much more subtle. For general defects, a generalized Cardy condition for arbitrary junctions sets too tight constraints. One reason for this is that the spectrum of junction fields also depends on the angle between the defects. One would have to expect a discrete spectrum that depends non-trivially on continuous parameters. The situation becomes even more delicate for very small angles. Due to effects that are very similar to those of the Casimir effect the spectrum becomes divergent and one has to introduce a method of regularization. Only one particular class of defects does not suffer from these issues – the one of topological defects that will be introduced shortly.

1.10.2 Factorizing and topological defects

The gluing condition (1.41) has two special solutions where its treatment simplifies a lot. The first one is when both sides of the equation vanish independently which is simply the case of two separate boundary conditions for the two conformal field theories. The corresponding interface is then dubbed *factorizing*. If the conformal boundaries of a theory are known then the factorizing defects follow easily. This shows, however, that there are many more possibilities for defects than there are for boundaries. In fact, any boundary can be realized as an interface between the respective theory and the trivial CFT with vanishing energy momentum tensor. It is, hence, fair to say that defects really are generalizations of boundaries.

The other special solutions occur if the holomorphic and the antiholomorphic parts of

the energy momentum tensor themselves are continuous over the defect. On the level of operators this becomes

$$L_m^{(1)}\mathcal{I} = \mathcal{I}L_m^{(2)} \quad \text{and} \quad \bar{L}_m^{(1)}\mathcal{I} = \mathcal{I}\bar{L}_m^{(2)} \quad \forall m \in \mathbb{Z}. \quad (1.43)$$

This gluing condition tells us that the defect is compatible with all conformal transformations. It in particular commutes with the Hamiltonian and the momentum operator and, hence, is tensionless and can be moved around without cost of energy or momentum. In fact, they can be deformed arbitrarily on the surface and do not affect the value of correlators as long as they do not cross any operator insertion. These types of defects are called *topological*. Since T and \tilde{T} are separately continuous across the defect, the spectrum of defect fields is organized in representations of the holomorphic and anti-holomorphic copy of the Virasoro algebra, just as the bulk spectrum. This in particular means that any defect field ϕ has a left and right conformal weight (h, \bar{h}) .

A detailed look on topological defects

Compared to general conformal defects, topological defects are very easy to handle. For rational conformal field theories there actually exists a classification. When realized as an operator, a topological interface simply acts as a constant map between isomorphic representations of the Virasoro algebra or an extended symmetry algebra. Its general form is

$$\mathcal{I}_A = \sum_{\mathbf{i}} d_{A\mathbf{i}} \|\mathbf{i}\|, \quad (1.44)$$

where the subscript A labels the interface, and the bold index \mathbf{i} refers to a pair of irreducible representations in the two adjacent conformal field theories,

$$\mathbf{i} \equiv (i, \bar{i}; \alpha, \beta). \quad (1.45)$$

Here, (i, \bar{i}) labels a pair of representation that appears $M_{i\bar{i}}^{(1)}$ and $M_{i\bar{i}}^{(2)}$ times in the Hilbert space of the respective CFT. The indices $\alpha = 1, 2, \dots, M_{i\bar{i}}^1$ and $\beta = 1, 2, \dots, M_{i\bar{i}}^2$ are the multiplicity labels of this pair on the two sides of the interface. The symbol $\|\mathbf{i}\|$ stands for the Ishibashi-type projector which acts as an intertwiner between the two pairs of representations, *i.e.*

$$\|\mathbf{i}\| : [\mathcal{H}_i \otimes \mathcal{H}_{\bar{i}}]^{(\alpha)} \rightarrow [\mathcal{H}_i \otimes \mathcal{H}_{\bar{i}}]^{(\beta)} \quad (1.46)$$

and

$$L_n \|\mathbf{i}\| = \|\mathbf{i}\| L_n, \quad \bar{L}_n \|\mathbf{i}\| = \|\mathbf{i}\| \bar{L}_n. \quad (1.47)$$

An important feature of topological interfaces is that they give rise to a simple fusion product. It simply has the geometric interpretation of moving the interface lines on top of each other, and interpreting the result as a topological interface between the two remaining CFTs. While fusion may also be defined for more general conformal interfaces as we will discuss in section 1.10.4, it is particularly straightforward in the topological case, where it can basically be realized by map composition. The coefficients $d_{AB\mathbf{i}}$ of the fusion product $\mathcal{I}_{AB} = \mathcal{I}_A \mathcal{I}_B$ is then simply given by

$$d_{AB\mathbf{i}} = \sum_{\gamma} d_{A(i\bar{i}, \alpha, \gamma)} d_{B(i\bar{i}, \gamma, \beta)} \equiv d_{A\mathbf{i}} d_{B\mathbf{i}}. \quad (1.48)$$

This fusion product can also be generalized to fusion of a topological interface with general conformal interfaces and in particular with boundary conditions.

Using Cardy's condition and the fusion product, the coefficients $d_{A\mathbf{i}}$ must satisfy the condition

$$\sum_{\mathbf{i}} S_{ij} S_{\bar{j}} \text{Tr} d_{A^* \mathbf{i}} d_{A\mathbf{i}} = \mathcal{N}_{j\bar{j}A}^A \in \mathbb{N}, \quad (1.49)$$

where A^* labels the conjugate interface $\mathcal{I}_{A^*} = \mathcal{I}_A^\dagger$ of \mathcal{I}_A , S_{ij} is an element of the modular S matrix, and the trace is over multiplicity labels. The $\mathcal{N}_{j\bar{j}A}^B$ are multiplicities of the pair of representations (j, \bar{j}) that appears for a quantization parallel to the interfaces. The condition (1.49) is a strong constraint on the possible values of coefficients $d_{A\mathbf{i}}$, and it also requires that linear superpositions of interfaces must have integer coefficients.

Topological interfaces which cannot be decomposed into a superposition of other interfaces with positive coefficients are called *elementary*. The set of elementary interfaces forms a basis for all topological interfaces. Obviously any interface for which at least one of the $\mathcal{N}_{j\bar{j}A}^A$ is equal to 1 is elementary. In fact, any elementary interface has at least $\mathcal{N}_{00A}^A = 1$, *i.e.* the vacuum in parallel quantization occurs with multiplicity 1.

Consider a set of elementary topological interfaces \mathcal{I}_A as above. It can be shown that the corresponding $\mathcal{N}_{i\bar{i}A}^B$ form a representation of a tensor product of fusion algebras,

$$\sum_B \mathcal{N}_{i\bar{i}A}^B \mathcal{N}_{j\bar{j}B}^C = \sum_{\mathbf{k}} N_{ij}^k N_{\bar{j}}^{\bar{k}} \mathcal{N}_{k\bar{k}A}^C. \quad (1.50)$$

In the last formula, the N_{ij}^k are the fusion coefficients of the Virasoro algebra.

In case of diagonal theories⁹ the set of d_{Ai} becomes particularly simple. In such a theory there are topological defects of the form [27]

$$\mathcal{I}_a = \sum_i \frac{S_{ai}}{S_{0i}} \|i\|. \quad (1.51)$$

These defects have $\mathcal{N}_{0a}^a = N_{0a}^a = 1$ and are therefore elementary. They provide a basis for the set of topological defects. One can see that there are as many elementary topological defects in the theory as there are primary fields. Even more, the algebra of topological defects with the product being defined by the fusion product is isomorphic to the fusion algebra of Verma modules, which in particular means that

$$\mathcal{I}_a \mathcal{I}_b = \sum_k N_{ab}^c \mathcal{I}_c. \quad (1.52)$$

All the above results for topological defects can be generalized straight forward to extended chiral algebras if one assumes that the defect is compatible with the full symmetry, *i.e.*

$$J_n^{(1)} \mathcal{I} = \mathcal{I} \sigma(J_n^{(2)}) \quad (1.53)$$

where the J s denote any symmetry generator and σ is an automorphism of the extended symmetry algebra.

When the conformal field theory admits a global symmetry G , we find among the topological interfaces the so-called symmetry defects. Each element $g \in G$ can be associated to a topological defect \mathcal{I}_g . These interfaces are defined by gluing any field to its image under the symmetry operation. Therefore, they implement an action of G through

$$\mathcal{I}_g^\dagger = \mathcal{I}_{g^{-1}}, \quad \mathcal{I}_g \mathcal{I}_h = \mathcal{I}_{gh} \quad \forall h, g \in G. \quad (1.54)$$

A broader class of interfaces are the so-called duality interfaces introduced in [78]. Their defining property is

$$\mathcal{I} \mathcal{I}^\dagger = \bigoplus_{g \in G} n_g \mathcal{I}_g, \quad (1.55)$$

where G is a symmetry group of the CFT and \mathcal{I}_g are the respective symmetry defects.

⁹This are those rational theories which are charge conjugation invariant ($i = \bar{i}$), and where the multiplicities for all chiral algebra representations are 1.

Duality defects were first introduced in the context of rational conformal field theories, where they can relate CFTs with the same chiral algebra but different modular invariants. A prominent example is Kramers-Wannier duality which is a self-duality of the critical Ising model that can be implemented by a defect [22]. However, the definition can be extended to non-rational examples such as the T-duality in toroidal compactified free bosons.

1.10.3 The folding trick

There exists a full correspondence between interfaces between CFT1 and CFT2 on the lower and upper half plane and boundaries of the tensor product $\overline{\text{CFT1}} \otimes \text{CFT2}$ defined only on the upper half plane.¹⁰ The conformal gluing condition (1.41) for interfaces between CFT1 and CFT2 then becomes the conformal boundary condition (1.36) in the tensor product $\overline{\text{CFT1}} \otimes \text{CFT2}$ with $T^{\bar{1}\otimes 2} = \overline{\tilde{T}^1} + T^2$ and $\tilde{T}^{\bar{1}\otimes 2} = \overline{T^1} + \tilde{T}^2$, the interface operator corresponds to a boundary state, and the defect (changing) fields become boundary (changing) fields. This correspondence is also called the *folding trick*.

As an example consider topological defect in a rational theory where every representation appears only once. Using (1.44), the defect operator is given by

$$\mathcal{I}_A = \sum_{\mathbf{i}=(i,\bar{i})} d_{A\mathbf{i}} \|\mathbf{i}\|, \quad (1.56)$$

where we now write $\|\mathbf{i}\| = (|i\rangle\rangle^2 \otimes |\bar{i}\rangle\rangle^2) ({}^1\langle\langle i| \otimes {}^1\langle\langle \bar{i}|)$, with $|i\rangle\rangle$ ($|\bar{i}\rangle\rangle$) being Ishibashi-type states in the left (right) moving sector of the respective theory. We distinguish between the theories on the two sides of the interface although they are assumed to be the same. The folding trick now exchanges the left- and right-moving degrees of freedom in CFT1 and conjugates. The result is the boundary state

$$|\mathcal{B}\rangle = \sum_{(i,\bar{i})} d_{A\mathbf{i}} (|i\rangle\rangle^2 \otimes |\bar{i}\rangle\rangle^1) \otimes (|\bar{i}\rangle\rangle^2 \otimes |i\rangle\rangle^1), \quad (1.57)$$

which is also called permutation boundary state [79].

¹⁰ $\overline{\text{CFT1}}$ is defined from CFT1 by interchanging the holomorphic and antiholomorphic sectors and mirroring it at the real axis.

1.10.4 On the fusion of interfaces

We now want to shortly discuss the fusion of two conformal interfaces. It is a generalization of the fusion of two topological defects that was introduced earlier. For a detailed text on the fusion of defects see [80]. The general idea is illustrated in figure 1.1. We have three conformal field theories glued by the interfaces \mathcal{I}_{12} and \mathcal{I}_{23} at separation ε . The fusion now corresponds to shrinking the intermediate region of CFT2 to zero size $\varepsilon \rightarrow 0$. Then CFT1 and CFT3 are glued by a new interface which we denote $I_{12} \star I_{23}$. In terms of a lattice theory this is equivalent to considering that the typical scale x at which the system is probed is much larger than the separation of the defects $\varepsilon \ll x$ which however must be large compared to the lattice spacing/UV cutoff Λ , *i.e.* $\Lambda \ll \varepsilon$.

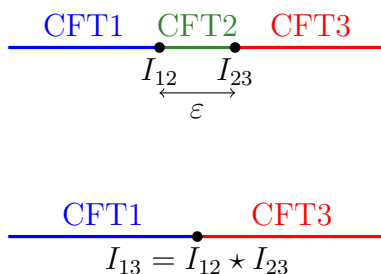


Figure 1.1: The fusion of two interfaces corresponds to shrinking the size of the intermediate region to zero, *i.e.* taking the limit $\varepsilon \rightarrow 0$. We here only draw the direction orthogonal to the defect.

The fusion in the quantum theory is defined by the composition of interface operators which in general requires regularization. One therefore defines

$$I_{12} \star I_{23} := \lim_{\varepsilon \rightarrow 0} [e^{-C/\varepsilon} I_{12} e^{-\varepsilon H} I_{23}] , \quad (1.58)$$

where H is the Hamiltonian of CFT2, and C/ε is called the Casimir energy between the two interfaces. The divergent (or vanishing) factor $e^{-C/\varepsilon}$ is an overall regularization factor that drops out of calculations of correlation functions. If one of the interfaces is topological there is no need of a regularization, *i.e.* the Casimir energy vanishes. This method of computing a fusion product uses a particular choice of regularization. One could in principle introduce other methods of regularization, which however should not alter the result of the fusion product if it was a physically reasonable procedure.

The definition of fusion of conformal interfaces with boundaries is straight forward when

using the fact that any boundary of a CFT can be seen as an interface between that CFT and the trivial CFT. The trivial CFT in particular has an everywhere vanishing energy momentum tensor, *s.t.* any interface between a CFT and the trivial CFT is factorizing. As an example, consider the fusion of a topological defect with a Cardy boundary state in a diagonal theory. It does not need a regularization factor and can be computed to be (see also [25])

$$\mathcal{I}_a|\mathcal{B}_b\rangle\rangle = \left(\sum_i \frac{S_{ai}}{S_{0i}} \|i\| \right) \left(\sum_j \frac{S_{jb}}{\sqrt{S_{j0}}} |j\rangle\rangle \right) = \sum_c N_{ab}^c |\mathcal{B}_c\rangle \quad (1.59)$$

Fusion of interfaces clearly distinguish them from boundaries. There is no analogous procedure for two boundaries which shows again, that interfaces can be regarded as generalizations of boundaries.

1.10.5 Reflection and transmission of interfaces

Two interesting quantities that characterise all conformal interfaces are the reflection coefficient \mathcal{R} and the transmission coefficient \mathcal{T} which are given by 2-point functions of the energy momentum tensor as follows [18]

$$\mathcal{R} \equiv \frac{\langle T_1 \bar{T}_1 + T_2 \bar{T}_2 \rangle_{\mathcal{I}}}{\langle (T_1 + \bar{T}_2)(\bar{T}_1 + T_2) \rangle_{\mathcal{I}}}, \quad \mathcal{T} \equiv \frac{\langle T_1 \bar{T}_2 + T_2 \bar{T}_1 \rangle_{\mathcal{I}}}{\langle (T_1 + \bar{T}_2)(\bar{T}_1 + T_2) \rangle_{\mathcal{I}}} \quad (1.60)$$

where T_1, \bar{T}_1 are the components of the energy momentum tensor at the point z and T_2, \bar{T}_2 are evaluated at the corresponding point reflected at the interface. In case of free theories, where one mostly has the possibility to define a notion of particles, the above two quantities really have the interpretation of a probability of a particle being transmitted or reflected at the interface.

The two coefficients always sum to identity. The two special cases discussed in section 1.10.2 correspond to the extreme values of \mathcal{T} and \mathcal{R} . Topological defects are fully transmissive, *i.e.* $\mathcal{T} = 1$ and $\mathcal{R} = 0$, whereas factorizing defects are purely reflective, *i.e.* $\mathcal{R} = 1$ and $\mathcal{T} = 0$. In unitary theories, the respective coefficients of general conformal defects lie between these two extremes.

Chapter 2

About Entanglement Measures

In the conceptual development of quantum physics the idea of *entanglement* has played an important role. For a long time, entanglement was simply seen as a qualitative feature of quantum theories that distinguishes from classical expectations. Quantitative checks that make this evident are Bell's inequalities. They also show the non-local features of quantum theories when it comes to entanglement – performing a local measurement may instantaneously affect the outcome of local measurements far away [2]. Bell's inequalities may be seen as a first attempt to quantify quantum correlations that – from the classical point of view – seem counter-intuitive when looking at entangled states.

The concept of entanglement developed from a qualitative feature to an important tool in quantum physics a lot because of the technological progress of the last decades. We can now coherently prepare, manipulate, and measure individual quantum systems, and, in particular, it has become possible to create and control quantum correlations. In the same time it has become evident that quantum correlations may be used to perform computational tasks that are very inefficient when only restricted to classical methods. Examples for this are the Deutsch-Jozsa algorithm [81], or Shor's algorithm for prime factorization [82].¹ This has led to the development of modern quantum information science.

Another very broad field of research concerns the understanding of the role played by entanglement in many-body systems, or to phrase it differently: what can we learn about quantum field theories by investigating entanglement. Its study may reveal new probably non-local features of quantum theories. We want to give three short examples where this is or very likely will be the case.

¹Among others these are examples for quantum algorithms that are more efficient than any **known** classical algorithm for the same problems. However, it is not known if it is really the case that these problems in principle cannot be solved classically with the same efficiency.

Monotonicity theorems: In quantum field theory the concept of renormalization group (RG) plays an important role [10]. It allows the systematic investigation of physical systems at different energy scales (or equivalently length scales). In particular, it allows to derive effective descriptions at lower energies by “integrating out” high energy degrees of freedom. This is also called a renormalization group flow and very often is parametrized by the coupling constants of the theory which themselves change under the flow. Fixed points of this flow must be scale invariant theories, and very often are conformally invariant too.

Monotonicity theorems make the physical expectation manifest that the number of degrees of freedoms reduces along the renormalization group flow. A necessary ingredients to such a theorem is a quantity that measures degrees of freedom. The respective theorem then states that this quantity decreases under RG flow. A prominent example is the Zamolochikov c -theorem [83] that states that for any two-dimensional renormalizable field theory, there exists a function $c(\lambda)$ of its coupling constants $\lambda = (\lambda_1, \lambda_2, \dots)$ which (i) decreases monotonically under the RG flow and (ii) equals to the central charge of the conformal field theory at the fix points of the flow. Another example is the g -theorem [84] that states that under boundary RG flows in two-dimensional field theories a function g decreases with $\log(g)$ being the boundary entropy at fixed points.

Both theorems can be proven using the concept of entanglement in the respective theorys [85, 86]. A measure thereof – the entanglement entropy that will be introduced later – serves to define c - and g -functions with the above properties. This matches the vague intuition that when the number of degrees of freedoms is reduced there is less that can be entangled. It seems plausible that measures of entanglement can be used to state and prove monotonicity theorems generally.

AdS/CFT correspondence: The holographic principle [31] is a statement that a gravitational theory describing a region of space (the bulk) is equivalent to a (non-gravitational) theory confined to the boundary of that region. That is, intrinsically non-geometric features can be equivalently described geometrically. The AdS/CFT-correspondence [33] is an explicit example of this principle. It relates (quantum) gravity on $(d + 1)$ -dimensional asymptotic Anti-de Sitter (AdS) space to a d -dimensional conformal field theory on the boundary.

One remarkable aspect of this correspondence is the interplay of geometry and entanglement, that is most evident in the proposal by Ryu and Takayanagi that entanglement entropy in the CFT is equivalently given by the area of a minimal surface in the AdS

geometry [34]. This is known as the *Ryu-Takayanagi* (RT) formula. Other connections between entanglement and the AdS/CFT correspondence will be discussed in chapter 4.

Black hole physics: Many more connections between geometry and entanglement have been proposed [36, 37, 38, 39, 40, 41, 42]. Also, more generally, concepts of quantum information theory and entanglement were fruitfully applied to gravity and, in particular, to black holes [43, 44, 45, 46, 47, 48, 49]. The latter objects are still mysterious in various senses, especially because their macroscopic geometric description needs to be consistent with microscopic descriptions at the black hole horizon, for small black holes or in the center of black holes. They seem to be the most promising candidates to reveal the connection between gravity, *i.e.* a description of the geometry of space-time by means of classical field theory, and quantum theory.

One of the key principle from quantum theory to understand gravity and in particular black holes is entanglement. Entanglement entropy might give an explanation for the huge entropy of black holes [87], or a black hole might even break entanglement through its horizon and spoil essential features that we expect from a solid quantum theory [45].

In what follows, we will review some mathematical aspects of entanglement and in particular talk about measures thereof. For more details we recommend [15], whose logic we follow here too.

2.1 Measures of entanglement

In the description of entanglement one wants to discover the mathematical structure that fully capture its behavior. A found description should cover a consistent characterization, should tell how it behaves under manipulations of a quantum system, and last but not least it should provide us with a possibility of quantification, or in other words we seek a consistent and well behaved measure of quantum correlations. Without going to deep into details, we want to mention that in the context of quantum information the definition of quantum correlation is maintained by considering so called LOCC operations [88]. These are those operations on a bipartite system that can be performed locally in each part (Local Operations), where one in addition allows all possible Classical Communication between them. The set of these operations is not completely local and can have a quite complicated structure. The key idea now is that (i) LOCC-operations *cannot* create entanglement, *i.e.* entanglement does not increase under LOCC transformation [89, 90]. Additional require-

ments are that (ii) separable states² contain no entanglement, (iii) every non-separable state is entangled, (iv) local unitary operations cannot change entanglement at all, and (v) there are maximally entangled states. The latter are known at least in bipartite systems with fixed d -dimensional sub-systems: any pure state that is local unitary equivalent to

$$|\psi_{\max.}^+\rangle = \frac{1}{\sqrt{d}} \sum_{i=0}^{d-1} |i\rangle \otimes |i\rangle \quad (2.1)$$

is maximally entangled. This is because any pure or mixed state³ of two d -dimensional systems can be obtained by performing LOCC operations on $|\psi\rangle$ [15].

In the case of pure states there exists a favorable measure of entanglement in a bipartite systems. This is the *entropy of entanglement* [89], which is defined as

$$E(\rho=|\psi\rangle\langle\psi|) = S(\text{Tr}_A\rho) = S(\text{Tr}_B\rho), \quad (2.2)$$

where S is the von-Neumann entropy $S(\rho) = -\text{Tr}(\rho \log \rho)$, and $\text{Tr}_{A(B)}$ stands for the partial trace over sub-system A (B). In the case of mixed states the entanglement entropy does not show good properties. There *e.g.* exist separable mixed states with non-vanishing entanglement entropy.⁴ Therefore, one has to introduce different measures that work for mixed states too. However, very often one demands that entanglement measures for general states of bipartite systems reduce to the entropy of entanglement when evaluated on pure states. Three examples of measures of this type are the following:

Entanglement cost: For a state ρ it quantifies the rate at which one can transform collections of maximally entangled states into an output state that approximates many copies of ρ , where the approximation becomes exact in the limit of infinite copies. A mathematical definition is

$$E_C(\rho) := \inf \left\{ r : \lim_{n \rightarrow \infty} \left(\inf_{\Psi} D(\rho^{\otimes n}, \Psi[\Phi(2^{rn})]) \right) \right\}, \quad (2.3)$$

where $\Phi(K)$ is the density operator that corresponds to the maximally entangled state in

²A state $\rho_{ABC\dots}$ of subsystems A, B, C, \dots is separable if it can be written in the form $\rho_{ABC\dots} = \sum_i p_i \rho_A^i \otimes \rho_B^i \otimes \rho_C^i \otimes \dots$ [91].

³Pure states can be represented by a vector $|\psi\rangle$ in the Hilbert space of the theory. Their density matrix simply is $\rho = |\psi\rangle\langle\psi|$. A mixed state is a statistical ensemble of pure states and cannot be described by a vector of the Hilbert space. Typical examples for mixed states are thermal states with $\rho = e^{-\beta H}/Z(\beta)$.

⁴An easy example is the maximally mixed state of two qbits, $\rho = \rho_1 \otimes \rho_2$ with $\rho_1 = \rho_2 = \text{diag}(1/2, 1/2)$. It is separable but the entanglement entropy between the two qubits is non-zero, $E = \log 2$.

K dimensions, Ψ denotes a general trace preserving LOCC transformation, and D is some suitable measure of distance in the space of density operators [92, 93]. So $D(\rho^{\otimes n}, \Psi[\Phi(2^{rn})])$ gives a distance between n copies of the state ρ and the maximally entangled state in 2^{rn} dimensions after the LOCC transformation Ψ . The formula gives us the value for r for which this distance is minimal in the limit of $n \rightarrow \infty$ and after minimizing with respect to all possible Ψ . The entanglement cost asks how many maximally entangled states – the “gold standard currency” in quantum information – do we have to pay to get back our state.

Distillable entanglement: This measure [89] asks about the reverse process: at which rate can we extract maximally entangled states from an input of many copies of ρ ? The precise mathematical description is

$$E_D(\rho) := \sup \left\{ r : \lim_{n \rightarrow \infty} \left(\inf_{\Psi} D(\Psi[\rho^{\otimes n}], \Phi(2^{rn})) \right) \right\}. \quad (2.4)$$

Entanglement of formation: This measure [94] represents the minimal possible average entanglement over all pure state decompositions of a given state ρ , where one takes the entanglement entropy as the measure for pure states. The mathematical definition is given by

$$E_F(\rho) := \inf \left\{ \sum_i p_i E(|\psi_i\rangle\langle\psi_i|) : \rho = \sum_i p_i |\psi_i\rangle\langle\psi_i| \right\}. \quad (2.5)$$

The entanglement of formation is closely related to the entanglement cost and in fact it can be shown that the asymptotic version of E_F , being

$$E_F^\infty(\rho) = \lim_{n \rightarrow \infty} \frac{E_F(\rho^{\otimes n})}{n}, \quad (2.6)$$

equals E_C .

We want to mention that these three definitions are interesting conceptually and from a mathematical point of view. However, their actual computation for a given state is in general very hard.

All examples so far are successful attempts to quantify the entanglement between two parts of a quantum system. The situation becomes more involved when considering multipartite systems. One reason is that it is not possible to single out maximally entangled

states as in the case of two-partite systems. There is no “gold standard” that can serve as a reference because in general there is no generic notion of maximally multi-entangled states [95]. Although there still exist good attempts to define well behaved measures for three-partite and even four-partite entanglement, we don’t want to present them here.

So far we considered finite-dimensional systems. Even in these cases, the actual computation of the exemplary measures given above can be very involved. The task becomes yet more delicate for infinite dimensional systems. However, at least for pure states the entanglement entropy still defines a solid and computable measure for entanglement in bipartite systems. Therefore we want to stick to this measure of entanglement.

Assume a quantum field theory with an Hamiltonian H . The actual physical system is described by a pure state $\rho(t) = |\Psi(t)\rangle\langle\Psi(t)|$, where $|\Psi(t)\rangle = e^{-iHt}|\Psi(0)\rangle$. We will be mostly interested in the groundstate entanglement, *s.t.* we have $\rho \equiv |\Omega\rangle\langle\Omega|$ for all times, where $|\Omega\rangle$ is the groundstate. The two subsystems are often defined by subregions of the space the theory is defined on, *e.g.* in a (1+1)-dimensional system one considers the entanglement between a spatial interval and its complement. If the theory is defined on a lattice, very often the entanglement entropy between a subset of all lattice sites and its complement is the quantity of interest. However, one can also consider other also non-geometric bipartitions, as *e.g.* at boundaries with a bipartition into left- and right-moving degrees of freedom.

The basic definition of the entanglement entropy in all these cases is the same and equivalent to the definition for finite systems. One has to calculate the reduced density matrix by tracing over all degrees of freedom of one subsystem. The entanglement entropy is then given by the von Neumann entropy of this reduced density matrix as in (2.2). However, especially in infinite systems the computation of this quantity can become very messy mostly due to the logarithm appearing in its definition. A method that makes life very often easier is the so called replica trick (see *e.g.* [96]). Therefore one considers K copies (or replicas) of the reduced system which brings us to the definition of the so-called Rényi entropy of the reduced density matrix ρ_A , which is given by

$$S_K(\rho_A) := \frac{1}{1-K} \log (\text{Tr} \rho_A^K) . \quad (2.7)$$

If one is able to derive the Rényi entropy for all integer $K > 1$ and in addition sets the constraints that $S_{\pm i\infty} = 0$, then there exist a unique analytic continuation of this quantity to the whole complex plane and one can take the limit $K \rightarrow 1$. In this limit, the Rényi

entropy approaches the von Neumann entropy and hence gives the entanglement entropy. Under the same condition, it is also possible to derive the entanglement entropy as

$$E(\rho) \equiv - \lim_{K \rightarrow 1} \frac{\partial}{\partial K} \text{Tr}(\rho_A^K) . \quad (2.8)$$

In many physically relevant cases, that are when we deal with a local Hamiltonian with finite-interaction strength and a unique ground state with a spectral gap, it is believed that the ground state entanglement entropy follows an area law [97]. It states that under the latter conditions the entanglement entropy in a spatial bipartite system depends on the area that separates the two regions. In (1+1)-dimensional gapped local spin models this area law is actually proven [98]. The prove highly depends on the Lieb-Robinson theorem, which is a statement on the existence of speed of sound in local Hamiltonian systems [99]. There also exists an area law for two-dimensional gapless systems, for which conformal field theories are an example, where it is proposed that the entanglement entropy is proportional to the logarithm of the size of the smaller subsystem which gives the dominant contribution. However, it is in addition also proportional to the separating area.

2.1.1 Entanglement measures in experiment

It is quite hard to directly access entanglement measures in experiment. This is because the entanglement measures are not directly related to a single physical quantity. They quantify the strength of entanglement between subsystems and, hence, in these subsystems any correlation between observables generically contributes. Experimental measurements quantify correlations in a specific situation which is surely not enough to assess the full entanglement structure of a system.

One way to determine the reduced density matrix can be quantum tomography. This is a method to determine a density matrix by repeatedly performing many different measurements (see *e.g.* [100, 101, 102] for articles on quantum tomography).

There is one quantity that is easier accessible by experiment – the n th Rényi entropy. This is because there is a way to arrange n copies of the system, *e.g.* a spin chain, in such a way that one can extract information about their partition function. This is for example done in [103]. They arrange n half chains in a star like formation (they call it a cross geometry) with a quantum switch in the center which controls the connection between the endpoints of the half chains by selectively forbidding tunneling processes between neighboring spins next to the center. They then measure the overlaps between groundstates of

different configurations by so-called Rabi oscillations of the quantum switch, which they claim to be proportional to the n th Rényi entropy.

Another example of an experiment where they take copies of a system is [104]. There they built two copies of a many body state out of ultra cold bosonic atoms in optical lattices and interfere them. This directly enables them to measure the second Rényi entropy, quantum purity⁵ and mutual information.

2.2 Entanglement entropy in two-dimensional CFT

For a number of key quantities in conformal field theory, the microscopic details of the theory became irrelevant and they then only depend on basic properties like the symmetry of the system, or the spatial dimension. The most prominent examples therefore are critical exponents at phase transitions. These features are called *universal* quantities. At least for a single large interval in a (1+1)-dimensional conformal field theory, the corresponding ground state entanglement entropy is such a quantity.

Assume an arbitrary conformal field theory in (1+1) dimensions and a subsystem A being the union of N disjoint intervals, *i.e.* $A = I_1 \cup \dots \cup I_N$. As argued in [16], the quantity $\text{Tr}\rho_A^K$ can be computed by considering the partition function $Z(K)$ of the given conformal field theory on a K -sheeted Riemann surface where the different sheets are glued together in a cyclic fashion with branchcuts along the intervals in A . The precise relation is

$$\text{Tr}\rho_A^K = \frac{Z(K)}{Z(1)^K}, \quad (2.9)$$

such that the entanglement entropy is given by

$$E = \lim_{K \rightarrow 1} (1 - \partial_K) \log Z(K). \quad (2.10)$$

The Riemann surface has a rather complicated geometry mainly because of the endpoints of the branchcuts, where one can expect very high curvature. It is possible to carry these complications from the world-sheet over to the space of states by considering a model of K independent copies of the original theory on the complex plane – one can imagine to fold all the single sheets together onto the plane. There the role of the branch cuts, that told us to jump from sheet n to sheet $n+1$, can be played by defects along the respective intervals. The action of the defects simply is to replace any field of the n th copy by the respective

⁵Quantum purity is a rather simple attempt to measure entanglement. It is given by $\text{Tr}\rho^2$.

2.2 Entanglement entropy in two-dimensional CFT

field in the $(n+1)$ st copy of the theory. This action is a realization of a \mathbb{Z}_K symmetry of the tensor product theory $\text{CFT}^{\otimes K}$.

As discussed in section 1.10.1, at an endpoint of a defect – which also can be seen as a junction between the defect and the identity – there must sit a junction field. In case of defects that implement a symmetry of the theory these junction fields are also called *twist fields*. Cardy's condition allows us to derive the full spectrum of \mathbb{Z}_K twist fields, however, only the twist field of lowest possible conformal dimension is needed to derive the above partition function. Any other twist field would correspond to some excited state and hence cannot correspond to the groundstate entanglement entropy. The last step now is to mod out the \mathbb{Z}_K symmetry which does not change partition functions of twist fields. However, the defects that previously implemented the symmetry become invisible and the non-local twist fields become local fields in the twisted theory $\text{CFT}^{\otimes K}/\mathbb{Z}_K$. Finally, the partition function on the K -sheeted Riemann surface is given by the $2N$ -point correlator of twist fields sitting at the endpoints of the respective intervals in A .⁶ When we denote the endpoints of interval I_j by u_j and v_j and call the lowest-weight twist field $T_K(z)$, then

$$Z(K) = d_K \left\langle T_K(u_1) T_K^\dagger(v_1) \cdots T_K(u_N) T_K^\dagger(v_N) \right\rangle_{\text{CFT}^{\otimes K}/\mathbb{Z}_K, \mathbb{C}}, \quad (2.11)$$

where the subscript tells that this $2K$ -point correlator is taken in $\text{CFT}^{\otimes K}/\mathbb{Z}_K$ on the complex plane \mathbb{C} .

In case of a single interval the situation becomes particularly easy because the two-point correlator is simply given by $\langle T_K(u) T_K^\dagger(v) \rangle = (v-u)^{-2\Delta_K}$ with Δ_K the conformal dimension of the twist field. The conformal weight Δ_K can be obtained by using Cardy's condition for the symmetry defect as shown in the following computation

$$q^{\Delta_K - \frac{Kc}{12}} = \langle T_K | q^{H_K} | T_K \rangle = \text{Tr}_{\mathcal{H}_K/\mathbb{Z}_K} (q^{H_K}) |_{\tau \gg 1} \quad (2.12)$$

$$= \text{Tr}_{\mathcal{H}_K} (\mathcal{I}_{\mathbb{Z}_K} \tilde{q}^{KH}) |_{\tau \gg 1} \quad (2.13)$$

$$= \text{Tr}_{\mathcal{H}} ((\tilde{q}^K)^H) |_{\tau \gg 1} = \sum_{(i\bar{i})} \chi_i(\tilde{q}^K) \chi_{\bar{i}}(\tilde{q}^K) |_{\tau \gg 1} \quad (2.14)$$

$$= q^{-\frac{c}{12K}}. \quad (2.15)$$

We have $q = e^{-2\pi i\tau}$, H_K is the Hamiltonian for propagation along the symmetry defect $\mathcal{I}_{\mathbb{Z}_K}$. In the first line the trace is over the full spectrum of H_K , *i.e.* the space of \mathbb{Z}_K -twist

⁶This is true up to some possible overall constant that makes it in particular dimensionless.

fields $\mathcal{H}_K/\mathbb{Z}_K$. The second line is Cardy's condition with $\tilde{q} = e^{\frac{2\pi i}{\tau}}$ being the S -transformed q . The trace there goes over the states of $\text{CFT}^{\otimes K}$ with its Hamiltonian $\sum_{i=1}^K H = KH$. The third line uses the action of $\mathcal{I}_{\mathbb{Z}_K}$. The trace is now over the states of the original CFT, where one "goes around the torus K times". The last line follows from the dominant contribution by the vacuum for large τ after another S -transformation. One can read of that

$$\Delta_K = \frac{c}{12} \left(K - \frac{1}{K} \right), \quad (2.16)$$

so that the ground state entanglement entropy of a single interval is given by

$$E = \frac{c}{3} \log(L) + \tilde{d}, \quad (2.17)$$

where $L = v - u$ and $\tilde{d} = \log(d_1) - \frac{d_1'}{d_1}$. For large L – measured in units of a UV-cutoff like a lattice spacing – the first term dominates and the entanglement entropy becomes in fact universal. Only the sub-leading contribution \tilde{d} depends on microscopic properties of the theory.

For later purpose we also want to consider the situation of a bipartition into two infinite intervals $A = \mathbb{R}^-$ and $B = \mathbb{R}^+$. The branch cut for the K -sheeted Riemann surface goes along B . The corresponding partition function is divergent so that we have to introduce cutoffs. The ultraviolet cutoff ϵ excludes a circle with respective radius around the origin, *i.e.* the point where the branch cut ends and we have to expect high curvature. The infrared cutoff L renders the system finite by excluding all points with distance larger than L from the origin. For large system sizes the partition function is independent of the specific choice of boundary conditions, *s.t.* we can choose periodic boundary conditions at ϵ and L in radial direction. The situation is now somewhat analogues to the derivation of the conformal weight of the twist field. In fact if we now want to compute the partition function in circular quantization this is like "going around a torus K times" as in (2.14) with $\tau = \frac{\log(\frac{L}{\epsilon})}{2\pi i}$, where i renders the respective torus euclidean. We are in the same limit because $L \ll \epsilon$, such that to leading order in L the regularized partition function on the K -sheeted Riemann surface is given by (2.15), *i.e.*

$$Z(K) = q^{-\frac{c}{12K}} = e^{\frac{c}{12K} \log(\frac{L}{\epsilon})}, \quad (2.18)$$

2.2 Entanglement entropy in two-dimensional CFT

which gives the entanglement entropy

$$E = \frac{c}{6} \log \left(\frac{L}{\epsilon} \right). \quad (2.19)$$

Sub-leading contributions to the entanglement entropy depend on the specific choice of UV cutoff and of course on the sub-leading contribution to the partition function which depends on the specific microscopic features of the theory – mainly its spectrum.

The regularized result for the entanglement entropy of two infinite interval is half the result of a large but finite interval and its complement. This matches the expectation of an area law in (1+1) dimensions which states that the result is proportional to the area separating the two sub-regions – which here is respectively one and two. The factor $\log(L)$ is also expected from the general proof of the area law for gap-less systems in two dimensions.

Chapter 3

Entanglement Entropy through Interfaces

Besides systems defined on Riemann surfaces without boundaries, one area of investigation is centered around the entanglement in systems with boundaries or interfaces. There are several possibilities to specify subsystems, leading to different entanglement entropies. One possibility is to single out a spatial interval terminating at the boundary. If the subsystem of length L ends on a boundary specified by some boundary condition b , the expression for the entanglement entropy becomes [16]

$$E^{(b)} = \frac{c}{6} \log L + \log g_b + \frac{\tilde{d}}{2}. \quad (3.1)$$

Comparing with (2.17), the factor $1/2$ in the overall coefficient of the leading term again reflects the area law. The quantity g_b is the universal ground-state degeneracy [84] of the boundary condition b . In string theory, g_b defines the mass of the D-brane [105]. The important observation [16] is that $\log g_b$ in (3.1) is a universal contribution to the entanglement entropy from the boundary. The other subleading terms are non-universal, where \tilde{d} denotes the same terms as in the bulk case (2.17).

Via the folding trick, this result can also be applied to interfaces between two CFTs if the interface splits the system symmetrically. In [106, 107, 108], both boundary and interface entanglement entropy were investigated by AdS/CFT methods based on the Ryu-Takayanagi formula [34, 35].

Naturally, it is of interest to generalize the results on defect and boundary entropies further. For the case of interfaces, one would like to consider situations not constrained by the requirement of geometric reflection symmetry. For the case of boundaries, one would like

to consider subsystems that are not specified by the geometry of the system, but by decomposing the Hilbert space into left- and right-movers [109, 28]. In this work, we will discuss the entanglement entropy through interfaces, and also show how the same techniques can be employed to determine the left/right entanglement entropy for boundaries.

The problem of entanglement through interfaces has been approached before in special examples, in particular for the case of free bosons in [30]. The interface splits the system into two parts, and one is interested in the entanglement entropy between the subspace on the two sides of the interface. A recent investigation from the AdS/CFT point of view of these setups can be found in [110].

The replica trick and conformal interfaces

In the following, we will briefly review a construction of $Z(K)$ for the above situation, which in principle allows to derive the entanglement entropy through general conformal interfaces connecting two conformal field theories via (2.10). It is analogous to the construction of $Z(K)$ for two infinite intervals at the end of section 2.2.

Consider a conformal interface \mathcal{I} along the imaginary axis of the complex plane, with CFT1 on $\text{Re } w > 0$ and CFT2 on $\text{Re } w < 0$. With time flowing along the defect line, the subsystems A and B consist of the positive and negative real axis, respectively. Following the replica trick, the corresponding K -sheeted Riemann surface consists of K copies of the complex plane, glued together cyclically along a branch cut on the positive real axis, as illustrated on the left of Figure 3.1.

In order to evaluate the partition function $Z(K)$ we introduce the cutoffs $|w| = \epsilon$ and $|w| = L$. We again impose periodic boundary conditions in radial direction and change to circular quantization, which is in fact the same as performing the conformal transformation $z = \log(w)$ with time flowing in imaginary z -direction.¹ The corresponding torus is illustrated on the right of Figure 3.1. We conclude that $Z(K)$ is given by a torus partition function with $2K$ interfaces inserted,

$$\begin{aligned} Z(K) &= \text{Tr}_1 \left(\mathcal{I}^\dagger e^{-\delta H_2} \mathcal{I} e^{-\delta H_1} \dots \mathcal{I} e^{-\delta H_1} \right) \\ &= \text{Tr}_1 \left(\mathcal{I}^\dagger e^{-\delta H_2} \mathcal{I} e^{-\delta H_1} \right)^K, \end{aligned} \tag{3.2}$$

¹This transformation is in fact compatible with the conformal gluing condition mainly because the shape of the defects is unaltered. Hence one does not have to deal with non-trivial transformation properties of the interface.

where H_1 and H_2 are the Hamilton operators in the respective CFT, and again

$$\delta = \frac{2\pi^2}{\log L/\epsilon}. \quad (3.3)$$

Obviously the evaluation and analytic continuation of (3.2) depends heavily on \mathcal{I} . For non-topological conformal defects, $Z(K)$ is in general very hard to compute. An explicit expression which permitted the computation of the entanglement entropy was obtained in [30] for the case of a single free boson, and we will compute the result for conformal defects of the free fermion and the Ising model later. For topological defects the expression for $Z(K)$ simplifies considerably, as we will see in the following section.

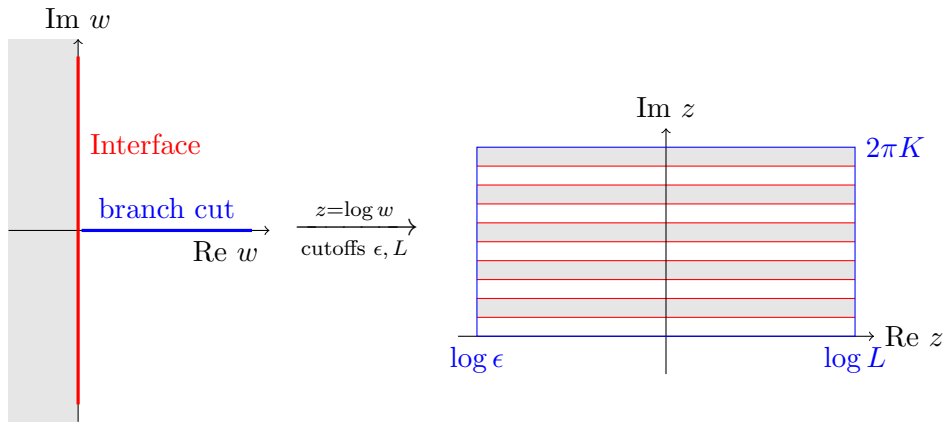


Figure 3.1: Sketch of the K -sheeted Riemann surface we use in the replica trick. After imposing a UV cutoff ϵ and a IR cutoff L , and imposing periodic boundary conditions in radial direction we get the torus with $2K$ defect insertions as shown on the right.

There is one feature of the entanglement entropy as we define it here which is rather obvious already at this stage. From (3.2) it is easy to see that the entanglement entropy computed by (2.10) is invariant under any rescalings of the interface. While interfaces generically have a standard normalisation derived from their properties under modular transformations, this means in particular that superpositions $M\mathcal{I}$ of identical interfaces \mathcal{I} yield the same entanglement as a single \mathcal{I} .

We will show that in all our examples the entanglement entropy is given by

$$E_{\mathcal{I}} = \frac{\sigma}{2} \log \left(\frac{L}{\epsilon} \right) + c_{\mathcal{I}} + \frac{\tilde{d}}{2} \quad (3.4)$$

Chapter 3 Entanglement Entropy through Interfaces

where $\sigma \leq \frac{c}{3}$ and $\sigma = \frac{c}{3}$ iff the interface is topological, $c_{\mathcal{I}}$ is a universal sub-leading contribution that only depends on topological data of the defect and \tilde{d} is the usual non-universal sub-leading contribution that we will omit in what follows.

3.1 Entanglement entropy through topological interfaces

In this section we will study the constant shifts in the entanglement entropy that occur in the presence of topological interfaces at the boundary between the two subregions. The latter objects are discussed in section 1.10.2 in some more detail and generality, where rational theories are of particular interest but we will also consider toroidal compactifications of free bosons. We will consider the case where the interface also respects a higher symmetry. We will show that this sub-leading contribution to the entanglement entropy is given by the negative of a relative entropy, and solely depends on the data of the interface. It has a solid physical meaning, which is why we interpret it as a universal contribution to the entanglement entropy. Originally the upcoming ideas and results were published in [26].

In the limit of a large IR cutoff L , or equivalently $\delta \ll 1$, the entanglement entropy through a topological interface \mathcal{I} follows straight forward from the torus partition function (3.2). The torus partition function includes K insertions of \mathcal{I} and of its adjoint \mathcal{I}^\dagger , which both commute with the Virasoro algebras and therefore in particular intertwine the Hamiltonian $H \propto L_0 + \tilde{L}_0$. Hence we can write

$$Z(K) = \text{Tr} (\mathcal{I} e^{-\delta H} \mathcal{I}^\dagger e^{-\delta H})^K = \text{Tr} ((\mathcal{I} \mathcal{I}^\dagger)^K e^{-2\delta H K}) . \quad (3.5)$$

For the general topological interface (1.44)

$$\mathcal{I}_A = \sum_{\mathbf{i}} d_{A\mathbf{i}} \|\mathbf{i}\| , \quad (3.6)$$

this reduces to

$$Z(K) = \sum_{(i, \bar{i})} \text{Tr} (d_{A\mathbf{i}} d_{A^*\mathbf{i}})^K \chi_i (e^{-2\delta K}) \chi_{\bar{i}} (e^{-2\delta K}) , \quad (3.7)$$

where $\chi_i(q)$ is the character of the representation i . In (3.7) and in the remainder of this section, Tr denotes the trace over multiplicity indices. Applying a modular S transformation we obtain

$$Z(K) = \sum_{(i, \bar{i})} \sum_{j, \bar{j}} \text{Tr} (d_{A\mathbf{i}} d_{A^*\mathbf{i}})^K S_{ij} S_{\bar{j}\bar{i}} \chi_j \left(e^{-\frac{2\pi^2}{\delta K}} \right) \chi_{\bar{j}} \left(e^{-\frac{2\pi^2}{\delta K}} \right) . \quad (3.8)$$

In the limit $\delta \ll 1$ only the vacuum with the energy $E_0 = -\frac{c}{12}$ contributes to the sum. The contribution of every other state in the theory is exponentially suppressed. The partition

Chapter 3 Entanglement Entropy through Interfaces

function is therefore approximately given by

$$Z(K) \approx \underbrace{\sum_{(i, \bar{i})} \text{Tr} (d_{A^*i} d_{Ai})^K S_{i0} S_{\bar{i}0}}_{\equiv A(K)} e^{\frac{\pi^2 c}{6\delta K}}. \quad (3.9)$$

The factor $A(K)$ contains the information about the topological interface. With this the entanglement entropy can be computed to be

$$\begin{aligned} E &= (1 - \partial_K) \log Z(K) \Big|_{K \rightarrow 1} \\ &\approx (1 - \partial_K) \left(\frac{\pi^2 c}{6\delta K} + \log A(K) \right) \Big|_{K \rightarrow 1} \\ &= \frac{c}{6} \log \frac{L}{\epsilon} + \left[\log A(1) - \frac{A'(1)}{A(1)} \right]. \end{aligned} \quad (3.10)$$

In the last line we have used (3.3), and a prime denotes the derivative with respect to K . Note that time in the channel described in (3.8) runs parallel to the interface. Using (1.49) we find that

$$A(1) = \mathcal{N}_{\mathbf{0}A}^A \quad (3.11)$$

is a non-negative integer. It is the multiplicity of the vacuum representation in the twisted torus partition function in quantization along the interface and its conjugate. In case of an elementary interface we have $A(1) = 1$. The derivative of $A(K)$ is given by

$$A'(1) = \sum_{(i, \bar{i})} S_{i0} S_{\bar{i}0} \text{Tr} (d_{A^*i} d_{Ai}) \log (d_{A^*i} d_{Ai}).$$

Inserting this in (3.10), the entanglement entropy becomes

$$E = \frac{c}{6} \log \frac{L}{\epsilon} + \left[\log \mathcal{N}_{\mathbf{0}A}^A - \frac{1}{\mathcal{N}_{\mathbf{0}A}^A} \sum_{(i, \bar{i})} S_{i0} S_{\bar{i}0} \text{Tr} (d_{A^*i} d_{Ai}) \log (d_{A^*i} d_{Ai}) \right]. \quad (3.12)$$

In CFT1 we now define

$$p_{(i\bar{i}, \alpha\alpha')}^A = \frac{d_{A^*i} d_{Ai} S_{i0} S_{\bar{i}0}}{\mathcal{N}_{\mathbf{0}A}^A}, \quad (3.13)$$

where the multiplicity labels α and α' both run from 1 to $M_{i\bar{i}}^1$. For every pair (i, \bar{i}) , the

3.1 Entanglement entropy through topological interfaces

matrix $p_{\mathbf{i}}^A \equiv p_{(i\bar{i}, \alpha\alpha')}^A$ is a positive-semidefinite Hermitian matrix², *i.e.* the eigenvalues of the $p_{\mathbf{i}}^A$ are real and positive. Moreover, by using (1.49) one gets

$$\sum_{(i, \bar{i})} \text{Tr} p_{\mathbf{i}}^A = 1. \quad (3.14)$$

The above conditions show that the set of these eigenvalues form a probability distribution. In quantization orthogonal to the interface, the value of $\text{Tr} p_{\mathbf{i}}^A$ is the probability of finding the system CFT1 in the Ishibashi-type state associated to the sector (i, \bar{i}) , after tracing out CFT2.³ Such a state is thermal within its sector, and the set of $p_{\mathbf{i}}^A$ should therefore be understood as defining a reduced density matrix. Note that the distribution corresponding to the identity defect in CFT1 is given by

$$p_{\mathbf{i}}^{id} = S_{i0} S_{\bar{i}0} \delta_{\alpha\alpha'} \quad (\alpha, \alpha' = 1, 2, \dots, M_{i\bar{i}}^1). \quad (3.15)$$

The entanglement entropy through a topological interface in unitary rational theories can now be written as

$$E = \frac{c}{6} \log \frac{L}{\epsilon} - \sum_{(i, \bar{i})} \text{Tr} p_{\mathbf{i}}^A \log \frac{p_{\mathbf{i}}^A}{p_{\mathbf{i}}^{id}}. \quad (3.16)$$

This is our first main result. The quantity

$$s(\mathcal{I}_A) := - \sum_{(i, \bar{i})} \text{Tr} p_{\mathbf{i}}^A \log \frac{p_{\mathbf{i}}^A}{p_{\mathbf{i}}^{id}} \quad (3.17)$$

is the negative of the relative entropy – the Kullback-Leibler divergence [112] – of the probability distribution associated to \mathcal{I}_A on the CFT1 side, measured with respect to the probability distribution associated to the identity \mathcal{I}_{id} of CFT1. One interpretation of this quantity is the amount of information that is lost when the probability distribution is wrongly assumed to be given by \mathcal{I}_{id} , while it is really given by \mathcal{I}_A .

Relative entropies are always non-negative, and vanish only if the compared probability distributions agree.⁴ Therefore we have $s(\mathcal{I}_A) \leq 0$, which corresponds to the intuition that an interface cannot enhance entanglement beyond the one of the identity defect in CFT1. We get $s(\mathcal{I}_A) = 0$ if and only if $p^A = p^{id}$. This is the case when $d_{A^*i} d_{Ai}$ is the identity matrix for all pairs of representations (i, \bar{i}) which appear in CFT1. A necessary condition

²Recall that in unitary theories $S_{i0} > 0$

³For an interpretation along these lines in terms of a three-dimensional topological field theory see [111].

⁴Continuous distributions have to agree almost everywhere.

Chapter 3 Entanglement Entropy through Interfaces

for the existence of an interface with this property is that the representation multiplicities of CFT2 must not be smaller than those of CFT1. Because both CFTs are unitary and have a single vacuum state, modular invariance in fact forces CFT1 and CFT2 to have identical spectra. Since the necessary condition $d_{A^*i}d_{Ai} = 1$ then means that the fusion product of the defect and its conjugate is the identity, we get

$$\exists \mathcal{I} : s(\mathcal{I}) = 0 \quad \Leftrightarrow \quad Z_{\text{CFT1}} = Z_{\text{CFT2}} \quad \text{and} \quad \mathcal{I}^\dagger \mathcal{I} = \mathcal{D}_{id} \quad \text{in CFT1.} \quad (3.18)$$

For general CFT1 and CFT2 we can give an upper bound for s , based on the restricted data we have been employing so far. Every interface \mathcal{I} between CFT1 and CFT2 can be associated with a set of diagonal matrices p_i . Each of these matrices p_i has at most $T_{i\bar{i}} = \min(M_{i\bar{i}}^1, M_{i\bar{i}}^2)$ eigenvalues different from 0. We seek for the maximal value of s under the linear constraint (3.14). This is only one constraint out of the set (1.49), such that this calculation will obviously lead to an upper bound. A maximal value of s would be achieved for the distribution

$$p_i = \text{diag}(p_{(i\bar{i},1)}, \dots, p_{(i\bar{i},T_{i\bar{i}})}, 0, \dots, 0) \quad \text{with} \quad p_{(i\bar{i},\alpha)} = \frac{S_{i0}S_{\bar{i}0}}{\sum_{(j,\bar{j})} T_{j\bar{j}} S_{j0} S_{\bar{j}0}}, \quad (3.19)$$

which yields the upper bound

$$s \leq \log \left(\sum_{(i,\bar{i})} T_{i\bar{i}} S_{i0} S_{\bar{i}0} \right). \quad (3.20)$$

The bound is strictly smaller than zero if there is at least one (i, \bar{i}) with $T_{i\bar{i}} < M_{i\bar{i}}^1$. As we have seen above, this is equivalent to having at least one pair (i, \bar{i}) where $M_{i\bar{i}}^1 \neq M_{i\bar{i}}^2$. The bound (3.20) is zero if and only if the theories CFT1 and CFT2 have the same spectrum. In cases where the CFTs on the two sides are identical, the distribution (3.19) is in particular obtained from the identity defect.

We want to point out that different interfaces can lead to the same distribution (3.13), and, thus, can give the same entanglement entropy. In particular, the fusion of any interface with a symmetry defect of the respective theory will leave the distribution unaltered. The reference distribution p^{id} of (3.15) is therefore also obtained from any symmetry defect in CFT1. On the other hand, every defect whose fusion product with a particular topological interface leaves the probability distribution of the interface unaltered must be a symmetry defect.

3.1 Entanglement entropy through topological interfaces

The distributions do not change if we superpose the same interface multiple times, too. From the interpretation of the probability distribution mentioned above this is straight forward. In agreement to our remark in section 3, an interface \mathcal{I} formally has the same probability distribution as $M\mathcal{I}$ for any rescaling $M \in \mathbb{C}^*$, and therefore in particular for superpositions of the same interface. However, the change in the entanglement entropy is in general difficult to compute for arbitrary superposition and fusion, because it is in general difficult to see how closely the probability distribution of the resulting interface follows p_i^{id} .

Let us consider the defects (1.51) with $d_{ai} = S_{ai}/S_{0i}$ in a rational theory with diagonal modular invariant as a more concrete example. By (3.13), the probability distribution of an interfaces (1.51) in a diagonal RCFT is simply

$$p_i^a = |S_{ia}|^2. \quad (3.21)$$

Our result (3.16) therefore is

$$E = \frac{c}{6} \log \frac{L}{\epsilon} - \sum_i |S_{ia}|^2 \log \left| \frac{S_{ia}}{S_{i0}} \right|^2. \quad (3.22)$$

Example 1, duality interfaces: As a class of examples let us consider the duality interfaces (1.55). Here $\mathcal{I}\mathcal{I}^\dagger$ projects the theory onto a sector invariant under a symmetry group G . Invariant states get dressed with a constant prefactor of $|G|$, the order of the group. On the level of equation (3.5) this is

$$Z(K) = \text{Tr} \left((\mathcal{I}\mathcal{I}^\dagger)^K e^{-2\delta HK} \right) = \text{Tr} \left((\oplus_{g \in G} \mathcal{D}_g)^K e^{-2\delta HK} \right) = |G|^K \text{Tr}_{inv} \left(e^{-2\delta HK} \right), \quad (3.23)$$

where in the last line the trace is taken only over the invariant subsector of the initial Hilbert space. This partition function is a projection of the initial partition function. This is in agreement with the fact that in orbifold theories correlators of invariant fields are obtained by projection from the initial theory. The prefactor $|G|^K$ drops out in the calculation of the entanglement entropy, so that effectively we consider entanglement in the projected system. However, in comparison to the system with only the trivial defect inserted, the projection contains a factor of $|G|^{-1}$. This leads to a shift in the entanglement entropy for duality interfaces. The entanglement entropy in the presence of such a duality

interface is therefore

$$E = \frac{c}{6} \log \frac{L}{\epsilon} - \log |G|. \quad (3.24)$$

In terms of the probability distributions introduced earlier, we find for the duality defects

$$p_{\mathbf{i}}^{duality} = p_{\mathbf{i}}^{id} |G| \text{ for } \mathbf{i} \text{ invariant, } p_{\mathbf{i}}^{duality} = 0 \text{ otherwise.} \quad (3.25)$$

The shift in the entanglement entropy encodes the information loss under a projection on the G -invariant subspace.

Example 2, Ising model: The critical Ising model, that will be discussed in more detail in section 3.2, is described by three primaries id , ϵ , σ . It is the simplest non-trivial example of a diagonal rational theory. The S matrix of the Ising model is given by

$$(S_{ij}) = \frac{1}{2} \begin{pmatrix} 1 & 1 & \sqrt{2} \\ 1 & 1 & -\sqrt{2} \\ \sqrt{2} & -\sqrt{2} & 0 \end{pmatrix}, \quad \text{with } i, j \in \{id, \epsilon, \sigma\}. \quad (3.26)$$

The three elementary topological defects of the Ising model are therefore

$$\begin{aligned} \mathcal{D}_{id} &= \|id\| + \|\epsilon\| + \|\sigma\|, \\ \mathcal{D}_{\epsilon} &= \|id\| + \|\epsilon\| - \|\sigma\|, \\ \mathcal{D}_{\sigma} &= \sqrt{2}\|id\| - \sqrt{2}\|\epsilon\|. \end{aligned}$$

The defect corresponding to the vacuum id is the identity defect. The defect \mathcal{D}_{ϵ} is a symmetry defect implementing the \mathbb{Z}_2 symmetry of the Ising model. The presence of these two defects does not result in a shift of the entanglement entropy. The third defect \mathcal{D}_{σ} implements Kramers-Wannier duality. It satisfies the fusion rules

$$\mathcal{D}_{\sigma} \mathcal{D}_{\sigma} = \mathcal{D}_{id} + \mathcal{D}_{\epsilon}. \quad (3.27)$$

From our formula (3.22) we deduce that the entanglement entropy of \mathcal{D}_{σ} is

$$E(\sigma) = \frac{c}{6} \log \frac{L}{\epsilon} - \log 2, \quad (3.28)$$

which also agrees with the result (3.24) for duality interfaces where the order of the group is 2. The result also reproduces the constant shift in the entanglement entropy observed

3.1 Entanglement entropy through topological interfaces

in [29], and in section 3.2.

Example 3, $su(2)_k$ interfaces and the large k limit: The diagonal WZW model based on the chiral algebra $su(2)$ at level k has irreducible representations labelled by half-integer spins s .⁵ We use the index convention $i = 2s$, *s.t.* the integer label i runs from 0 to k . The modular S matrix elements are given by

$$S_{ij} = \sqrt{\frac{2}{k+2}} \sin\left(\frac{\pi(i+1)(j+1)}{k+2}\right). \quad (3.29)$$

Using our result (3.22), the entanglement entropy through an elementary defect \mathcal{D}_a of the form (1.51) is given by

$$E(\mathcal{D}_a) = \frac{c}{6} \log \frac{L}{\epsilon} - \frac{2}{k+2} \sum_{i=0}^k \sin^2\left(\frac{\pi(a+1)(i+1)}{k+2}\right) \log \frac{\sin^2\left(\frac{\pi(a+1)(i+1)}{k+2}\right)}{\sin^2\left(\frac{\pi(i+1)}{k+2}\right)}. \quad (3.30)$$

Note that the defect \mathcal{D}_k implements the \mathbb{Z}_2 -symmetry acting on the representation labels as $a \rightarrow k - a$ and hence does not change the entanglement entropy.

At $k \rightarrow \infty$ one obtains the WZW model based on $su(2)$. The central charge is $c = 3$, and the model can be formulated in terms of three bosons on a target space S^3 at large radius with non-vanishing H -flux. The \mathbb{Z}_2 -symmetry then corresponds to the reflection symmetry of the three-sphere.

At arbitrary k , the theory contains elementary defects \mathcal{D}_a for every $a = 0, \dots, k$. For a possible geometric interpretation in a targetspace, we recall a few facts on the interpretation of symmetry preserving boundary states respective D-branes. Quite generally, symmetry preserving D-branes on group manifolds wrap conjugacy classes [113, 114], which in addition can be twisted by automorphisms. In particular, the symmetry preserving (Cardy-)states of a WZW model wrap ordinary conjugacy classes of the underlying group G (in our case $G = SU(2)$). To give an interpretation to defects, we first use the folding trick to map defects to permutation boundary conditions for the WZW model based on $G \times G$. Geometrically, the corresponding branes wrap twisted conjugacy classes where the automorphism is the permutation of the two factors, and the conjugacy class $[g_1, g_2]$ of $(g_1, g_2) \in G \times G$ takes the form [115]

$$[g_1, g_2] = \{(h_1^{-1} g_1 h_2, h_2^{-1} g_2 h_1) \mid h_1 \in G_1, h_2 \in G_2\}. \quad (3.31)$$

⁵A good overview on WZW models can for example be found in [61]

The multiplication map

$$\begin{aligned} m : G \times G &\rightarrow G \\ (g_1, g_2) &\mapsto g_1 g_2 \end{aligned}$$

maps these conjugacy classes to the conjugacy classes in the diagonal G . Indeed, the twisted conjugacy classes of $G \times G$ correspond precisely to the pre-images of the conjugacy classes of G under the multiplication map [115]. In the case of $G = SU(2)$ they take the form $S^3 \times S^2$, as the regular untwisted conjugacy classes of $SU(2)$ are generically isomorphic to S^2 . The conjugacy classes of ± 1 are special and correspond to points. This gives a geometric interpretation to the fact that the defects \mathcal{D}_a carry the same labels as Cardy boundary states. Indeed, the label a corresponds to a polar angle distinguishing the different 2-spheres $S^2 \subset S^3$ of a single $SU(2)$.

Let us first compute the entanglement entropy in the large k limit while keeping a label a fixed. In the limit $k \rightarrow \infty$, the correction $s(\mathcal{D}_a)$ to the universal bulk entanglement entropy $\propto \log L$ obtained from the defect \mathcal{D}_a can be computed by the integral

$$\begin{aligned} s(\mathcal{D}_a) &= - \lim_{k \rightarrow \infty} \frac{2}{k+2} \sum_{i=0}^k \sin^2 \left(\frac{\pi(a+1)(i+1)}{k+2} \right) \log \frac{\sin^2 \left(\frac{\pi(a+1)(i+1)}{k+2} \right)}{\sin^2 \left(\frac{\pi(i+1)}{k+2} \right)} \\ &= -2 \int_0^1 dx \sin^2(\pi(a+1)x) \log \left(\frac{\sin^2(\pi(a+1)x)}{\sin^2(\pi x)} \right). \end{aligned} \quad (3.32)$$

In particular, we see that in the large k limit, the probability distribution of the interface is a continuous sine-square distribution

$$p_a(x) = 2 \sin^2(\pi(a+1)x), \quad x \in [0, 1]. \quad (3.33)$$

The distributions of sphere-like conjugacy classes are related to a conjugacy class corresponding to a point.

The integration can be performed by elementary methods. Let us first split the logarithmic term. The first of the two summands,

$$\int_0^1 dx \sin^2(\pi(a+1)x) \log(\sin^2(\pi(a+1)x)) = \frac{1}{\pi} \int_0^\pi dy \sin^2 y \log(\sin^2 y) = \frac{1}{2} - \log 2 \quad (3.34)$$

3.1 Entanglement entropy through topological interfaces

is independent of a ! For the second summand we use $2 \sin^2 x = 1 - \cos(2x)$ and obtain

$$\begin{aligned} - \int_0^1 dx \sin^2(\pi(a+1)x) \log(\sin^2(\pi x)) &= \\ &= -\frac{1}{2\pi} \int_0^\pi dy \log(\sin^2 y) + \frac{1}{2\pi} \int_0^\pi dy \cos(2(a+1)y) \log(\sin^2 y). \end{aligned} \quad (3.35)$$

The first integral on the right-hand side of (3.35) is $-\int_0^\pi dy \log \sin^2 y = 2\pi \log 2$. For the second integral we use partial integration to obtain

$$\begin{aligned} \int_0^\pi dy \cos(2(a+1)y) \log(\sin^2 y) &= \\ &= -\frac{1}{a+1} \int_0^\pi dy \sin(2(a+1)y) \cot(y) = -\frac{\pi}{a+1}. \end{aligned} \quad (3.36)$$

Finally, combining (3.34) and (3.36), (3.32) becomes

$$s(\mathcal{D}_a) = -\frac{a}{a+1}, \quad a \ll k. \quad (3.37)$$

In particular, the contribution to the entanglement entropy from such an elementary defect \mathcal{D}_a is given by a rational number!

However, there is a second class of defects, for which the approximations made in the calculation leading to the result (3.37) do not hold. This is in particular the case if we pick a such that $a+1$ divides $k+2$ and take the limit keeping the ratio $(a+1)/(k+2)$ fixed, which in particular means that a itself is no longer fixed. Let us for example consider the case $a = k/2$ (k even), geometrically corresponding to the equatorial two-sphere, which is the fixed point under the involution $a \rightarrow k - a$. In this case the probabilities p_i^a vanish for i odd, and take the value $2/(k+2)$ for i even. Using similar methods as above, the entanglement entropy in the limit of large k becomes

$$s(\mathcal{D}_{\frac{k}{2}}) = -\log 4 \quad (k \rightarrow \infty). \quad (3.38)$$

Since $\log 4 > 1$, we see that $-s(\mathcal{D}_{\frac{k}{2}})$ differs substantially from the value (3.37). In fact, plotting of $-s(\mathcal{D}_a)$ at finite even k one observes a peak in the entanglement at $a = k/2$. Similar, less pronounced peaks are obtained at other values where $a+1$ divides $k+2$.

For generic defects, $a+1$ does not divide $k+2$, but of course $(a+1)/(k+2)$ is still a rational number that we denote l/n , where l, n are coprime. It is natural to ask what

happens if instead of a (as in the computation leading to (3.37)) we keep l/n fixed when taking the large k limit. In this case we find from (3.30) the expression

$$s(\mathcal{D}_{\frac{l(k+2)}{n}-1}) = -\log(2n) - H(n) \quad (k \rightarrow \infty), \quad (3.39)$$

where $H(n)$ is the entropy of a probability distribution given by $p_m = \frac{2}{n} \sin^2(\frac{\pi m}{n})$ for $m = 1, 2, \dots, n$,

$$H(n) = \sum_{m=1}^n \frac{2}{n} \sin^2(\frac{\pi m}{n}) \log\left(\frac{2}{n} \sin^2(\frac{\pi m}{n})\right). \quad (3.40)$$

Note that the values of s in (3.39) are multiply degenerate, as the right-hand side does not depend on l . The entropies (3.39) are bounded from below by $s(D_{\frac{k}{2}})$, showing again that the defect corresponding to the equatorial two-sphere gives the minimal entanglement entropy. On the other hand, for $n \gg l$ they quickly approach the value -1 from below, such that this asymptotic expression in fact comes rather close to the approximation (3.37).

We will not go further into details, and instead plot the correction to the entanglement entropy $-s(\mathcal{D}_a)$ at a finite value of k together with the approximation (3.37) in figure 3.2. The plot illustrates that the values of $s(\mathcal{D}_a)$ approach the asymptotic values (3.37) rather well for generic values of a . It also illustrates the peaks of the values at the special points where (3.39) deviates strongly from (3.37).

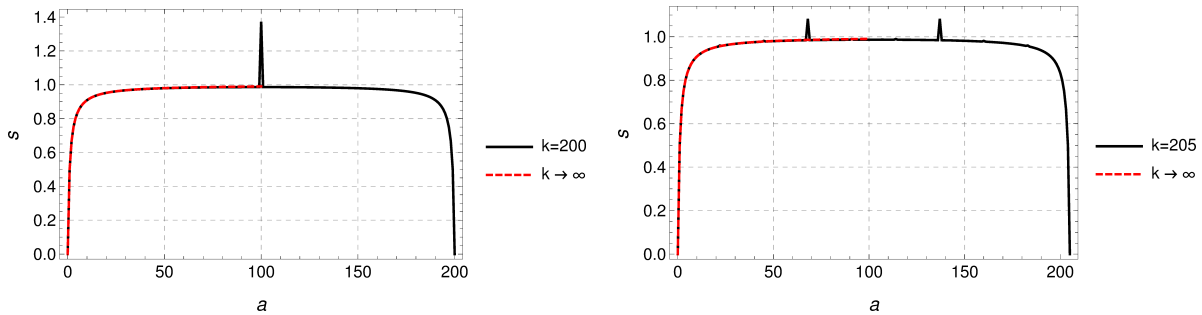


Figure 3.2: Plots of $-s(\mathcal{D}_a)$ for large values of k , together with the asymptotic values (3.37). The peaks in the plots are captured by the asymptotic expression (3.39).

A nice pattern also arises when we consider the fusion product of elementary defects at fixed labels a and b in the limit of large k . For finite k , the fusion $\mathcal{D}_{a \times b} = \mathcal{D}_a \mathcal{D}_b$ can be decomposed as

$$\mathcal{D}_{a \times b} = \sum_c N_{ab}^c \mathcal{D}_c \quad (3.41)$$

3.1 Entanglement entropy through topological interfaces

in terms of elementary defects, where N_{ab}^c are the fusion coefficients of $su(2)_k$, which are

$$N_{ab}^c = \begin{cases} 1 & |a-b| \leq c \leq \min\{a+b, 2k-a-b\} \\ 0 & \text{else} \end{cases}. \quad (3.42)$$

Using the fact that for large k the number of vacua on the defects contained in the fusion product is

$$\mathcal{N}_{0_{a \times b}}^{a \times b} = \min(a, b) + 1, \quad (3.43)$$

the probability distribution for $\mathcal{D}_{a \times b}$ is given by

$$p_i^{a \times b} = \frac{2}{\min(a, b) + 1} \frac{\sin^2\left(\frac{\pi(a+1)(i+1)}{k+2}\right) \sin^2\left(\frac{\pi(b+1)(i+1)}{k+2}\right)}{(k+2) \sin^2\left(\frac{\pi(i+1)}{k+2}\right)}. \quad (3.44)$$

The final expression for $s(\mathcal{D}_{a \times b})$ for large k can be reduced to a rather simple form, by splitting off the part involving the logarithm of the factor $\min(a, b) + 1$ in (3.44). As explained in appendix B.1, where we only use elementary methods one can show that in all cases

$$s(\mathcal{D}_{a \times b}) = -\frac{p}{q} + \log(\min(a, b) + 1), \quad (3.45)$$

where p and q are natural numbers that depend on the labels a and b . We want to emphasize that the argument in the logarithm is the number of elementary defects in the decomposition of the fusion product. However, the fact that this logarithm directly reflects the number of elementary defects in the decomposition is true only if each of these elementary defects appears with multiplicity 1.

3.1.1 Left/Right entanglement entropy

In this section let us consider a system with a boundary. As mentioned earlier, the entanglement entropy of an interval that ends on a boundary receives a correction by the boundary entropy $s = \log g$, where g is the universal non-integer ground-state degeneracy as shown in [84]. The entanglement entropy we are here interested in is the left/right entanglement entropy (LREE) considered before in [109] for the free boson and in [116, 28] for generic CFTs. The two subsystems consist of the left- and right-moving (respective chiral and anti-chiral) part of the Hilbert space.

As discussed in section 1.9, a conformal boundary can be written as

$$|\mathcal{B}\rangle = \sum_{\mathbf{i}} b_{B\mathbf{i}} |\mathbf{i}\rangle, \quad (3.46)$$

where $|\mathbf{i}\rangle$ are the Ishibashi states, and the coefficients $b_{B\mathbf{i}}$ are constrained by Cardy's condition. We here choose the more precise description with $\mathbf{i} = (i, \alpha, \beta)$ and include the multiplicity labels α and β that distinguish the different copies of the representation i appearing in the chiral and anti-chiral part of the space of states, respectively.

In section 1.9, we also discuss that rather than looking at the full non-chiral theory on a half-plane with a boundary one can equivalently consider a chiral theory on the full plane. One “unfolds” the theory and the boundary becomes a topological interface. We want to make this more precise, now. The resulting defect must be topological because the boundary condition $T = \bar{T}$ for the energy-momentum tensor becomes simply a continuity condition along the defect. Unfolding the Ishibashi states leads to an interface-like operators $\|\mathbf{i}\|$ that project onto a representations \mathbf{i} that appear in the both the chiral and anti-chiral part of the conformal field theory. We therefore associate to the boundary state (3.46) an interface operator

$$\mathcal{I}_B = \sum_{\mathbf{i}} b_{B\mathbf{i}} \|\mathbf{i}\|, \quad (3.47)$$

in the unfolded chiral theory that maps states from the anti-chiral part of the theory folded onto the lower half plane into states of the chiral part in the upper half plane.

The computation of the entanglement entropy now is analogous to the one in the previous sections. The partition function on the K -sheeted Riemann surface becomes

$$Z(K) = \sum_i \text{Tr} (b_{B^*i} b_{Bi})^K \text{Tr}_{\mathcal{H}_i} (e^{-2\delta H}) = \sum_i \text{Tr} (b_{B^*i} b_{Bi})^K \chi_i (e^{-2\delta K}) \quad (3.48)$$

which after the modular S transformation is given by

$$Z(K) = \sum_i \text{Tr} (b_{B^*i} b_{Bi})^K S_{ij} \chi_j \left(e^{-\frac{2\pi^2}{\delta K}} \right) \approx \sum_i \text{Tr} (b_{B^*i} b_{Bi})^K S_{i0} e^{\frac{2\pi^2 c}{\delta K^2}}. \quad (3.49)$$

For the general boundary state with vacuum multiplicity \mathcal{N}_{0B}^B in parallel quantization we can again write the entanglement entropy in terms of a probability distribution. The

3.1 Entanglement entropy through topological interfaces

distribution is defined by the traces of the matrices

$$p_{\mathbf{i}}^B = \frac{b_{B^* \mathbf{i}} b_{B \mathbf{i}} S_{i0}}{\mathcal{N}_{0B}^B}. \quad (3.50)$$

In (3.50) the index notation is simplified in the same way as in the previous chapters — while the indices \mathbf{i} on the right-hand side contain one multiplicity label for chiral and one for anti-chiral representations, and we again suppress summations over interior labels, the index \mathbf{i} on the left-hand side includes two multiplicity labels of the same kind. The LREE at a system with boundary condition B then reads

$$E = \frac{c}{12} \log \frac{L}{\epsilon} - \sum_i \text{Tr} p_{\mathbf{i}}^B \log \frac{p_{\mathbf{i}}^B}{S_{i0}}. \quad (3.51)$$

Note that the prefactor of the leading order term is half of the prefactor in the case of a full theory with a topological interface. This matches the expectation from the area law as mentioned in [16].

A natural question is whether it is again possible to interpret the result in terms of a relative divergence. For interfaces there is a generic “neutral” interface (the identity defect) with respect to which one can compute the relative entropy. This is no longer the case for boundaries, because there is no “neutral” boundary on the full plane that could serve as a reference point.

Technically, one can try to interpret the denominator in the logarithm of (3.51) as a distribution corresponding to the entries S_{i0} times appropriate identity matrices. However, the sum over the traces of these matrices is in general not equal to 1, and therefore not a probability distribution. In the cases where it is, we indeed obtain the relative entropy with respect to a permutation boundary state, where each $b_{\mathbf{i}}$ is a permutation matrix. However, in general we conclude that the interpretation as a relative entropy fails in the case of the left/right entanglement entropy at boundary states.

A consequence of losing the interpretation of the LREE as a relative entropy is that the sub-leading contribution

$$s = - \sum_i \text{Tr} p_{\mathbf{i}}^B \log \frac{p_{\mathbf{i}}^B}{S_{i0}} \quad (3.52)$$

is not necessarily negative any more. Following the same logic as in the case of interfaces

in full non-chiral theories, we can give an upper bound

$$s \leq \log \left(\sum_i S_{i0} \right). \quad (3.53)$$

This bound however is not necessarily negative, and actually s sometimes will become positive.

As an example consider boundary states in diagonal rational theories. Elementary boundary states which preserve the rational symmetry can be labeled by irreducible representations b of the symmetry algebra. The coefficients of the elementary boundary states in this case are

$$b_{bi} = \frac{S_{bi}}{\sqrt{S_{i0}}}. \quad (3.54)$$

Using (3.50) and (3.52) we can compute the left/right entanglement entropy to be

$$E = \frac{c}{12} \log \frac{L}{\epsilon} - \sum_i |S_{bi}|^2 \log \frac{|S_{bi}|^2}{S_{i0}}. \quad (3.55)$$

This reproduces the result obtained previously in [28]. The LREE of the Cardy brane labeled by the identity gives a shift

$$s = - \sum_i S_{0i}^2 \log S_{0i}, \quad (3.56)$$

which is always positive. It is an even stricter upper bound than (3.53), too.

Example, Ising model: The left/right entanglement entropy for boundary states of the Ising model has been investigated in [28]. We quote the results here for illustration. The Cardy states in the Ising model are explicitly given in terms of Ishibashi states by

$$\begin{aligned} |id\rangle &= \frac{1}{\sqrt{2}} (|id\rangle\rangle + |\epsilon\rangle\rangle + 2^{\frac{1}{4}} |\sigma\rangle\rangle), \\ |\epsilon\rangle &= \frac{1}{\sqrt{2}} (|id\rangle\rangle + |\epsilon\rangle\rangle - 2^{\frac{1}{4}} |\sigma\rangle\rangle), \\ |\sigma\rangle &= |id\rangle\rangle - |\epsilon\rangle\rangle. \end{aligned} \quad (3.57)$$

3.1 Entanglement entropy through topological interfaces

The sub-leading contributions to the LREE we can compute from (3.52) are

$$s = \frac{3 \log 2}{4} \text{ for } |id\rangle, |\epsilon\rangle, \quad \text{and} \quad s = 0 \text{ for } |\sigma\rangle. \quad (3.58)$$

Example, $su(2)_k$ boundary states and the $k \rightarrow \infty$ limit: Analogously to the example of $su(2)_k$ defects in the previous section we consider the LREE of boundary states in the WZW models $su(2)_k$ in the limit of large k . For finite k , the theory is diagonal and rational, and the formula (3.55) applies which has been computed in [28] too. The Cardy states (3.54) are labeled by spin eigenvalues $s = b/2$ for $b = 0, 1, \dots, k$. The universal sub-leading contribution to the LREE by the state B_b at finite k is

$$s(b) = - \sum_{i=0}^k \frac{2}{k+2} \sin^2(\pi(b+1)\frac{i+1}{k+2}) \log \frac{\sin^2(\pi(b+1)\frac{i+1}{k+2})}{\sin(\pi\frac{i+1}{k+2})} + \log \sqrt{\frac{2}{k+2}}. \quad (3.59)$$

We have split off a term depending only on k from the argument of the logarithm, and used that $\sum_i p_i^b = 1$. The shift term proportional to $-\log(k+2)$ in (3.59) can be identified with (the logarithm of) the radius of the target space. The target space of the $su(2)_k$ WZW model is the (fuzzy) sphere S^3 at radius $R = \sqrt{k}$. As in the defect case, the sum in (3.59) can be computed as an integral in the large k limit. Solving this integral with the same methods as used in the previous section we obtain

$$s(b) = -\frac{2b+1}{2b+2} + \frac{1}{2} \log 2 + \log R \quad , \text{ for large } k. \quad (3.60)$$

The positive (and infinite) contribution from the radius is similar to the radius contribution to the LREE of Dirichlet branes of the compactified boson [109], that we will also compute in (3.93).

Example, fusion of a defect with a boundary in the $su(2)_k$ WZW model: As an extension to the latter result we consider the fusion of an elementary defect operator \mathcal{D}_a with a Cardy boundary state $|b\rangle$. This yields a new boundary state $|B\rangle = \mathcal{D}_a|b\rangle$. From (1.51) and (3.54) we see that the coefficients of $|B\rangle$ are given by

$$b_{Bi} = \frac{S_{ai}S_{bi}}{S_{0i}^{3/2}}. \quad (3.61)$$

In quantization parallel to the boundary the number of vacua in the self-spectrum of $|B\rangle$ is

$$\mathcal{N}_{0B}^B = \sum |b_{Bi}|^2 S_{0i} = \min(a, b) + 1, \quad (3.62)$$

as in the case of the fusion products of two elementary defects in example 3 in the last section. The sub-leading contribution to the left/right entanglement entropy can be written as

$$s(a \times b) = \log(\min(a, b) + 1) - \frac{\sum_i |b_{Bi}|^2 S_{0i} \log |b_{Bi}|^2}{\min(a, b) + 1}. \quad (3.63)$$

The quantity $\min(a, b) + 1$ is also the number of elementary branes in the decomposition

$$|B\rangle = \sum_c N_{ab}^c |c\rangle \quad (3.64)$$

of the fusion product.

In the large k limit of the $su(2)_k$ WZW model, the LREE of the fusion product differs from the entropy of the original boundary state $|b\rangle$ by a rational term and the logarithm of the number of elementary branes in the decomposition. Indeed, in this limit the numerator in the second term of the right-hand side of (3.63) becomes

$$\begin{aligned} & \sum_i |b_{Bi}|^2 S_{0i} \log |b_{Bi}|^2 \xrightarrow{k \rightarrow \infty} \\ & - \log \sqrt{\frac{2}{k+2}} + \frac{2}{\pi} \int_0^\pi \frac{\sin^2((a+1)x) \sin^2((b+1)x)}{\sin^2(x)} \log \left(\frac{\sin^2((a+1)x) \sin^2((b+1)x)}{\sin^3(x)} \right) dx. \end{aligned} \quad (3.65)$$

A similar calculation as before leads to

$$s(a \times b) = \log(\min(a, b) + 1) + \frac{1}{2} \log 2 + \log R - \frac{p}{q}, \quad k \rightarrow \infty, \quad (3.66)$$

for some $p, q \in \mathbb{N}$. The difference between the LREE of the boundary state after fusion (3.66) and the original boundary state (3.60) for large k is therefore

$$s(a \times b) - s(b) = \log(\min(a, b) + 1) - \frac{p}{q} + \frac{2b+1}{2b+2}. \quad (3.67)$$

3.1.2 Results for bosonic tori

The following also originates from [26].

Entanglement entropy through topological defects: The interface operators of d free bosons compactified on a torus are explicitly known [117]. We here shortly review the result and will compute the entanglement entropy through these interfaces.

The ground states of the theory form an even, self dual lattice $\Gamma \subset \mathbb{R}^{d,d}$. The lattice vectors are of the form $\gamma = (p, \bar{p})$, where the d -dimensional vectors p and \bar{p} denote left- and right-moving momenta. We will consider topological interfaces that preserve the full $u(1)^d$ symmetry of the torodial compactified bosons. They are specified by a gluing matrix $\Lambda \in O(d|\mathbb{R}) \times O(d|\mathbb{R})$. Similarly to the rational case discussed earlier, the interface operators can be written as linear combinations of operators between $u(1)^d$ highest weight representations:

$$\mathcal{I}_{12}(\Lambda) = \sum_{\gamma \in \Gamma_{12}^\Lambda} d_{\Lambda\gamma} ||\gamma||. \quad (3.68)$$

As before, $||\gamma||$ is an intertwiner of the representation space specified by the lattice vector $\gamma \in \Gamma$. The prefactors $d_{\Lambda\gamma}$ are constrained by Cardy's condition. The summation is restricted to a sublattice that is specified by a gluing condition Λ for the lattices Γ_1 and Γ_2 on the two sides of the interface,

$$\Gamma_{12}^\Lambda = \{\gamma \in \Gamma_1 \mid \Lambda\gamma \in \Gamma_2\} = \Gamma_1 \cap \Lambda^{-1}\Gamma_2 \subset \Gamma_1. \quad (3.69)$$

The gluing conditions Λ should lead to a sublattice Γ_{12}^Λ of full rank. Cardy's condition then demands that $d_{\Lambda\gamma} = g_{12}^\Lambda \exp(2\pi i\varphi(\gamma))$, where $\varphi \in (\Gamma_{12}^\Lambda)^\star$ and

$$(g_{12}^\Lambda)^2 = |\Gamma_1/\Gamma_{12}^\Lambda| \quad (3.70)$$

is the index of the sublattice Γ_{12}^Λ inside the lattice Γ_1 , which can *e.g.* be defined as the quotient of the volumina of the fundamental domain of the two lattices. The topological interface operator now splits into a lattice and an oscillator part and can be written as

$$\mathcal{I}_{12} = \mathcal{I}_{12}^0(\Lambda) \prod_{n>0} \mathcal{I}_{12}^n(\Lambda), \quad (3.71)$$

where

$$\mathcal{I}_{12}^0 = g_{12}^\Lambda \sum_{\gamma \in \Gamma_{12}^\Lambda} e^{2\pi i\varphi(\gamma)} |\Lambda\gamma\rangle \langle \gamma| \quad (3.72)$$

gives the map for the zero modes and

$$\mathcal{I}_{12}^n = \exp \left(-\frac{1}{n} (a_{-n}^2 \Lambda_{11} a_n^1 + \tilde{a}_{-n}^2 \Lambda_{22} \tilde{a}_n^1) \right) \quad (3.73)$$

for $n > 0$ gives the contribution of the higher modes. It is understood that modes of CFT1 act from the right and modes of CFT2 from the left of \mathcal{I}_{12}^0 .

In order to determine the entanglement entropy we proceed in the known way. The partition function of the K -sheeted Riemann surface for the topological defect (3.5) is

$$\begin{aligned} Z(K) &= \text{Tr} \left((\mathcal{I}\mathcal{I}^\dagger)^K e^{-2\delta KH} \right) \\ &= (g_{12}^\Lambda)^{2K} \sum_{(p,\bar{p})=\gamma \in \Gamma_{12}^\Lambda} \chi_p \left(i\frac{\delta}{\pi} K \right) \bar{\chi}_{\bar{p}} \left(i\frac{\delta}{\pi} K \right), \end{aligned} \quad (3.74)$$

where the χ_p are the $u(1)$ characters. After a modular S transformation we express $Z(K)$ in terms of characters depending on the variable $i\pi/(K\delta)$, which leads to a summation over lattice vectors in the dual lattice Γ_{12}^\vee . In the limit $\delta \ll 1$ the lattice sum is dominated by the contribution of the vacuum $p = \bar{p} = 0$,

$$\begin{aligned} Z(K) &= (g_{12}^\Lambda)^{2K} \sum_{(q,\bar{q}) \in \Gamma_{12}^\vee} a_{(q,\bar{q})} \chi_q \left(i\frac{\pi}{K\delta} \right) \bar{\chi}_{\bar{q}} \left(-i\frac{\pi}{K\delta} \right) \\ &\approx (g_{12}^\Lambda)^{2K} a_{(0,0)} e^{\frac{\pi^2 d}{6\delta K}}. \end{aligned} \quad (3.75)$$

We now use that the interfaces with the normalization (3.70) are elementary. For $K = 1$, we obtain the ordinary defect partition function, where in parallel quantization only a single vacuum should propagating. We therefore conclude that $a_{(0,0)} = 1/(g_{12}^\Lambda)^2$.

Now, using $\delta = 2\pi^2/\log(L/\epsilon)$, $c = d$ for the central charge of d bosons, and (3.70), the entanglement entropy is given by

$$E = (1 - \partial_K) \log(Z(K)) \Big|_{K=1} = \frac{c}{6} \log \frac{L}{\epsilon} - \log |\Gamma_1/\Gamma_{12}^\Lambda|. \quad (3.76)$$

In the case $d = 1$, *i.e.* for a free boson compactified on a circle, conformal interfaces between CFT1 and CFT2 are classified by two winding numbers k_1 and k_2 . For generic compactification radii these interfaces are not topological, but they become so by choosing radii to satisfy the relation $R_1/R_2 = k_2/k_1$ [118]. In this case the index of the sublattice

3.1 Entanglement entropy through topological interfaces

is [118, 117]

$$|\Gamma_1/\Gamma_{12}^\Lambda| = |k_1 k_2|, \quad (3.77)$$

and the entanglement entropy through the topological interface is given by

$$E = \frac{1}{6} \log \frac{L}{\epsilon} - \log |k_1 k_2|. \quad (3.78)$$

The entanglement entropy computed here is in agreement with the result of [30].

All the above topological interfaces are duality interfaces according to our previous definition. A subclass of them are symmetry interfaces that describe automorphisms of the toroidal CFT. They are associated to gluing matrices in the T-duality group $O(d, d, \mathbb{Z})$. In particular, for those matrices we get $\Gamma_{12}^\Lambda = \Gamma_1$, which means that the defect couples to the full momentum lattice and no ground states are projected out. In this case, there is obviously no contribution to the entanglement entropy from the interface.

The broader class of duality interfaces is specified by gluing matrices in $O(d, d, \mathbb{Q})$. These interfaces can in particular be related to orbifold constructions. In the case of a single circle, where $R_1/R_2 = k_2/k_1$ [118, 117], the theory with radius R_1 can be obtained from the theory with radius R_2 by orbifolding with respect to the shift symmetry

$$X \mapsto X + 2\pi R_1. \quad (3.79)$$

The orbifold group generated by this symmetry is $\mathbb{Z}_{|k_1 k_2|}$, and hence of order $|k_1 k_2|$. It is clear that \mathcal{IT}^\dagger projects the theory with R_2 onto the sector invariant under the orbifold group. We see that for circle theories the contribution to the sub-leading term of the entanglement entropy is set by the order of this orbifold group,

$$E = \frac{1}{6} \log \frac{L}{\epsilon} - \log |G|, \quad (3.80)$$

in agreement with the general result (3.24).

Left/Right entanglement entropy in bosonic tori: Now, we want to consider the left/right entanglement entropy at boundaries for d free bosons compactified on a torus. The boundary conditions can be written as [117, 119]

$$(a_n + O\tilde{a}_{-n})|B\rangle = 0, \quad (3.81)$$

Chapter 3 Entanglement Entropy through Interfaces

where $O \in O(d|\mathbb{R})$. The ground states solving this condition are associated to lattice vectors in

$$\Gamma^O = \left\{ \begin{pmatrix} -Ox \\ x \end{pmatrix} \cap \Gamma \mid x \in \mathbb{R}^d \right\}, \quad (3.82)$$

where Γ is the charge lattice of the torus model. The boundary state is a superposition of Ishibashi states $|p, \bar{p}\rangle\rangle$ built from the ground states $(p, \bar{p}) \in \Gamma^O$,

$$|B\rangle = g \sum_{(p, \bar{p}) \in \Gamma^O} e^{i\varphi(p, \bar{p})} |p, \bar{p}\rangle\rangle, \quad (3.83)$$

where the function $\varphi \in (\Gamma^O)^*$ specifies the D -brane moduli and the g -factor is fixed by the condition that only a single vacuum appears in parallel quantization. As in the general section on LREE, we unfold the boundary state and associate an interface between left- and right-moving degrees of freedom of the free boson theory. We therefore introduce the projections $\pi(\Gamma^O)$ and $\bar{\pi}(\Gamma^O)$ of the lattice Γ^O onto the left- and right-moving parts respectively. The interfaces therefore maps ground states as $\pi(\Gamma^O) \ni p \rightarrow -Op \in \bar{\pi}(\Gamma^O)$. The boundary entropy, *i.e.* g -factor, is given by

$$g = \text{vol}(\pi(\Gamma^O)), \quad (3.84)$$

the volume of the fundamental cell of $\pi(\Gamma^O)$.

The computation of the LREE now proceeds in analogy to the case of topological interfaces of rational theories. The partition functions on the K -sheeted surface are approximated by

$$Z(K) = g^{2K} \sum_{(p, \bar{p}) \in \Gamma^O} \chi_p(i\frac{\delta}{\pi}K) \xrightarrow{S \text{ trsf, } \delta \ll 1} g^{2K-2} e^{\frac{\pi^2}{12\delta K}}, \quad (3.85)$$

where we used again that the vacuum in parallel quantization has multiplicity 1 for $K = 1$. Using $c = d, \delta = 2\pi^2 / \log(L/\epsilon)$ we obtain the LREE

$$E = \frac{c}{12} \log \frac{L}{\epsilon} - \log \text{vol}(\pi(\Gamma^O)). \quad (3.86)$$

The subleading part of the LREE is determined by the g factor of the boundary state. To relate this quantity to the torus geometry, let us recall that Γ is a Narain lattice given by

$$\Gamma = \left\{ \begin{pmatrix} \frac{1}{2}F^{-1}N + F^T(1+B)M \\ -\frac{1}{2}F^{-1}N + F^T(1-B)M \end{pmatrix} \mid M, N \in \mathbb{Z}^d \right\}, \quad (3.87)$$

3.1 Entanglement entropy through topological interfaces

where $G = FF^T$ is the metric and B the Kalb-Ramond field on the target space torus, and N and M are the momentum and winding quantum numbers, respectively. Let us for now consider a $D1$ brane in $d = 2$ dimensions for the geometric case where B is zero. If the $D1$ brane was located in infinite flat space, we would specify the direction of the brane by specifying the momenta perpendicular to it; a localisation of the brane to its world-volume direction would then be achieved by integration over these momenta. On a torus, the momenta are part of a lattice. We can fix our brane by choosing the elementary generator of transverse momenta that couple to the brane to be given by

$$N^0 = \begin{pmatrix} N_1^0 \\ N_2^0 \end{pmatrix}, \quad (3.88)$$

with two integers N_i^0 that we assume to be relatively prime. This choice determines the winding modes our $D1$ brane can couple to. The elementary winding generator $M^0 = (M_1^0, M_2^0)$ is again specified by two coprime integers M_1^0, M_2^0 , and have to satisfy the orthogonality constraint

$$N_1^0 M_1^0 + N_2^0 M_2^0 = 0. \quad (3.89)$$

The equation is solved by $M_1^0 = -N_2^0, M_2^0 = N_1^0$. By this we have fixed a $D1$ brane for which the lattice Γ^0 is precisely spanned by the two generators N^0 and M^0 for N and M in (3.87), respectively. It can be checked explicitly that these lattice vectors solve (3.81) with

$$O = \begin{pmatrix} \cos(2\theta) & \sin(2\theta) \\ \sin(2\theta) & -\cos(2\theta) \end{pmatrix} \in O(2, \mathbb{R}), \quad (3.90)$$

where $\theta = \arctan(- (E^{-1}N^0)_1 / (E^{-1}N^0)_2)$ [118]. To compute the g -factor we now have to compute the volume of (the unit cell of) this lattice, projected to the left-movers. After some algebra one obtains

$$g^2 = \frac{1}{2 \det E} ((N_2^0)^2 G_{11} + (N_1^0)^2 G_{22} - 2G_{12} N_2^0 N_1^0). \quad (3.91)$$

Mapping N_i^0 to the winding numbers of the brane $N_1^0 = k_2, N_2^0 = -k_1$, we see that

$$g^2 = \frac{\text{length}^2}{2 \text{vol}}, \quad (3.92)$$

where *length* refers to the length of the brane and *vol* to the volume of the torus. This is in agreement with geometrical expectations. Note also, that in the special case of a

rectangular torus with diagonal metric where the radii are related by a rational number the above result agrees with the one for topological interfaces of the latter section.

The left/right entanglement entropy has been computed before for the case of a free boson in [109]. To compare the results, note that in one dimension the left-moving momenta are given by $a_0 = N/2R + MR$ and the right-moving momenta by $\bar{a}_0 = N/2R - MR$. The matrix O in the gluing condition reduces to a choice of sign. For Dirichlet branes we have $O = 1$, and only ground states without winding contribute to the boundary state. We therefore have $\Gamma^O = \{(N/2R, N/2R)\}$, and the volume of the projected unit cell is $1/2R$. Similar considerations also hold for Neumann branes. Our result (3.86) for the LREE of a single boson compactified on a circle thus gives

$$E = \frac{1}{12} \log \frac{L}{\epsilon} - \begin{cases} \log R & \text{for } O = -1 \text{ (Neumann b.c.)} \\ \log \frac{1}{2R} & \text{for } O = 1 \text{ (Dirichlet b.c.)} \end{cases} . \quad (3.93)$$

This in particular reproduces the results of [109].

3.2 Entanglement entropy through Ising interfaces

In what follows, our discussion focusses on the two-dimensional Ising model, where defects have been analysed by integrability [19, 120] and conformal field theory [20, 121] techniques. There are altogether three classes of defects preserving conformal invariance. Two of them have a simple description in terms of a square lattice model. At the position of the interface, the couplings between the spins are different than in the bulk of the lattice. In formulas, the energy-to-temperature ratio is given by

$$\frac{\mathcal{E}}{T} = - \sum_{i,j} (K_1 \sigma_{i,j} \sigma_{i+1,j} + K_2 \sigma_{i,j} \sigma_{i,j+1}) + (1-b) K_1 \sum_j \sigma_{0,j} \sigma_{1,j} \quad (3.94)$$

where $\sigma_{i,j} = \pm 1$ are the spin variables, and $\sinh(2K_1) \sinh(2K_2) = 1$ so that the bulk theory is critical. Along the (vertical) interface, couplings are rescaled by the factor b that parametrizes deformations of the interface. In the special case $b = 1$ the situation reduces to the case without any defect, on the other hand, for $b = \pm\infty$ or $b = 0$, one obtains two isolated subsystems, separated by a totally reflective defect. One furthermore distinguishes between ferromagnetic interfaces for which the parameter b takes values $b \in (0, \infty)$ and anti-ferromagnetic interfaces which are parametrized by $b \in (-\infty, 0)$.

In a spin chain interpretation, the defect sits on a particular link of the spin chain, and we consider the entanglement entropy of the subsystems located left and right of the defect link. When the system propagates in time, the defect link sweeps out a one-dimensional line in two-dimensional space-time, which is the defect line of the conformal field theory.

For the three topological defects – that is when they are fully transmissive and $b = 1$ – the result for the entanglement entropy through the defect is also given in the previous section. We expect it to vanish in the totally reflective case that corresponds to factorizing defects, and that for generic b the entanglement entropy will depend on b , as this parameter determines the “strength” of the defect.

The entanglement entropy for subsystems separated by a defect in the Ising model as well as other fermionic chains was studied before with different methods. Numerical results were presented in [122], subsequently an analytical analysis appeared in [123]. In particular, the same result for the leading order part of the entanglement entropy was derived using the spectrum of the reduced density matrix in the lattice model. The paper [123] initiated a series of following papers addressing related topics, see e.g. [124, 125, 126, 127, 128].

3.2.1 Conformal interfaces of the Ising model

Interfaces and boundary conditions

A convenient description of defects in the Ising model arises, when we employ the folding trick. Here, as illustrated in figure 3.3, an Ising model interface is mapped to a boundary condition of the tensor product of two Ising models. The latter is well known to be equivalent to a \mathbb{Z}_2 orbifold of a free boson compactified on a circle of radius $R = 1$ [20, 121].

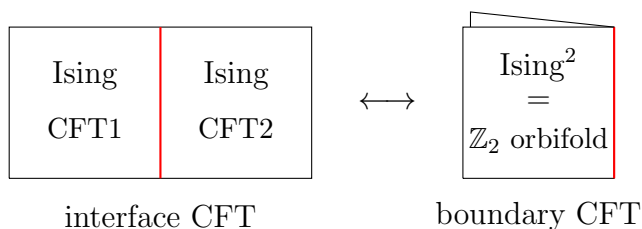


Figure 3.3: The folding trick transforms interfaces (red) of the critical Ising model to boundary conditions of the $c = 1$ \mathbb{Z}_2 -orbifold theory.

The boundary conditions of the orbifold theory come in two continuous families, [20, 121, 18]:

- Dirichlet conditions $|D, \phi\rangle\rangle$ with $\phi \in [0, \pi]$,
- Neumann conditions $|N, \tilde{\phi}\rangle\rangle$ with $\tilde{\phi} \in [0, \pi/2]$.

In string theory language, ϕ is the position of a D0-brane on the circle with a \mathbb{Z}_2 identification, whereas $\tilde{\phi}$ is the Wilson line on a D1-brane which belongs to the position of the dual D0-brane on the dual circle (of radius $\tilde{R} = 1/2$). Unfolding converts the boundary states $|\mathcal{B}\rangle\rangle$ of $(\text{Ising})^2$ to interfaces of the Ising model.

For Dirichlet interfaces one can relate ϕ and the parameter b of the interface model (3.94) as in [20, 121] by comparing the CFT spectrum with the exact diagonalization of the transfer matrix [129]:

$$\tan(\phi - \pi/4) = \frac{\sinh(K_1(1 - b))}{\sinh(K_1(1 + b))} \longleftrightarrow \cot(\phi) = \frac{\tanh(bK_1)}{\tanh(K_1)} \quad (3.95)$$

A special case is $\phi = \pi/4$ corresponding to $b = 1$ which means there is no interface. Hence the interface operator is given by the identity operator. Another special case is $\phi = 3\pi/4$ which belongs to $b = -1$. This operator belongs to the \mathbb{Z}_2 -symmetry of the Ising model.

3.2 Entanglement entropy through Ising interfaces

At the special values $\phi = 0, \pi/2$ and π , corresponding to $b = \infty, 0$ and $-\infty$, respectively, the interfaces reduce to separate boundary conditions for the two Ising models given by

$$(++) \oplus (--), \quad (ff) \quad \text{and} \quad (+-) \oplus (-+), \quad (3.96)$$

where $+, -, f$ denote the three conformal boundary conditions of the Ising model, namely spin-up, spin-down and free [130].

For Neumann interfaces, or order-disorder interfaces, the relation between $\tilde{\phi}$ and \tilde{b} is similar but with $\tilde{\phi} \in [0, \pi/2]$ and thus $\tilde{b} \geq 0$ (see e.g. in [80]). Again, for the special value $\tilde{\phi} = \pi/4$ we have $\tilde{b} = 1$. This means that this Neumann interface is topological. On the other hand, at the values $\tilde{\phi} = 0, \pi/2$ the interfaces reduces to separate boundary conditions

$$(+f) \oplus (-f) \quad \text{and} \quad (f+) \oplus (f-). \quad (3.97)$$

Since we are dealing with general conformal interfaces the reflection coefficient \mathcal{R} and the transmission coefficient \mathcal{T} that were introduced in section 1.10.5 are of importance. For the interfaces of the Ising model the reflection and transmission coefficients are given by

$$\mathcal{R} = \begin{cases} \cos^2(2\phi) & \text{Dirichlet} \\ \cos^2(2\tilde{\phi}) & \text{Neumann} \end{cases}, \quad \text{and} \quad \mathcal{T} = \begin{cases} \sin^2(2\phi) & \text{Dirichlet} \\ \sin^2(2\tilde{\phi}) & \text{Neumann} \end{cases}, \quad (3.98)$$

with $\mathcal{R} + \mathcal{T} = 1$. Note that for topological Dirichlet interfaces, where $\phi = \pi/4$ or $3\pi/4$, there is no reflection, namely $\mathcal{R} = 0$. On the other hand, for $\phi = n\pi/2$ the reflection coefficient is $\mathcal{R} = 1$, and thus the interface reduces to factorizing one. For Neumann interfaces the statements are alike.

Free fermion description

While the description in terms of the free boson provides an overview over the possible interfaces, to construct the explicit interface operator one needs to undo the folding. This is best done in the language of free fermions. Recall that the Ising model can be regarded as a system of a free real Majorana fermion, where modular invariance is achieved by a projection on even fermion number (where the fermion number is the sum of left and right fermion number). In a free fermion theory one distinguishes between the NS-sector and the R-sector. In the NS sector, the fermions $\psi, \bar{\psi}$ (denoting left and rightmovers) are half integer moded and there is a non-degenerate ground state. In the R-sector the

fermions are integer moded and the ground state degenerates. The Ising model has three primary fields with respect to the Virasoro algebra, $1, \sigma, \epsilon$ of left-right conformal dimensions $(0, 0), (1/16, 1/16), (1/2, 1/2)$. In terms of the free fermion $(0, 0)$ is the NS-vacuum, $(1/2, 1/2)$ the first excited state of the NS-sector and $(1/16, 1/16)$ a R-ground state (after the degeneracy of the ground states has been lifted by the GSO-projection).

Having an interface between two 2D free fermion conformal field theories as on the left of figure 3.3, its interface operator has the general form [117, 80]

$$I_{1,2}(\mathcal{O}) = \prod_{n>0} I_{1,2}^n(\mathcal{O}) I_{1,2}^0(\mathcal{O}) \equiv I_{1,2}^>(\mathcal{O}) I_{1,2}^0(\mathcal{O}), \quad (3.99)$$

where we have split the operator into two factors; $I_{1,2}^0(\mathcal{O})$ is a map of the ground states of the free fermion theory, whereas $I_{1,2}^>$ contains the higher oscillator modes. The latter can be factorized further; in $I_{1,2}^n$ only the $\pm n$ th modes of the fermion field appear pairwise, such that all $I_{1,2}^n$ commute. It is given by

$$I_{1,2}^n = \exp \left(-i\psi_{-n}^1 \mathcal{O}_{11} \bar{\psi}_{-n}^1 + \psi_{-n}^1 \mathcal{O}_{12} \psi_n^2 + \bar{\psi}_{-n}^1 \mathcal{O}_{21} \bar{\psi}_n^2 + i\psi_n^2 \mathcal{O}_{22} \bar{\psi}_n^2 \right), \quad (3.100)$$

where the $\psi_{\mp n}^{1/2}$ are the modes of CFT1/CFT2 which are acting from the left/right on I^0 – the ground state operators. The matrix $\mathcal{O} \in O(2)$ specifies the interface and can be given in terms of a boost matrix $\Lambda \in O(1, 1)$ which guarantees that the interface preserves conformal invariance, see [117, 80] for more details. Their exact relation is given by

$$\mathcal{O}(\Lambda) = \begin{pmatrix} \Lambda_{12} \Lambda_{22}^{-1} & \Lambda_{11} - \Lambda_{12} \Lambda_{22}^{-1} \Lambda_{21} \\ \Lambda_{22}^{-1} & -\Lambda_{22}^{-1} \Lambda_{21} \end{pmatrix}. \quad (3.101)$$

The matrices with $\det \Lambda = +1$ correspond to Dirichlet boundary conditions in the orbifold theory whereas $\det \Lambda = -1$ corresponds to the Neumann boundary conditions.

For $\det \Lambda = +1$ the relation gives

$$\Lambda = \begin{pmatrix} \cosh \gamma & \sinh \gamma \\ \sinh \gamma & \cosh \gamma \end{pmatrix} \leftrightarrow \mathcal{O} = \begin{pmatrix} \cos(2\phi) & \sin(2\phi) \\ \sin(2\phi) & -\cos(2\phi) \end{pmatrix}, \quad (3.102)$$

and for $\det \Lambda = -1$

$$\Lambda = \begin{pmatrix} \cosh \tilde{\gamma} & -\sinh \tilde{\gamma} \\ \sinh \tilde{\gamma} & -\cosh \tilde{\gamma} \end{pmatrix} \leftrightarrow \mathcal{O} = \begin{pmatrix} \cos(2\tilde{\phi}) & \sin(2\tilde{\phi}) \\ -\sin(2\tilde{\phi}) & \cos(2\tilde{\phi}) \end{pmatrix}. \quad (3.103)$$

Indeed, ϕ and $\tilde{\phi}$ precisely correspond to the parameters describing the D0 and D1 brane moduli space. From now on we omit the tildes. Then we can write $\cos(2\phi) = \tanh \gamma \Leftrightarrow e^\gamma = \cot \phi$ in both cases. To obtain the interface operators of the Ising model from those of the free fermion theory, one still has to GSO-project on total even fermion number. This requires taking linear combinations of the free fermion interfaces. In the Ising model the type-0-GSO projection allows us to distinguish three cases: The interface operators for $\det \Lambda = 1$ that carry either positive or negative RR charge and can be written as ⁶

$$I^\pm(\Lambda) = \frac{1}{2} (I^{\text{NS}}(\Lambda) \pm I^{\text{R}}(\Lambda)) + (\Lambda \rightarrow -\Lambda), \quad (3.104)$$

and these for $\det \Lambda = -1$ which are the neutral operators

$$I^n(\Lambda) = \frac{1}{\sqrt{2}} (I^{\text{NS}}(\Lambda) + I^{\text{NS}}(-\Lambda)). \quad (3.105)$$

The operators I^{NS} and I^{R} act on the Neveu-Schwarz and Ramond sector of the free fermion theory, respectively. They are given by

$$I^{\text{NS}}(\Lambda) = \prod_{n \in \mathbb{N} - \frac{1}{2}} I^n(\Lambda) I^{0,\text{NS}}, \quad \text{with } I^{0,\text{NS}} = |0\rangle_{\text{NS NS}} \langle 0|, \quad (3.106)$$

and

$$I^{\text{R}}(\Lambda) = \prod_{n \in \mathbb{N}} I^n(\Lambda) I^{0,\text{R}}, \quad (3.107)$$

$$\begin{aligned} \text{with } I^{0,\text{R}} &= \sqrt{|\sin(2\phi)|} \left(|+\rangle_{\text{R R}} \langle +| + |-\rangle_{\text{R R}} \langle -| \right) S(\Lambda) \\ &= \sqrt{2} \left(\cos(\phi) |+\rangle_{\text{R R}} \langle +| + \sin(\phi) |-\rangle_{\text{R R}} \langle -| \right). \end{aligned}$$

Here, $|\pm\rangle_{\text{R}}$ denote R-ground states and S is the spinor representation of $O(1,1)$.

3.2.2 Derivation of the partition functions

In the following we explicitly derive the partition function (3.2) for the interface operators introduced in section 3.2.1. We start with a single NS operator which is the simplest case. Step by step we show how to derive $Z(K)$ for the more complicated R, neutral, and charged

⁶ See [80] for more details on the construction

operator.

The partition function for a single NS operator $I = I^{\text{NS}}(\Lambda)$

In the NS sector of the free fermion theory we can formally write the Hilbert space \mathcal{H} of the theory as a tensor product $\otimes_n \mathcal{H}_n$ where $\mathcal{H}_n = \text{span} \{ |0\rangle, \psi_{-n} \bar{\psi}_{-n} |0\rangle, \psi_{-n} |0\rangle, \bar{\psi}_{-n} |0\rangle \}$. Then each $I^n(\mathcal{O})$ as in (3.100) has a matrix representation in \mathcal{H}_n given by

$$I^n = \begin{pmatrix} 1 & -i \mathcal{O}_{22} & 0 & 0 \\ -i \mathcal{O}_{11} & -\det \mathcal{O} & 0 & 0 \\ 0 & 0 & \mathcal{O}_{12} & 0 \\ 0 & 0 & 0 & \mathcal{O}_{21} \end{pmatrix}, \quad (3.108)$$

and we can write $I^{\text{NS}} = \otimes_n I^n$. In this notation the propagator is given by $e^{-\delta H} \equiv P = \otimes_n P^n$ with

$$P^n = \text{diag}(1, e^{-2\delta n}, e^{-\delta n}, e^{-\delta n}). \quad (3.109)$$

Using the above notation with CFT1 = CFT2 the partition function (3.2) of the K -sheet can be written as

$$Z(K) = \prod_{n \in \mathbb{N} - \frac{1}{2}} \text{Tr} \left(I^n P^n (I^n)^\dagger P^n \right)^K \quad (3.110)$$

$$= \prod_{n \in \mathbb{N} - \frac{1}{2}} (\lambda_{n,1}^K + \lambda_{n,2}^K + \lambda_{n,3}^K + \lambda_{n,4}^K), \quad (3.111)$$

where $\lambda_{n,i}$, $i = 1, \dots, 4$, are the eigenvalues of $D^n = [I^n P^n (I^n)^\dagger P^n]$.

Explicit calculation: We have two distinguishable interfaces: the Dirichlet-interface with $\det \Lambda = 1$ and the Neumann-interface with $\det \Lambda = -1$. However, in both cases the matrices D^n are similar and their eigenvalues are given by

$$\lambda_{n,1} \equiv e^{-2n\delta} p_n^+ = e^{-2n\delta} \left(\cosh(2n\delta) + \cos^2(2\phi) + \cosh(n\delta) \sqrt{2 \cosh(2n\delta) + 2 \cos(4\phi)} \right),$$

$$\lambda_{n,2} \equiv e^{-2n\delta} p_n^- = e^{-2n\delta} \left(\cosh(2n\delta) + \cos^2(2\phi) - \cosh(n\delta) \sqrt{2 \cosh(2n\delta) + 2 \cos(4\phi)} \right),$$

$$\lambda_{n,3} = e^{-2n\delta} \sin^2(2\phi) = \lambda_{n,4},$$

3.2 Entanglement entropy through Ising interfaces

so that the partition function on the K -sheeted surface with $2K$ defect insertions is given by

$$Z(K) = \prod_{n \in \mathbb{N} - \frac{1}{2}} e^{-2Kn\delta} (2 \sin^{2K}(2\phi) + (p_n^+)^K + (p_n^-)^K). \quad (3.112)$$

At this stage one could proceed further by directly using formula (2.10) on the latter result for $Z(K)$. The logarithm makes the infinite product a sum. Taking the derivative w.r.t. K in every summand it is then easy to write down a result for the entanglement entropy by means of an infinite sum. One could then evaluate the sum – and thus the entanglement entropy – numerically for every $\delta > 0$ and ϕ up to arbitrary accuracy. However, we are mainly interested in small δ – which means large L – behaviour of the entanglement entropy, since L is introduced as a IR cutoff. In this limit we can derive the EE analytically by proceeding as in the following.

For odd K the partition function (3.112) can be written as

$$Z(K) = \prod_{n \in \mathbb{N} - \frac{1}{2}} \left(\prod_{k=1}^K 2e^{-2n\delta} (2 \cos^2(\nu_k) - 1 + \cosh(2n\delta)) \right), \quad (3.113)$$

with $\nu_k = \arcsin(\sin(2\phi) |\sin(\frac{k\pi}{K})|)$. For even K we have to add $4e^{-2Kn\delta} \sin^{2K}(2\phi)$ to every factor in (3.113). Additionally, we state that the fraction $\theta[0,0](\tau, z)/\eta(\tau)$ of the well known θ -function and η -functions as defined in (A.1) and (A.7) can be written as

$$\frac{\theta[0,0](\tau, z)}{\eta(\tau)} = e^{\frac{\pi i \tau}{12}} \prod_{n \in \mathbb{N} - \frac{1}{2}} 2e^{-2n\pi i \tau} (2 \cos^2(\pi z) - 1 + \cos(2n\pi \tau)). \quad (3.114)$$

Thus we can conclude that the K -sheet partition function for odd K can be expressed as

$$Z(K) = e^{-\frac{K\delta}{12}} \prod_{k=1}^K \frac{\theta[0,0]\left(\frac{i\delta}{\pi}, \frac{\nu_k}{\pi}\right)}{\eta\left(\frac{i\delta}{\pi}\right)}. \quad (3.115)$$

Using the behaviour of η and θ under S -transformations we can write

$$Z(K) = e^{-\frac{K\delta}{12}} \prod_{k=1}^K e^{-\frac{\nu_k^2}{\delta}} \frac{\theta[0,0]\left(i\frac{\pi}{\delta}, -i\frac{\nu_k}{\delta}\right)}{\eta\left(i\frac{\pi}{\delta}\right)} \quad (3.116)$$

$$\xrightarrow{\delta \ll 1} Z(K) = e^{\frac{\pi^2 K}{12\delta}} e^{-\frac{\varphi(K)}{\delta}} \left(1 + e^{-\frac{\mu}{\delta}}\right),$$

where $\varphi(K) = \sum_{k=1}^K \nu_k^2$, and μ is constant in δ .

For even K , $Z(K)$ can not be given in terms of θ and η as above. One might wonder if we really can use (3.116) to calculate the entanglement entropy although it is just valid for odd K . In Appendix B.2 we actually show why it really suffices to consider (3.116).

The partition function for a single R-operator $I = I^R(\Lambda)$

In the Ramond sector the modes are integer and the zero-mode map is slightly more difficult, $I^{0,R} = \sqrt{2} \left(\cos(\phi) |+\rangle_{R,R} \langle +| + \sin(\phi) |-\rangle_{R,R} \langle -| \right)$. The latter allows us to write

$$I^R = \cos(\phi) I_+^R + \sin(\phi) I_-^R, \quad \text{with} \quad I_{\pm}^R = \sqrt{2} |\pm\rangle \langle \pm| \prod_{n \in \mathbb{N}} I^n, \quad (3.117)$$

where $I_-^R(\Lambda) \cdot I_+^R(\Lambda')$ vanishes. Proceeding similar to the case of NS-operators one gets

$$Z(K) = 2^K (\cos(\phi)^{2K} + \sin(\phi)^{2K}) \prod_{n \in \mathbb{N}} (\lambda_{n,1}^K + \lambda_{n,2}^K + \lambda_{n,3}^K + \lambda_{n,4}^K), \quad (3.118)$$

where again $\lambda_{n,i}$, $i = 1, \dots, 4$, are the eigenvalues of $[I^n P^n (I^n)^\dagger P^n]$.

Explicit calculation: The eigenvalues for the R-interface are similar to the eigenvalues for the NS interface but with $n \in \mathbb{N}$. Thus, for odd K we can write

$$Z(K) = 2^K (\cos(\phi)^{2K} + \sin(\phi)^{2K}) \prod_{k=1}^K \left(\prod_{n \in \mathbb{N}} 2e^{-2\delta n} (2 \cos^2(\nu_k) - 1 + \cosh(2\delta n)) \right), \quad (3.119)$$

where again $\nu_k = \arcsin(\sin(2\phi) |\sin(\frac{k\pi}{K})|)$. This time the latter is given in terms of $\frac{\theta[\frac{1}{2}, 0](\tau, z)}{\eta(\tau)}$ because of n being integer. One important difference between the θ -function we use here and the θ -function used in the case of the NS-interface is that there appears an additional factor of $2 \cos(\pi z)$. One can show that

$$\prod_{k=1}^K \cos(\nu_k) = \cos(\phi)^{2K} + \sin(\phi)^{2K}$$

for odd K so that in this case the partition function reduces to

$$\begin{aligned} Z(K) &= e^{-\frac{K\delta}{6}} (\cos(\phi)^{2K} + \sin(\phi)^{2K}) \prod_{k=1}^K \frac{1}{\cos(\nu_k)} \prod_{k=1}^K \frac{\theta[\frac{1}{2}, 0] \left(\frac{i\delta}{\pi}, \frac{\nu_k}{\pi} \right)}{\eta \left(\frac{i\delta}{\pi} \right)} \\ &= e^{-\frac{K\delta}{6}} \prod_{k=1}^K \frac{\theta[\frac{1}{2}, 0] \left(\frac{i\delta}{\pi}, \frac{\nu_k}{\pi} \right)}{\eta \left(\frac{i\delta}{\pi} \right)}. \end{aligned} \quad (3.120)$$

The same steps as for the NS interface now lead us to

$$Z(K) = e^{\frac{\pi^2}{12\delta} K} e^{-\frac{\varphi(K)}{\delta}} \left(1 + e^{-\frac{\mu}{\delta}} \right), \quad (3.121)$$

in the limit $\delta \ll 1$.

In the Ramond sector only the Dirichlet interfaces have non-trivial components, so we do not consider Neumann boundary conditions, although they would not make any difference for $Z(K)$.

The partition function for the neutral interface operator

The neutral interface operator is given by $I^n(\Lambda) = \frac{1}{\sqrt{2}} (I^{\text{NS}}(\Lambda) + I^{\text{NS}}(-\Lambda))$ with Neumann boundary conditions, i.e. $\det \Lambda = -1$. Some simple algebra leads to

$$\begin{aligned} 2 I^n(\Lambda) e^{-\delta H} I^n(\Lambda)^\dagger e^{-\delta H} &= I^{\text{NS}}(\Lambda) e^{-\delta H} I^{\text{NS}}(\Lambda) e^{-\delta H} + I^{\text{NS}}(-\Lambda) e^{-\delta H} I^{\text{NS}}(-\Lambda) e^{-\delta H} \\ &\quad + I^{\text{NS}}(-\Lambda) e^{-\delta H} I^{\text{NS}}(\Lambda) e^{-\delta H} + I^{\text{NS}}(\Lambda) e^{-\delta H} I^{\text{NS}}(-\Lambda) e^{-\delta H} \\ &= 2 (I^{\text{NS}}(\Lambda) e^{-\delta H} I^{\text{NS}}(\Lambda) e^{-\delta H}) \\ &\quad + 2 (I^{\text{NS}}(\Lambda) e^{-\delta H} I^{\text{NS}}(-\Lambda) e^{-\delta H}) \\ &\equiv 2 (D_+ + D_-), \end{aligned} \quad (3.122)$$

with D_\pm given by the tensor product of the matrices

$$D_\pm^n = \begin{pmatrix} 1 + e^{-2\delta n} \mathcal{R} & i(e^{-4\delta n} + e^{-6\delta n})\sqrt{\mathcal{R}} & 0 & 0 \\ -i(e^{-2\delta n} + e^{-4\delta n})\sqrt{\mathcal{R}} & e^{-4\delta n} + e^{-2\delta n} \mathcal{R} & 0 & 0 \\ 0 & 0 & \pm e^{-2\delta n} \mathcal{T} & 0 \\ 0 & 0 & 0 & \pm e^{-2\delta n} \mathcal{T} \end{pmatrix}, \quad (3.123)$$

where we here used the reflection coefficient $\mathcal{R} = \cos(2\phi)^2$ and the transmission coefficient $\mathcal{T} = \sin(2\phi)^2$ as introduced in (1.60). We can see that both D_+ and D_- can be diagonalized simultaneously. With straightforward linear algebra we can now calculate the partition function for the K -sheet with a neutral interface insertion. It is given by

$$\begin{aligned} Z(K) &= \text{Tr}(D_+ + D_-)^K \\ &= 2^{K-1} \prod_{n \in \mathbb{N} - \frac{1}{2}} e^{-2Kn\delta} \left(+2 \sin^{2K}(2\phi) + (p_n^+)^K + (p_n^-)^K \right) + \\ &\quad + 2^{K-1} \prod_{n \in \mathbb{N} - \frac{1}{2}} e^{-2Kn\delta} \left(-2 \sin^{2K}(2\phi) + (p_n^+)^K + (p_n^-)^K \right). \end{aligned} \quad (3.124)$$

The important factor of 2^{K-1} can be understood with the following simpler example: Consider the matrices $M_{\pm}(x) = \otimes_i \text{diag}(x, \pm x)$. It is now easy to convince oneself that

$$[M_+(x) + M_-(x)] \cdot [M_+(y) + M_-(y)] = 2[M_+(xy) + M_-(xy)],$$

which allows us to directly conclude that $[M_+(x) + M_-(x)]^K = 2^{K-1}[M_+(x^K) + M_-(x^K)]$. The generalization to D_+ and D_- is straight forward.

The first summand in (3.124) is the same as for the single NS-interface. In a very similar way as in section 3.2.2, the second summand can also be written in terms of $\theta[0, 0]/\eta$. We here only state the result in the limit $\delta \ll 1$:

$$Z(K) = 2^{K-1} e^{\frac{\pi^2 K}{12\delta}} \left(e^{-\frac{\varphi(K)}{\delta}} + e^{-\frac{\chi(K)}{\delta}} \right), \quad (3.125)$$

where $\chi(K) = \sum_{k=1}^K \mu_k^2$ with $\mu_k = \arcsin(\sin(2\phi) |\cos(\frac{k\pi}{K})|)$.

The partition function for the charged interface operator

The charged interface operator is given by $I^{\pm}(\Lambda) = \frac{1}{2} (I^{\text{NS}}(\Lambda) \pm I^{\text{R}}(\Lambda)) + (\Lambda \rightarrow -\Lambda)$ with Dirichlet boundary conditions, i.e. $\det \Lambda = 1$. With similar considerations as for the neutral interface we can write

$$\begin{aligned} 2I^{\pm}(\Lambda) e^{-\delta H} I^{\pm}(\Lambda)^{\dagger} e^{-\delta H} &= (D_+ + D_-) \oplus 2 \cos^2(\phi) (D_+^{\text{R}+} + D_-^{\text{R}+}) \oplus \\ &\quad \oplus 2 \sin^2(\phi) (D_+^{\text{R}-} + D_-^{\text{R}-}), \end{aligned} \quad (3.126)$$

3.2 Entanglement entropy through Ising interfaces

where $D_{\pm}^{\text{R}+}$ corresponds to the vacuum $|+\rangle$ and $D_{\pm}^{\text{R}-}$ corresponds to $|-\rangle$ in a similar way to the single Ramond interface. There is no difference between the positively and the negatively charged interface. In matrix representation all the D 's are tensor products of matrices similar to (3.123) but with integers for the Ramond operators. Thus the partition function on the K -sheet surface with charged interface insertions can be written as

$$\begin{aligned}
Z(K) &= \frac{1}{2^K} \text{Tr} \left[(D_+ + D_-)^K \oplus 2^K \cos(\phi)^{2K} (D_+^{\text{R}+} + D_-^{\text{R}+})^K \oplus \right. \\
&\quad \left. \oplus 2^K \sin(\phi)^{2K} (D_+^{\text{R}-} + D_-^{\text{R}-})^K \right] \\
&= \frac{1}{2} \left(\prod_{n \in \mathbb{N} - \frac{1}{2}} e^{-2Kn\delta} (+2 \sin^{2K}(2\phi) + (p^+)^K + (p^-)^K) + \right. \\
&\quad + \prod_{n \in \mathbb{N} - \frac{1}{2}} e^{-2Kn\delta} (-2 \sin^{2K}(2\phi) + (p^+)^K + (p^-)^K) + \\
&\quad + 2^K (\cos(\phi)^{2K} + \sin(\phi)^{2K}) \prod_{n \in \mathbb{N}} e^{-2Kn\delta} (+2 \sin^{2K}(2\phi) + (p^+)^K + (p^-)^K) + \\
&\quad \left. + 2^K (\cos(\phi)^{2K} + \sin(\phi)^{2K}) \prod_{n \in \mathbb{N}} e^{-2Kn\delta} (-2 \sin^{2K}(2\phi) + (p^+)^K + (p^-)^K) \right). \tag{3.127}
\end{aligned}$$

Using the same logic as in the previous sections, the partition function for odd K reduces to

$$Z(K) = e^{\frac{\pi^2 K}{12\delta}} \left(e^{-\frac{\varphi(K)}{\delta}} + f(K) e^{-\frac{\chi(K)}{\delta}} \right), \tag{3.128}$$

in the limit $\delta \ll 1$. The functions ϕ and χ are given as before and $f(K)$ is given by

$$f(K) = \frac{1}{2} \left(1 + (\cos(\phi)^{2K} + \sin(\phi)^{2K}) \prod_{k=1}^K \frac{1}{\cos(\mu_k)} \right) \neq 1. \tag{3.129}$$

3.2.3 Derivation of the entanglement entropy

Before we explicitly derive the entanglement entropy we want to show that – for $\delta \ll 1$ – it is the same in all previous cases up to an additional $\log 2$ term for the neutral interface. Our formula of choice again is

$$E = (1 - \partial_K) \log Z(K)|_{K \rightarrow 1}. \tag{3.130}$$

We want to state again that any overall factor C^K in $Z(K)$ with C constant in K does not contribute to the entanglement entropy.

At first we want to write down the preliminary result for the single NS-interface where $Z(K)$ is given by (3.116) so that the entanglement entropy can be written as

$$E^{\text{NS}} = (-\varphi(1) + \partial_K \varphi(1)) \frac{1}{\delta}. \quad (3.131)$$

Next we consider the single R-interface where the partition function is given by (3.121). Its EE is simply the same as for the NS-interface

$$E^{\text{R}} = (-\varphi(1) + \partial_K \varphi(1)) \frac{1}{\delta} = E^{\text{NS}}. \quad (3.132)$$

Now we want to derive the EE for the neutral interface. Inserting its partition function (3.125) in (3.130) gives

$$\begin{aligned} E^{\text{n.}} &= \log \left(e^{-\varphi(1)/\delta} + e^{-\chi(1)/\delta} \right) + \frac{1}{\delta} \frac{\partial_K \varphi(1) e^{-\varphi(1)/\delta} + \partial_K \chi(1) e^{-\chi(1)/\delta}}{e^{-\varphi(1)/\delta} + e^{-\chi(1)/\delta}} - \log 2 \\ &= (-\varphi(1) + \partial_K \varphi(1)) \frac{1}{\delta} - \log 2 \\ E^{\text{n.}} &= E^{\text{NS}} - \log 2, \end{aligned} \quad (3.133)$$

where we can simplify to the second line because we are in the limit $\delta \ll 1$ and because $\varphi(1) = 0 > \chi(1) = -4\phi^2$.

At last we want to derive the EE for the charged interface operator where $Z(K)$ is given by (3.128). As in the case of the neutral interface operator every term with a factor $e^{-\chi(1)/\delta}$ can be neglected. Consequently also $f(K)$ in (3.128) has no contribution to the entanglement entropy when we are in the limit $\delta \ll 1$. It again simply reduces to the EE for the single NS-interface:

$$E^{\pm} = E^{\text{NS}}. \quad (3.134)$$

3.2.4 Explicit derivation of E^{NS}

To derive the entanglement entropy explicitly we have to calculate $\partial_K \varphi(1)$. Therefore we proceed similar as in [30] and write $\varphi(K) = \sum_{k=1}^K \nu_k^2 \equiv \sum_{k=1}^K f\left(\frac{k}{K}\right)$, which can be written

3.2 Entanglement entropy through Ising interfaces

in a Taylor series around $k/K = 0$ and further massaged as

$$\begin{aligned}\varphi(K) &= \sum_{k=1}^K \sum_{m=0}^{\infty} f_m \left(\frac{k}{K}\right)^m = \sum_{m=0}^{\infty} \frac{f_m}{K^m} \sum_{k=1}^K k^m \\ &= \sum_{m=0}^{\infty} \frac{f_m}{K^m} \frac{B_{m+1}(K+1) - B_{m+1}}{m+1},\end{aligned}\tag{3.135}$$

where $B_n(x), B_n$ are the Bernoulli polynomials and Bernoulli numbers, respectively, as given in Appendix A.2. Its derivative in the limit $K \rightarrow 1$ is then given by

$$\begin{aligned}\partial_K \varphi(K)|_{K \rightarrow 1} &= \sum_m \frac{f_m}{m+1} \underbrace{\partial_K B_{m+1}(K+1)}_{=\partial_K(B_{m+1}(K)+(m+1)K^m)} \Big|_{K \rightarrow 1} - \frac{f_m m}{m+1} \underbrace{(B_{m+1}(2) - B_{m+1})}_{=(m+1)} \\ &= \sum_m \frac{f_m}{m+1} \partial_K B_{m+1}(K)|_{K \rightarrow 1} + f_m m - f_m m \\ &= \sum_m \frac{f_m}{m+1} \partial_K B_{m+1}(K)|_{K \rightarrow 1}.\end{aligned}\tag{3.136}$$

At this stage we use the formula (A.12) to obtain

$$\partial_K \varphi(K)|_{K \rightarrow 1} = f(0) + \frac{1}{2} f'(0) + \int_0^{\infty} \frac{if'(it) - if'(-it)}{1 - e^{2\pi t}} dt.\tag{3.137}$$

Both $f(0)$ and $f'(0)$ vanish, so that the entanglement entropy is given by

$$E^{\text{NS}} = \frac{1}{\delta} \int_0^{\infty} \frac{if'(it) - if'(-it)}{1 - e^{2\pi t}} dt = \frac{\pi^2 \sigma(s)}{\delta} = \frac{\sigma(s)}{2} \log\left(\frac{L}{\epsilon}\right),\tag{3.138}$$

where we defined $s = |\sin(2\phi)| = \sqrt{\mathcal{T}}$ and

$$\begin{aligned}\sigma(s) &= \frac{2}{\pi} \int_0^{\infty} \frac{\operatorname{arcsinh}(s \sinh(\pi t)) \left(\coth(\pi t) - 1\right) s \cosh(\pi t)}{\sqrt{1 + s^2 \sinh^2(\pi t)}} dt \\ &= \frac{2}{\pi^2} \int_0^{\infty} u \left(\sqrt{1 + \frac{s^2}{\sinh^2(u)}} - 1 \right) du.\end{aligned}\tag{3.139}$$

For the last step we substituted $u = \operatorname{arcsinh}(s \sinh(\pi t))$.

3.2.5 Comments on the result and special cases

The result (3.138) shows that the EE through a single NS interface has a logarithmic scaling with respect to the (large) size L of the system. Up to an additional term “ $\log 2$ ” for the neutral interface operator this is exactly the behaviour of the EE through a conformal interface in the 2D Ising model, too. The interface itself affects the EE mainly through the factor $\sigma(s)$ which is given in integral form in (3.139). The square of the “variable” $s = |\sin(2\phi)|$ just is the transmission coefficient of the interface \mathcal{T} , but can be given in terms of the scaling factor b and the coupling constant K_1 of the Ising model as in (3.95), too. In figure 3.4, we show the explicit dependence of the factor σ on the transmission coefficient \mathcal{T} .

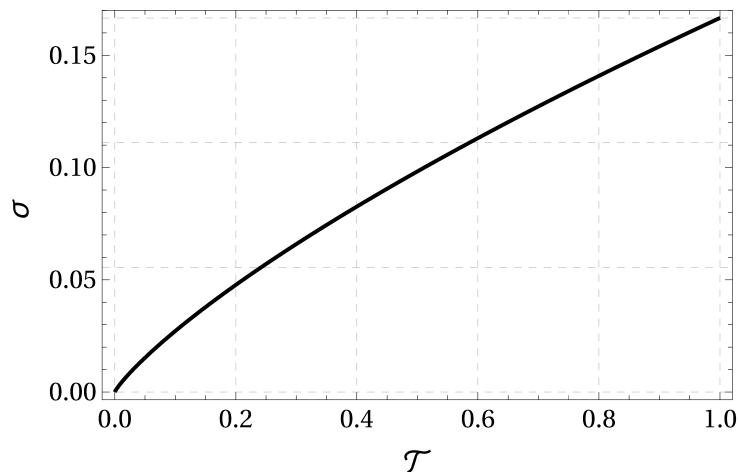


Figure 3.4: The prefactor σ as a function of the transmission coefficient \mathcal{T} . As expected, it vanishes for totally reflecting interfaces, where $\mathcal{T} = 0$, and reproduces the familiar result $\sigma(\mathcal{T} = 1) = 1/6 = c/3$ for topological interfaces in the Ising model.

There are two special cases to mention. First, we want to consider topological interfaces where the transmission coefficient is maximal, $\mathcal{T} = 1$. This case includes the identity in the free fermionic CFT and in the Ising model which is why it should reproduce the universal scaling of the entanglement entropy without interfaces. In fact, with $\sigma(1) = 1/6 = c/3$ we obtain the right result from [16].

Secondly, in the limit of totally reflecting interface, when $\mathcal{T} \rightarrow 0$, one can show that $\sigma(\mathcal{T}) = \mathcal{O}(\mathcal{T} \log \sqrt{\mathcal{T}})$, so that for vanishing transmittance also the entanglement entropy vanishes. This fits the fact that all the oscillator parts of the two CFTs are decoupling for an interface with $\mathcal{T} \rightarrow 0$. As shown in figure 3.4, $\sigma(\mathcal{T})$ increases monotonically between these

3.2 Entanglement entropy through Ising interfaces

two extremal cases. The latter observation supports the intuitive guess that entanglement changes according to the transmittance of the interface. The lower the transmittance the lower the strength of interaction between the two CFTs connected by the interface.

We also want to discuss the sub-leading terms although it vanishes but for the neutral interface operator. As expected, for the topological defects they match the result from 3.1. We want to analyze its origin a little more here for the non-topological interfaces at hand. An important contribution to that term for the Ramond and the charged interface comes from the ground state map.⁷ In our cases the ground state map is rather easy, it just separates the Hilbert space of the CFT in direct sums. Let us consider a Hilbert space $\mathcal{H} = \mathcal{H}_0 \oplus \mathcal{H}_1$ and two density operators ρ_0 and ρ_1 acting on the respective Hilbert space, such that

$$\rho = \alpha \rho_0 \oplus \beta \rho_1, \quad (3.140)$$

where α and β are real numbers. It is then easy to see that the von Neumann entropy on the full Hilbert space S_ρ can be given in terms of the entropies on \mathcal{H}_0 and \mathcal{H}_1 :

$$E_\rho = \alpha E_{\rho_0} + \beta E_{\rho_1} - (\alpha \log \alpha + \beta \log \beta). \quad (3.141)$$

As an example let us consider the single Ramond interface. Because of the ground state map the (reduced) density matrix can be written as $\rho = \cos^2\phi \rho_+ + \sin^2\phi \rho_-$ and since $E_{\rho_+} = E_{\rho_-}$ the von Neumann entropy reads

$$E^R = E_\rho = E_{\rho_+} - (\cos^2\phi \log \cos^2\phi + \sin^2\phi \log \sin^2\phi). \quad (3.142)$$

However, E_{ρ_+} itself has an additional sub-leading term that exactly cancels the contribution of the ground state map.

Another contribution to the sub-leading term comes from the GSO-projection which separates the Hilbert space of the free fermion in a direct sum $\mathcal{H} = \mathcal{H}_0 \oplus \mathcal{H}_1$, graded by the fermion number. As an example consider the interface operator $I^{\text{NS}}(\Lambda)$ on the full NS Hilbert space. Then the projected interfaces on \mathcal{H}_0 and \mathcal{H}_1 are

$$I_\pm = \frac{1}{\sqrt{2}}(I^{\text{NS}}(\Lambda) \pm I^{\text{NS}}(-\Lambda)), \quad (3.143)$$

⁷Especially for bosonic interfaces this is often called the *lattice part* of the interface operator. This name comes from the change of the lattice structure of the torus by the ground state mapping (see also section 3.1.2).

where I_+ is the previously called neutral interface operator. A density operator is given by $I^\dagger I$, such that $\rho = \frac{1}{2}(\rho_+ + \rho_-)$ and thus

$$E^{\text{NS}} = E_\rho = \frac{1}{2}(E_+ + E_-) + \log 2, \quad (3.144)$$

where in the limit of large L it can be shown that $E_+ = E_-$, so that we get $E^{\text{NS}} = E^{\text{n}} + \log 2$ or

$$E^{\text{n}} = E^{\text{NS}} - \log 2. \quad (3.145)$$

It is noteworthy that the sub-leading term does not depend on the most significant property of the interfaces, namely the transmittance \mathcal{T} , in all our cases. A similar result is known for entanglement entropy through interfaces in the free boson theory [30]. There the sub-leading term only depends on the winding numbers k_1, k_2 on both sides of the interface and is simply given by “ $-\log |k_1 k_2|$ ”.

As a final comment in this section we want to state that one can also express the pre-factor σ in terms of the Logarithm and Dilogarithm Li_2 in a similar way as in [30]. It then looks like

$$\sigma(s) = \frac{s}{6} - \frac{1}{6} - \frac{1}{\pi^2} \left((s+1) \log(s+1) \log s + (s-1) \text{Li}_2(1-s) + (s+1) \text{Li}_2(-s) \right). \quad (3.146)$$

This indeed agrees with formulas (22-26) of [123].

3.2.6 Supersymmetric interfaces

Let us now consider a situation with $N = 1$ supersymmetry by adding a free boson to the theory of a free fermion. We can combine our results with those of [30] to obtain the entanglement entropy through a supersymmetric interface. Compatibility of the interface with $N = 1$ supersymmetry requires that the interface intertwines the supercurrents G^1, G^2 of the two theories

$$(G_r^1 - i\eta_S^1 \bar{G}_{-r}^1) I_{1,2} = \eta I_{1,2} (G_r^2 - i\eta_S^2 \bar{G}_{-r}^2), \quad (3.147)$$

where $\eta, \eta_S^2, \eta_S^1 = \pm 1$. The signs η_S^i specify the preserved SUSY of the two theories and the GSO projection requires to sum over both choices for η in the final step. As explained in [117] the choices of sign can be absorbed in the gluing matrix $\Lambda \in O(1, 1)$ for the fermions, such that specific entries in the gluing matrix for bosons and fermions can differ by signs. Since the entanglement entropy does not depend on these choices, we simply assume that

3.2 Entanglement entropy through Ising interfaces

bosons and fermions are glued by the same matrix Λ (or equivalently \mathcal{O}) that we used in the current paper, implying that the preserved SUSY is the same on the two sides of the interface.

The implementation of the GSO projection has been discussed in section 3.2.1 and can be taken over to the supersymmetric situation.

The full interface operator of the supersymmetric theory can be written as a tensor product of a bosonic and a fermionic piece:

$$I_{1,2}(\Lambda, k_1, k_2, \varphi) = I_{1,2}^{\text{bos}}(\Lambda, k_1, k_2, \varphi) \otimes I_{1,2}^{\text{ferm}}(\Lambda) . \quad (3.148)$$

Interfaces of the theory of a free boson compactified on a circle were considered in [118, 30]. They depend on two integers, k_1 and k_2 , specifying topological winding numbers, as well as two continuous moduli, ϕ_1, ϕ_2 . The origin of these parameters is easiest to understand in the “folded” picture, where the interface is mapped to a D-brane on a torus. In the simplest case of a one-dimensional brane wrapping the torus $S^1 \times S^1$, the integers can be understood as winding numbers of the D1-brane around the two 1-cycles. The continuous moduli correspond in this picture to position and Wilson line. The gluing matrix Λ is restricted by the torus geometry

$$\tanh \gamma = \frac{(k_1 R_1)^2 - (k_2 R_2)^2}{(k_1 R_1)^2 + (k_2 R_2)^2} .$$

We choose the fermionic gluing matrix to be the same as the bosonic one. The entanglement entropy has been computed in [30] with the result

$$E^{\text{bos}} = \frac{\sigma(s)^{\text{bos}}}{2} \log \frac{L}{\epsilon} - \log |k_1 k_2| , \quad (3.149)$$

where

$$\sigma(s)^{\text{bos}} = \frac{s}{2} - \frac{2}{\pi^2} \int_0^\infty u \left(\sqrt{1 + \frac{s^2}{\sinh^2(u)}} - 1 \right) du . \quad (3.150)$$

The Hilbert space of the supersymmetric theory is the tensor product of the bosonic and fermionic Hilbert spaces. The partition functions $Z(K)$ hence takes the product form $Z(K) = Z^{\text{bos}}(K) \cdot Z^{\text{ferm}}(K)$. Due to the logarithm in (3.130) the entanglement entropy can then be written as

$$E^{\text{SUSY}} = E^{\text{bos}} + E^{\text{ferm}} , \quad (3.151)$$

where in the fully supersymmetric model E^{bos} is given in (3.149) and E^{ferm} is $E^{\text{NS}} = E^{\text{R}}$.⁸ Explicitly,

$$E^{\text{SUSY}} = \frac{s}{4} \log \frac{L}{\epsilon} - \log |k_1 k_2|. \quad (3.152)$$

The prefactor $\sigma(s)$ of the logarithmic term simplifies significantly. Here, contributions from the oscillators of the bosonic and fermionic part of the system cancel out in the limit $\delta \rightarrow 0$, such that only the term $s/2$ remains. This is similar to the computations in [117], where the limit of two parallel interfaces approaching each other was considered. Note that the constant contribution $\log |k_1 k_2|$ has a topological interpretation: The winding and momentum modes of the compactified boson are quantized and part of a lattice. The combination $|k_1 k_2|$ is the index $\text{ind } \hat{\Lambda}$ of the sublattice of windings and momenta to which the interface couples. Here, $\hat{\Lambda} \in O(d, d|\mathbb{Q})$ is the gluing matrix for integer charge vectors and, as opposed to Λ , does not depend on the moduli. On the other hand, the quantity $s = |\sin 2\phi| = \sqrt{\mathcal{T}}$ specifies the precise geometry of the sublattice and determines the transmissivity, which is the same for bosons and fermions (for equal Λ) and also in the supersymmetric system. The supersymmetric entanglement can thus be rewritten as

$$E^{\text{SUSY}} = \frac{\sqrt{\mathcal{T}} c}{6} \log \frac{L}{\epsilon} - \log \text{ind } \hat{\Lambda}. \quad (3.153)$$

In figure 3.5 we compare the three results for σ in the free bosonic, free fermionic, and their supersymmetric combination.

It is very suggestive that this form of the entanglement entropy generalizes to supersymmetric torus compactifications in higher dimensions. As was shown in [117] the index of the sublattice is a useful quantity to characterize topological information of an interface, in other words, the information that does not change under deformations of the interface or bulk theories. In a similar way, \mathcal{T} naturally exists for any interface and characterizes the transmissivity, in other words, how far away the interface is from being topological. In the case of higher dimensional tori, $\Lambda \in O(d, d)$ is a $2d \times 2d$ matrix consisting of $d \times d$ blocks and the transmissivity is given in terms of the determinant of the lower-right block Λ_{22} , $\mathcal{T} = |\det \Lambda_{22}|^{-2}$.

Similar results exist for $\mathcal{N} = 1$ supersymmetry preserving defects in the holographic description of [110]. The prefactor of the leading term of the entanglement entropy through

⁸One can also consider the GSO projection of the supersymmetric model. It has the same structure but with E^{ferm} given by E^{n} or E^{\pm} . In the final result, there appears an additional contribution $\log 2$ for the neutral interfaces, as discussed before.

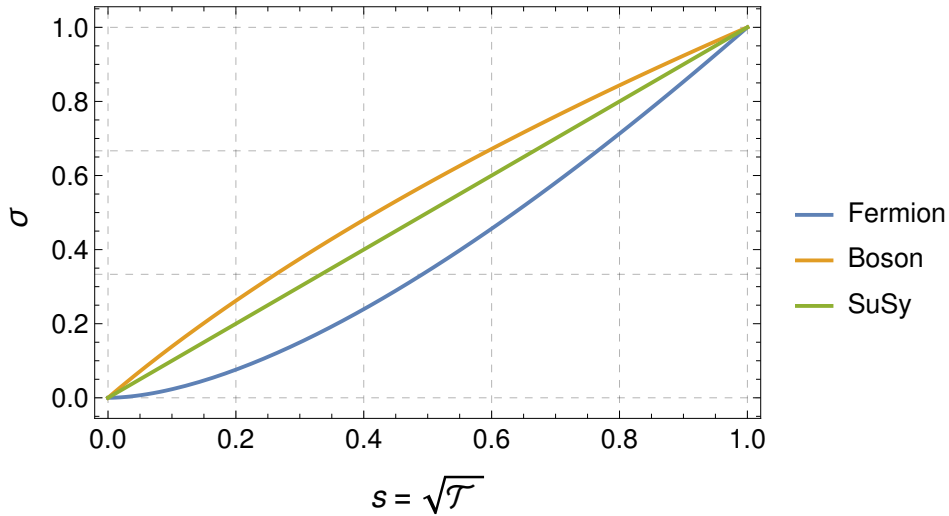


Figure 3.5: Comparison of σ (normalized to 1) in the three examples of free theories. The complicated dependencies of σ on the transmission coefficient simplifies significantly in the supersymmetric combination of the interfaces. This is because contributions from the oscillators of the bosonic and fermionic part of the system cancel out in the limit $\delta \rightarrow 0$, such that only the term $\propto s = \sqrt{\mathcal{T}}$ remains.

their defects simplifies in the exact same way. However, the conformal field theories and the defects that they describe by dual (2+1)-dimensional Janus solutions are not the free theories and defects we considered in our work. This raises the suggestion that the EE through defects that preserve $\mathcal{N} = 1$ SUSY generally show a similar easy dependency on the transmissivity.

Chapter 4

Classical Holographic Codes

In this chapter we want to present models that serve as toy models for the AdS/CFT correspondence. They are in particular designed to mimic some of the important information theoretical structures of the duality. They may serve as simple models that improve our intuition on the general information theoretical structure, and in particular may improve our understanding of the correlation structure of holographic theories and its connection to geometry. Most of the chapter was originally published in [60].

Before we go into more details about the AdS/CFT correspondence and the particular toy models that we will present here, let us specify what we mean by a “toy model”. Assume some (complicated) model, theory or concept that we ultimately want to learn about. A toy model is an ideally simpler model that captures some of its features. It does not have to capture all its features, because if it could it would no longer be a “toy model”, but the model itself. The concept that we want to understand better is the AdS/CFT correspondence, and the toy models we will consider capture specific information theoretical features. However, they will not exhibit other essential features of the correspondence. Another example of a toy model for AdS/CFT is the Sechdev-Ye-Kitaev (SYK) model that captures features related to scrambling and out-of-time-correlation functions [131]. Both have to do with the description of chaos in quantum systems. Other examples are $O(N)$ -vector models that are believed to be dual to higher spin theories [132]. They nicely capture the large- N expansion and ideas of RG-flows in general AdS/CFT.

We now first want to give a rather short introduction to the AdS/CFT correspondence with a focus on the features we are finally interested in, which is then followed by presenting the toy models including our classical code that we dubbed *classical holographic code*.

4.1 Holography and the AdS/CFT correspondence

The origin of the holographic principle lies in the description of black holes. Black holes are exact solutions to Einstein's equation, so there should be nothing random about them and on the classical level one would not expect it to have entropy. This, however, leads to a violation of the second law of thermodynamics. Just consider a hot gas with entropy that is thrown into a black hole. When it crosses the event horizon, the entropy would be gone since we could no longer see the random properties of the gas.

A resolution of this problem is to declare black holes to objects with statistic properties where the entropy is encoded on the horizon. It must be encoded on the horizon since we can not get any information from inside the horizon. The entropy is proportional to the logarithm of the number of microstates of the object. Typically one would expect that this is proportional to the volume of the object. However, for black holes it is proportional to the surrounding area [133, 134]. Among others, this at the beginning deeply puzzling result inspired the formulation of the holographic principle [31]:

A gravitational theory describing a region of space is equivalent to a (non-gravitational) theory living only on the surface of that region.

The AdS/CFT correspondence is an explicit example of this principle. However, so far holography is still just a conjecture and it is not clear if the holographic principle holds in all circumstances. Some physicists even suggest that the entire universe is encoded on a lower dimensional boundary – the so-called cosmological horizon. There might exist a painting of our three dimensional universe on a great two-dimensional canvas [135].

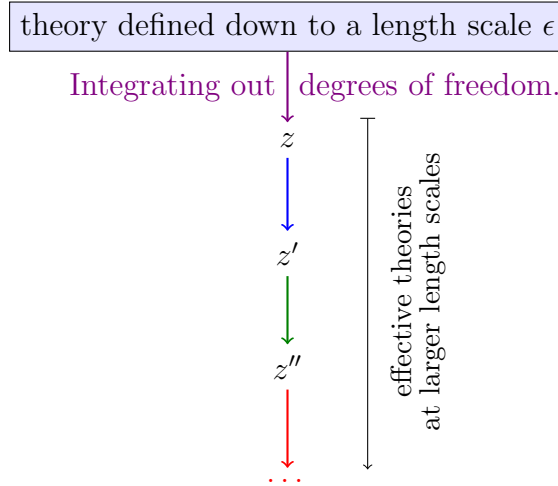
The AdS/CFT correspondence was originally discovered [33] by studying D_p -branes and black holes in string theory. But the fact that such an equivalence may exist can be directly motivated from several aspects of gauge theories and gravity. Here we closely follow [136].

4.1.1 Geometrizing the renormalization group flow

Consider a Quantum Field Theory (QFT) in d -dimensional Minkowski spacetime with coordinates (t, \vec{x}) . Normally, due to ultraviolet (UV) divergences one has to introduce a cutoff. We use a short-distance cutoff ϵ . The well-known renormalization group (RG) flow gives a description how to describe the theory effectively at larger length scales $z \gg \epsilon$

4.1 Holography and the AdS/CFT correspondence

by integrating out short-distance degrees of freedom [10]. The RG flow gives rise to a continuous family of effective theories in d -dimensional Minkowski spacetime labeled by the RG scale z .



It is now possible to visualize this continuous family of d -dimensional theories in $(d + 1)$ dimensions with the RG scale z becoming a spatial coordinate. The outcome should be a $(d + 1)$ -dimensional theory that has the following properties by construction:

1. Since an effective theory at scale z can only describe physics at larger scales than z , the theory should be intrinsically non-local. There is still some degree of locality in the z direction, since degrees of freedom of the original theory at different scales are not strongly correlated.
2. The original theory is invariant under reparametrization of the RG scale. Thus, the theory should be invariant under reparametrization of z .
3. An effective theory at z_0 can describe all the physics for $z \geq z_0$. Thus, the $(d+1)$ -dimensional description has not more degrees of freedom than the d -dimensional theory at the length scale $z = \epsilon$.

Especially the third property is very interesting. *If* the $(d + 1)$ -dimensional theory exists then the third property together with the holographic principle suggests that it is a gravitational theory.

This specific realization of the holographic principle gives a first hint for the AdS/CFT correspondence. The following part gives an even more impressive hint that there should

exist a string theory description for any gauge theory. It comes from 't Hooft's large- N_c expansion [137].

4.1.2 The large- N_c expansion

Consider a non-Abelian gauge theory and treat its number of colors N_c as a parameter. Take N_c to be large and expand physical quantities in $1/N_c$.¹ For example, consider the Euclidean partition function for $U(N_c)$ Yang-Mills theory with coupling g :

$$Z = \int DA_\mu \exp\left(-\frac{1}{4g^2} \int d^4x \operatorname{Tr} F^2\right). \quad (4.1)$$

with A_μ being the gauge field and F the corresponding field strength. The vacuum-to-vacuum amplitude can be expanded in $1/N_c$ as

$$\log Z = \sum_{h=0}^{\infty} N_c^{2-2h} f_h(\lambda) = N_c^2 f_0(\lambda) + f_1(\lambda) + \frac{1}{N_c^2} f_2(\lambda) + \dots, \quad (4.2)$$

where $\lambda = g^2 N_c$ is the 't Hooft coupling and $f_h(\lambda)$, $h \in \mathbb{N}$, are functions of λ only. The remarkable aspect of this expansion is that at fixed λ , Feynman diagrams are organized by their topologies. To be more specific, $f_h(\lambda)$ includes the contributions of all diagrams which can be drawn on a two-dimensional compact orientable surface with h holes without crossing of any lines. Since these surfaces are classified by their number of holes, the large- N_c expansion (4.2) can be seen as an expansion in terms of the topology of two-dimensional compact surfaces.

Amazingly, this is similar to the perturbative expansion of a closed string theory. The worldsheet of a closed string is a two-dimensional compact surface and the string perturbative expansion is given by a sum over the topologies of two-dimensional surfaces. Again, take a look at the vacuum-to-vacuum amplitude which in string theory can be written as (see for example [14])

$$\mathcal{A} = \sum_{h=0}^{\infty} g_s^{2-2h} F_h(\alpha') = \frac{1}{g_s^2} F_0(\alpha') + F_1(\alpha') + g_s^2 F_2(\alpha') + \dots, \quad (4.3)$$

where g_s is the string coupling, $2\pi\alpha'$ is the inverse string tension and $F_h(\alpha')$ is the contribution of two-dimensional surfaces with h holes.

¹For self-contained reviews of the expansion see e.g. [137, 138, 139].

4.1 Holography and the AdS/CFT correspondence

The crucial conclusion is that (4.2) can be interpreted as a perturbative expansion of a string theory with

$$f_h(\lambda) \leftrightarrow F_h(\alpha') \quad (4.4)$$

and, thus

$$g_s \sim 1/N_c \quad , \quad \alpha' \equiv \alpha'(\lambda) = \text{some function of } \lambda \text{ only.} \quad (4.5)$$

This motivates the conjecture that for any non-Abelian gauge theory there should exist a dual string theoretical description. However, it is left open what the specific string theory is.

4.1.3 The reason for AdS

So far we have considered general gauge theories. Now we want to consider conformal field theories and see how this restricts a possible dual description. First, assume that the d -dimensional CFT in fact has a dual $(d+1)$ -dimensional string or gravity description. We now want to derive some properties of the $(d+1)$ -dimensional spacetime. The most general metric in this spacetime that is consistent with d -dimensional Poincaré symmetry can be written as

$$ds^2 = \Omega^2(u) (-dt^2 + d\vec{x}^2 + du^2), \quad (4.6)$$

where u is the extra spatial direction. The directions (t, \vec{x}) are the coordinates of the field theory which are also called the boundary directions. This comes from the picture that the field theory lives on the boundary at $u = 0$.

A conformal field theory is in particular invariant under rescaling

$$(t, \vec{x}) \rightarrow C(t, \vec{x}), \quad (4.7)$$

with C some constant. As in section 4.1.1 we want u to represent a length scale in the boundary theory. Thus, under (4.7) the additional coordinate has to scale simultaneously, $u \rightarrow Cu$, and the dual description should be invariant under

$$(t, \vec{x}, u) \rightarrow C(t, \vec{x}, u). \quad (4.8)$$

For this to be the case $\Omega(u)$ has to scale as $\Omega(u) \rightarrow C^{-1}\Omega(u)$ under $u \rightarrow Cu$. The only solution to this is

$$\Omega(u) = \frac{R}{u} \quad (4.9)$$

where R is some constant. Therefore, the metric (4.6) should look like

$$ds^2 = \frac{R^2}{u^2}(-dt^2 + d\vec{x}^2 + du^2) \quad (4.10)$$

which is the metric of $(d + 1)$ -dimensional anti-de Sitter spacetime, AdS_{d+1} .

The conclusion of this section now is that a dual gravitational or string theoretical description of a conformal field theory should be in an (at least asymptotically) AdS spacetime. A specific example is the famous Maldacena duality of $\mathcal{N} = 4$ super-Yang-Mills theory and type IIB string theory on an $AdS_5 \times S^5$ background [33].

4.1.4 Some properties of the duality

Let us assume the existence of a system where the AdS/CFT correspondence holds, *i.e.* there is a (quantum) gravity on $(d + 1)$ -dimensional asymptotic AdS spacetime with a dual d -dimensional CFT confined on the boundary of that spacetime. This duality possesses many interesting features, and we want to highlight just a few of them that will play a role in the later toy models.

Operator representation and subregion duality: We here briefly review the standard construction of local fields in the interior of AdS (the bulk) from the CFT on the boundary [140, 141]. We work in global coordinates with a metric that asymptotically has the form

$$ds^2 \sim -(r^2 + 1)dt^2 + \frac{dr^2}{r^2 + 1} + r^2 d\Omega_{d-1}^2, \quad (4.11)$$

where r is the radial coordinate and $d\Omega_{d-1}$ is the area element of S^{d-1} . In this coordinates the boundary is at $r = \infty$ and the dual CFT lives on $S^{d-1} \times \mathbb{R}$, with \mathbb{R} being the time direction. The AdS/CFT dictionary gives the relation [140, 142]

$$\lim_{r \rightarrow \infty} r^\Delta \phi(r, X) = \mathcal{O}(X), \quad X \in S^{d-1} \times \mathbb{R}, \quad (4.12)$$

between a bulk field ϕ and its dual conformal operator \mathcal{O} with the scaling dimension Δ in the conformal field theory. Only in the limit $r \rightarrow \infty$, the representation of ϕ in the CFT is local and unique. For generic $x \in AdS_{d+1}$ it can be represented as

$$\phi(x) \leftrightarrow \int_{S^{d-1} \times \mathbb{R}} dX K(x, X) \mathcal{O}(X) + \dots \quad (4.13)$$

4.1 Holography and the AdS/CFT correspondence

where K is some smearing function (also called kernel) that solves the bulk equations of motions and must reproduce (4.12), and omitted terms are suppressed by orders of $1/N_c$. The object on the right-hand side is non-local, and generically has support everywhere on $S^{d-1} \times \mathbb{R}$. However one can in general reduce the support and make the representation less “non-local”, *i.e.* even without access to the whole boundary one can hope to represent/reconstruct local operators in the bulk.

Therefore, consider a constant time slice, *i.e.* fix $t_0 \in \mathbb{R}$, and choose a connected subregion A in S^{d-1} . Now consider the domain of dependency $D(A)$ of A inside of $S^{d-1} \times \mathbb{R}$, that is the set of points X that are in causal contact with A but not with A^c , *i.e.* any inextendible causal curve² passing through X must intersect A . Now define $J^\pm(D(A))$ as the union of all causal curves evolving from/to $D(A)$. The *causal wedge* $W_C(A)$ of the subregion A [143] is then

$$W_C(A) \equiv J^+(D(A)) \cap J^-(D(A)) . \quad (4.14)$$

The crucial point now is that the construction of representations of bulk fields in the CFT can be implemented purely within the causal wedge [141]. That is if $x \in W_C(A)$ then we can represent $\phi(x)$ in the CFT as the non local operator (to leading order in $1/N_c$)

$$\int_{D(A)} dX K(x, X) \mathcal{O}(X) , \quad (4.15)$$

with some other smearing function K .

An immediate consequence is that some bulk field operator $\phi(x)$ can (and must) have different non-local representations in the CFT because x can lie in multiple causal wedges.

As an example let us consider a constant time slice of AdS_3 with three boundary regions A , B and C as in figure 4.1. The causal wedge $W_C(A)$ at constant time is the region bounded by A and the red dashed line that connects the endpoints of A . Respectively for B and C . In this example the operator $\phi(y)$ can be represented in A but not in the complement $A^c = B \cup C$. The operator $\phi(x)$ lies in neither of the causal wedges and, hence, cannot be represented on any region A , B or C . However, it can be represented on the union of any two of these regions, *i.e.* on $A \cup B$, $A \cup C$ and $B \cup C$. That is referred to as *subregion duality*.

The Ryu-Takayanagi formula: We here want to state a result of [34] that reveals a

²A curve is called causal if its tangent vector is never spacelike.

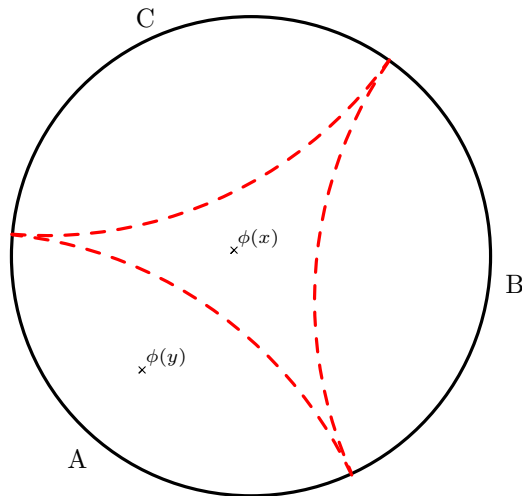


Figure 4.1: Example for subregion duality. $\phi(y)$ can be represented in A but not in the complement $A^c = B \cup C$. The operator $\phi(x)$, however, cannot be represented on any region A , B or C . But, still, it can be represented on the union of any two of these regions, *i.e.* on AB , AC and BC .

deep connection between the entanglement structure of states in a CFT and geometry in the AdS space. Let us assume that the state of the CFT is represented by a particular asymptotic AdS solution. The quantity one wants to compute is the entanglement entropy $E_A = S(\rho_A)$ of a connected spatial region A . Therefore, consider the minimal surface γ_A in the respective asymptotic AdS solution whose boundary coincides with the boundary of A , *i.e.* $\partial\gamma_A = \partial A$. “Minimal” here refers to the area of that surface. The volume that is bounded by A and γ_A is called the *entanglement wedge* ϵ_A . The so-called *Ryu-Takayanagi formula* now states that E_A is given by a sum of the bulk entanglement entropy E_{ϵ_A} and a term proportional to the area of the minimal cut. If we assume that the bulk contribution is negligible, then the Ryu-Takayanagi formula becomes

$$E(A) = \frac{\text{Area}(\gamma_A)}{4G}, \quad (4.16)$$

where G is Newton’s constant [35].

In general the causal wedge $W_C(A)$ lies in the entanglement wedge ϵ_A , *i.e.* $W_C(A) \subseteq \epsilon_A$. One might now ask if operator reconstruction is also possible in ϵ_A . We can at least “reconstuct” one object out of $C(A)$ namely the area of the minimal cut γ_A . It seems plausible that one can in principle get access to more information that lies behind the

causal wedge. It is, however, not fully clear to what extent one can expect this. At least in [144] it is suggested that one can represent any local operator in the entanglement wedge ϵ_A on the boundary region A .

4.2 Holographic quantum error-correcting codes

4.2.1 Qutrit example

In this section, we briefly review a simple toy model for the AdS/CFT correspondence based on quantum error correction. It is formulated as a qutrit³ code that encodes one logical qutrit into three physical ones such that the logical qutrit can be reconstructed even if one of the physical ones is lost. The key idea is to identify the bulk degrees of freedom with logical qutrits and the boundary degrees of freedom with the physical qutrits (see [53]). The logical qutrit $|\tilde{\psi}\rangle$ is encoded as

$$\begin{aligned} |\tilde{0}\rangle &= \frac{1}{\sqrt{3}} (|000\rangle + |111\rangle + |222\rangle) , \\ |\tilde{1}\rangle &= \frac{1}{\sqrt{3}} (|012\rangle + |120\rangle + |201\rangle) , \\ |\tilde{2}\rangle &= \frac{1}{\sqrt{3}} (|021\rangle + |102\rangle + |210\rangle) , \end{aligned} \tag{4.17}$$

where we indicated the logical qutrit by a tilde to distinguish it from the physical ones [145]. The logical qutrit is encoded in a subspace of the larger Hilbert space of three qutrits, that we also denote by A , B , and C . The code subspace is spanned by the GHZ-type states (4.17),

$$|\tilde{\psi}\rangle = \sum_{i=0}^2 c_i |\tilde{i}\rangle. \tag{4.18}$$

In consequence, no single physical qutrits can carry any information about the encoded state, as its reduced density matrix is maximally mixed. However, from any two physical qutrits the logical one can be reconstructed with certainty. That is due to the existence of operators U_{IJ} , where $I, J = A, B, C$, acting non-trivially only on the two of the physical qutrits I and J , such that

³A qutrit is very similar to a qubit. However, there is one additional base vector spanning its Hilbert space. Therefore, the qutrit state is described by $|\psi\rangle = \sum_{i=0}^2 c_i |i\rangle$.

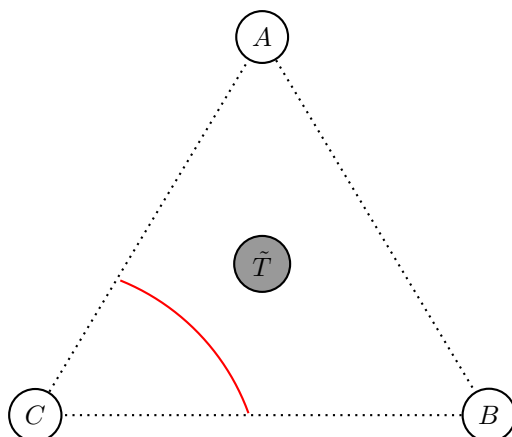


Figure 4.2: Simplistic toy model for the AdS/CFT correspondence. One logical qutrit \tilde{T} (representing the bulk degrees of freedom) is encoded in three physical qutrits A , B and C (representing the boundary degrees of freedom). The red line sketches minimal surface in the bulk. The logical qutrit can be reconstructed from any two of the boundary qutrits, while only one of these contains no information about it. Furthermore, logical operations on \tilde{T} can also be performed by acting on only two of the physical qutrits. These features are also captured in a classical version of this code we introduce in section 4.3.1.

$$U_{IJ}|\tilde{i}\rangle = |i\rangle_I \otimes |\chi\rangle_{JK}, \quad |\chi\rangle = \frac{1}{\sqrt{3}}(|00\rangle + |11\rangle + |22\rangle), \quad (4.19)$$

which means that all the information about the logical qutrit can be mapped on the single physical qutrit I by U_{IJ} which is explicitly constructed in [53].

Therefore, it is clear that access to any two qutrits out of the three ($I, J, K \in \{A, B, C\}$) suffices to learn about the logical qutrit. One simply acts on these two physical qutrits with the operator U_{IJ} and obtains qutrit I in the state $|i\rangle$ of the logical qutrit. From this it also follows immediately that the action of a logical operator \tilde{O} , acting as $\tilde{O}|\tilde{i}\rangle = \sum_j \tilde{O}_{ji}|\tilde{j}\rangle$, can be represented as an operator O_{IJ} acting non-trivially on any two physical qutrits but trivially on the respective third. It is of the form

$$O_{IJ} = U_{IJ}^\dagger O_I U_{IJ}, \quad (4.20)$$

where O_I denotes an operator acting solely on qutrit I as $O_I|i\rangle_I = \sum_j \tilde{O}_{ij}|j\rangle_I$ such that $O_{IJ}|\tilde{i}\rangle = \sum_j \tilde{O}_{ji}|\tilde{j}\rangle$. That is, any logical operation \tilde{O} on the logical qutrit can be performed by acting with the corresponding O_{IJ} on any two physical qutrits. As it was pointed out in [53], this models “subregion duality” in AdS/CFT. Furthermore, this simple toy model

obeys a version of the RT formula [55], as we demonstrate next.

As it is clear from above, an arbitrary (mixed) state $\tilde{\rho}$ on the code subspace can be written as

$$\tilde{\rho} = U_{AB} \left(\rho_A \otimes |\chi\rangle\langle\chi|_{BC} \right) U_{AB}^\dagger. \tag{4.21}$$

Interpreting the physical qutrits A , B and C as boundary degrees of freedom, we can calculate the entanglement entropy between regions (here: points) in the boundary, see figure 4.2. From (4.21), one easily obtains the entanglement entropies

$$\begin{aligned} S(\tilde{\rho}_C) &= \log(3), \\ S(\tilde{\rho}_{AB}) &= \log(3) + S(\tilde{\rho}), \end{aligned} \tag{4.22}$$

where $\tilde{\rho}_C$ and $\tilde{\rho}_{AB}$ are the reduced density matrices of qutrits C and AB , respectively. That fulfills the RT-formula with area operator $\log(3)$ [55]. Closely related to entanglement entropy is the mutual information that is, in the present case, given by

$$I_{qu}(C, AB) = S(C) + S(AB) - S(C, AB) = 2 \log(3). \tag{4.23}$$

The mutual information, however, does not capture contributions from the bulk entropy in this model.⁴ Therefore, restricting the states of the boundary qutrits to the class of pure states it is evident that the RT formula can be stated in terms of the mutual information $I_{qu}(A, A^c)$. In this form the RT formula states that the mutual information between a boundary region A and its complement A^c is given by twice the area of the minimal surface in the bulk.

4.2.2 Holographic pentagon code

The ideas outlined in the previous section led to the investigation of extended networks of concatenated quantum error-correcting codes [54, 56]. Here, we restrict ourselves to the holographic pentagon code, see figure 4.3, introduced as a toy model for AdS/CFT in [54] and briefly outline some of the ideas behind its construction.

The basic building block of the networks of [54] are perfect tensors. These are defined as tensors $T_{a_1, a_2, \dots, a_{2n}}$ with the property that they are proportional to isometric tensors from A to A^c for all subsets A of the tensor indices with $|A| \leq |A^c|$. In particular, perfect tensors

⁴This does not necessarily hold for more elaborate models, as bulk matter can back-react and, in principle, it can modify the geometry.

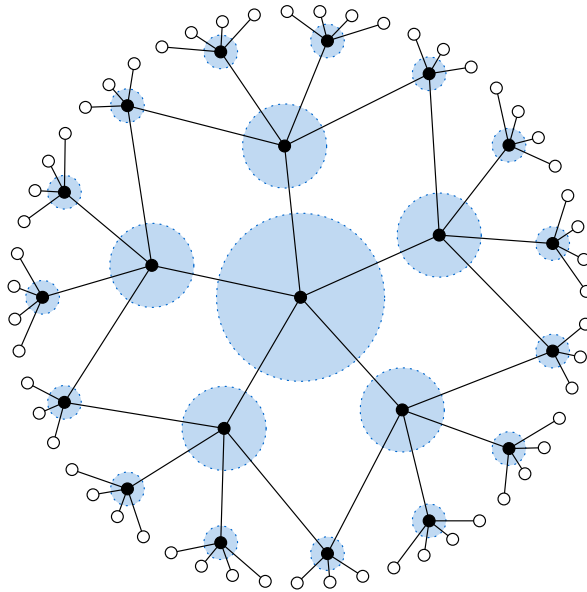


Figure 4.3: Holographic pentagon code. The pentagon tiling of AdS defines a network of negative curvature. Each vertex represents a perfect tensor (indicated by blue discs) in the bulk that takes one qubit as input (represented as black dots). The boundary contains the outputs of the network (represented by white dots). The network of perfect tensors establishes an isometry from the bulk Hilbert space to the boundary Hilbert space and provides a toy model for the AdS/CFT correspondence.

are related to quantum states of $2n$ v -dimensional spins as

$$|\psi\rangle = \sum_{a_1, a_2, \dots, a_{2n}} T_{a_1 a_2 \dots a_{2n}} |a_1 a_2 \dots a_{2n}\rangle. \quad (4.24)$$

These states $|\psi\rangle$ have the special property that they are maximally entangled along any possible bi-partition into sets of n spins and therefore show a very particular entanglement structure. Specifically, states of this kind are referred to as absolutely maximally entangled states [146] and possess interesting properties [147]. Interpreted as a map from one spin to the remaining $2n-1$ spins, a perfect tensor establishes the encoding map of a quantum error-correcting code. It encodes one logical spin into $2n-1$ spins and allows the recovery of the logical one even if up to $n-1$ spins are lost. One explicit example for a perfect quantum error-correcting code that gives rise to a state of the kind described in (4.24) is given by the five qubit code in [148]. The qutrit code described in the previous section provides a further example.

For the construction of the holographic pentagon code, the key idea is to uniformly tile AdS space with pentagons. This tiling defines a network with perfect tensors at each vertex, see figure 4.3. This tensor network describes an isometric tensor from the bulk (the inputs of the tensor network) to the boundary (its output) and can be seen as a quantum error-correcting code that maps the logical qubits in the bulk to the physical qubits on the boundary. Interestingly, in this network the lattice RT formula holds (see (4.35)). Furthermore, the representation of bulk logical operators on different regions of the boundary is analogous to the reconstruction of bulk operators from CFT operators on the boundary. In consequence, this model captures these important features of the AdS/CFT correspondence.

4.3 Classical holographic codes

In this section, we introduce *classical holographic codes*. These are constructed similarly to the holographic quantum error-correcting codes considered in [54]. Spacetime with non-negative curvature is uniformly tiled. Connecting neighboring tiles we define a network of probabilistic maps. Furthermore, we impose certain constraints on these, as described in section 4.3.2. We mainly focus our attention to a network with pentagon symmetry and use bits as bulk and boundary degrees of freedom. However, there are many different constructions possible using, for example, different tilings or trits instead of bits. It is possible to think about the whole network as a classical error-correcting code. However, we do not refer to our construction as an error-correcting code.⁵ Besides introducing classical holographic codes, we also discuss their features and find some similarities with expectations from AdS/CFT. In particular, we elaborate on close similarities with quantum error-correcting codes that have recently been considered as toy models for AdS/CFT [53, 54, 56, 55].

4.3.1 Classical trit example

To start our discussion on classical holographic codes, we introduce a classical probabilistic code that resembles key features of the quantum case discussed in 4.2.1. Similar to this case, we consider an encoding of a logical trit into three physical ones. Furthermore, we

⁵There are probabilistic codes used for error correction especially in telecommunication. The most prominent examples are Low-Density-Parity-Check-Codes [149] and Turbo-Codes [150]. However, there is no straight forward connection between these and the classical holographic codes as we define them here.

require that the information about the logical trit is zero in each of the individual physical trits, while the knowledge of two of the physical trits provides us with full knowledge about the logical one. One particular code satisfying these constraints is

$$\begin{aligned}\tilde{0} &\rightarrow p(000) = p(111) = p(222) = \frac{1}{3}, \\ \tilde{1} &\rightarrow p(012) = p(120) = p(201) = \frac{1}{3}, \\ \tilde{2} &\rightarrow p(021) = p(102) = p(210) = \frac{1}{3},\end{aligned}\tag{4.25}$$

where $p(X_1X_2X_3)$ denotes the probability that the trit string $X_1X_2X_3$ ($X_i \in \{0, 1, 2\}$) appears. In the encoding (4.25), each of the strings has the same probability, given by $\frac{1}{3}$. That is, we encode one logical trit in three physical trits in such a way that the logical one is mapped to three different strings of three trits with equal probability. One can convince oneself that the knowledge of one physical trit does not give any information about the logical one, while by knowing any two physical trits we can obtain the logical one with certainty. Labelling the physical trits by A , B and C , as above, that implies that the logical trit can be obtained from either AB , AC or BC , but not from A , B or C alone.⁶ That establishes a subregion duality analogous to the one in the quantum case.

These properties are also reflected in the Shannon entropy S_S . For any of the physical trits I , the entropy is given by

$$S_S(I) = - \sum_i p_i \log(p_i) = \log(3),\tag{4.26}$$

where $I = A, B, C$ and the p_i are given by the respective marginal probability distributions. That implies that there is no information about the logical trit in any of the physical ones, as we stated above. Considering any of the sets AB , AC or BC , we find

$$\begin{aligned}S_S(IJ) &= - \sum_{ij} p_i \tilde{p}_j \log(p_i \tilde{p}_j) \\ &= \log(3) + S_S(\tilde{I}),\end{aligned}\tag{4.27}$$

where $I, J = A, B, C$, the p_i are the probabilities appearing in (4.25) and the \tilde{p}_j give the probabilities for the logical trit \tilde{I} to be \tilde{X} ($\tilde{X} \in \{\tilde{0}, \tilde{1}, \tilde{2}\}$) and we used $\sum_i p_i = 1 = \sum_j \tilde{p}_j$.

⁶Therefore, codes like the one given by (4.25) can be used for secret sharing, as we discuss in more detail in section 4.4.3.

First, we notice that these results are formally the same as in the quantum case discussed in 4.2.1. That is, a RT formula – at least formally – holds. However, the RT formula is concerned with entanglement entropy, while here we considered the Shannon entropy. To connect both, we move to the mutual information that, for pure states, is equal to two times the entanglement entropy. We find that the mutual information I_{cl} between one physical trit A and the remaining two is given by

$$I_{cl}(A, BC) = S_S(A) + S_S(BC) - S_S(ABC) = \log(3), \quad (4.28)$$

where we used $S_S(BC) = S_S(ABC) = \log(3) + S_S(\tilde{I})$. Due to the symmetry of the encoding the same statement also holds for the other two trits B and C . That is, the classical mutual information is smaller than the one in the quantum case, (4.23), by a factor of $\frac{1}{2}$. However, it also is proportional to the “area” of the minimal cut.

Let us next investigate whether we can implement logical operations in the bulk (*i.e.* on the logical trit) by acting on a subset of the boundary degrees of freedom (the physical trits), see figure 4.2. First, let us implement an operation that implements addition by $\oplus 1$ by solely acting on the physical trits B and C .⁷ The operation that succeeds in this task is to apply $\oplus 1$ to B and $\oplus 2$ to C . The same operation can be implemented on A and B by applying $\oplus 1$ to A and $\oplus 2$ to B . Finally, to implement it on A and C , one has to apply $\oplus 2$ to A and $\oplus 1$ to C . To perform the logical operation $\oplus 2$ by acting on two of the physical trits, one has to either act with $\oplus 2$ on B and $\oplus 1$ on C , with $\oplus 2$ on A and $\oplus 1$ on B or with $\oplus 1$ on A and $\oplus 2$ on C . Therefore, operators acting on the logical trit can be reconstructed on either AB , AC or BC , but not on A , B or C alone.

In summary, the classical code we considered shares essential features with the quantum code that we reviewed in section 4.2.1.

Furthermore, it is interesting to note that the encoding (4.25) can be obtained from (4.17) by imposing complete decoherence.⁸ Mapping the classical logical trit given by \tilde{i} ($\tilde{i} \in \{\tilde{0}, \tilde{1}, \tilde{2}\}$) to the logical qutrit state $|\tilde{i}\rangle$ and subsequent encoding according to (4.17),

⁷Here and in the remainder of this section, $\oplus n$ for some integer n denotes the addition by $n \bmod 3$.

⁸Note that the classical encoding (4.25) neither does have to be obtained in this way nor does it have to be interpreted in this way. Also, already at this point, we want to mention that the classical codes on extended networks, we introduce in the next section, cannot be obtained by decoherence of the boundary state of *e.g.* the holographic pentagon code.

we obtain

$$\rho_{\tilde{i}} = |\tilde{i}\rangle\langle\tilde{i}| = \frac{1}{3} \begin{pmatrix} 1 & 1 & 1 & 0_{1 \times 6} \\ 1 & 1 & 1 & 0_{1 \times 6} \\ 1 & 1 & 1 & 0_{1 \times 6} \\ 0_{6 \times 1} & 0_{6 \times 1} & 0_{6 \times 1} & 0_{6 \times 6} \end{pmatrix} \quad (4.29)$$

in a basis containing the qutrit states appearing in (4.17), where we denote the basis by $\{|v_j\rangle\}_{j=1,\dots,9}$, and the ordering depends on \tilde{i} . Removing the coherences in $\rho_{\tilde{i}}$, for example, by a randomly selected projective measurement with projectors $P_j = |v_j\rangle\langle v_j|$, we arrive at a mixed state $\rho_{\tilde{i}}^{(dec)} = \frac{1}{3} \sum_{j=1}^3 |v_j\rangle\langle v_j|$. This is a statistical mixture of pure states $|v_j\rangle\langle v_j|$ that appear with probability $p(v_j) = \frac{1}{3}$. Therefore, by reinterpreting the qutrits as classical trits, we obtain the encoding (4.25).

At this point, we would like to insert another brief comment. There is the question how the randomness in the description of the system can be justified physically. In our opinion, there are (at least) three possible ways. One is that there is a lack of knowledge about the details of the system that forces a probabilistic description, like in thermodynamics (cf. section 4.5). Another way to justify the randomness in the code is to imagine an agent at each vertex that generates the randomness that is necessary for the functioning of the code, for example, by sending individual photons to a beam splitter and subsequently collapsing the quantum superposition of the photons. In this way the agent can create the required random numbers. Similarly, one could think of strong local decoherence at each of the vertices that kills the coherences and leaves us with a probabilistic mixture, as described above. However, in our opinion, it also is enough to just state that the codes we consider are intrinsically random.

4.3.2 Classical codes on hyperbolic space

We study classical probabilistic codes on a uniform pentagon-tiling of AdS space that feature some of the key properties of tensor-network-based quantum codes [54, 55, 56, 53] under which there are the Ryu-Takayanagi formula and important bulk reconstruction properties. The tiling gives rise to a network, that we also refer to as graph, as *e.g.* visible in figure 4.4. Via the network, we define a (probabilistic) mapping from the bits sitting on the vertices in the interior to those on the open edges at the boundary. The mapping is defined as follows: We order the network into layers of vertices defined by the graph distance from the center. From the negative curvature of the graph it follows that each vertex shares at most two edges with vertices of the previous layer. We now declare each

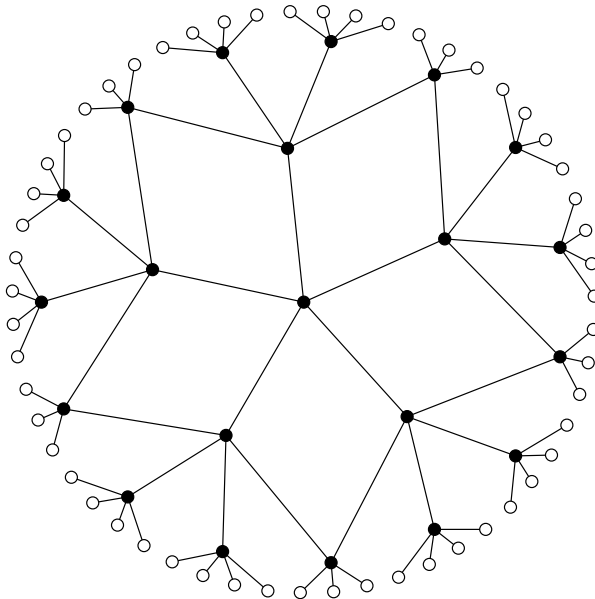


Figure 4.4: Network to realize a classical holographic code. Each vertex in the interior of the graph represents a tile with a specific fixed volume in AdS space. Furthermore, each of these vertices takes one bit as input (the input bits are then interpreted as bulk degrees of freedom) and (probabilistically) maps the input together with the input from the in-going edges to the out-going edges. The final output of the code is then given by the bits sitting at the boundary of the network. These are interpreted as boundary degrees of freedom. In this way a map from bulk degrees of freedom to boundary degrees of freedom is established that gives rise to a duality between bulk and boundary.

node to a map $n \rightarrow m$, where n is the number of inputs given by the bit at the vertex and edges from the previous layer, and m is the number of output bits. There are three possible mappings appearing in this pentagon-tiling, shown in Figure 4.4, that are $3 \rightarrow 3$, $2 \rightarrow 4$, and, in the center, $1 \rightarrow 5$.

Inspired by the quantum codes of [54], where the mapping from the bulk to the boundary is due to the insertion of one and the same perfect six-tensor at each vertex, we demand that each mapping originates from a single set of strings of six bits, $\mathfrak{S} = \{s_i \mid i = 1, \dots, N\}$, with the number of strings, N , not yet fixed. We define the mapping as follows: The first bits in the strings define the input, where we always take the very first bit in the strings as the bulk input (see fig. 4.5). We now assume a discrete uniform probability distribution on the set \mathfrak{S} , *i.e.* all probabilities $p(s_i) = 1/N$ are equal. The probability density of the outcome of the mappings for a given input string s_{in} is then defined by the conditional probabilities

$$p_{\text{out}}(s_{\text{out}} | s_{\text{in}}), \quad (4.30)$$

where $s_{\text{in}} \cup s_{\text{out}} \in \mathfrak{S}$. The domain of the $3 \rightarrow 3$ mapping should contain all possible strings of three bits. This gives a first condition on \mathfrak{S} and tells us that $|\mathfrak{S}| = N \geq 8$.

As we discussed in section 4.2.2, a perfect tensor gives rise to an absolutely maximally entangled state. In [54], this particular entanglement structure was used to show the desired features. Here, we demand rather similar conditions for \mathfrak{S} , where we use the mutual information as a measure of correlations. As it turns out, it is not possible to find a set \mathfrak{S} of bit-strings of length six, where any bipartition of the strings has maximal mutual information, which in a sense would be the classical analogue to perfect tensors. These analogues exist only for some special combinations of the length of the strings and the “dimension” d of the d its involved. It is not clear whether such a set of strings of length six exists. Therefore, in the following, we prefer to use milder conditions on the set \mathfrak{S} that still will be sufficient to obtain the results of section 4.4. The same properties then follow automatically for sets of maximally correlated strings. We demand that any bipartition into substrings of non-equal size is maximally correlated, and that any bipartition into strings of length three is maximally correlated if one of the two substrings contains only neighboring bits. Here, the term neighboring bits refers to either bits that are next to each other in the full (cyclic) six-string or to bits where the edges, that are allocated to these, are next to each other (see fig. 4.5 for the allocation). Therefore, the order in which the bits appear in the string and whether a particular bit acts as edge in- or outputs matters. As illustrated in figure 4.5, we choose the bits to be arranged counter clockwise.

As we show in appendix C.1, from the above properties, it follows that $|\mathfrak{S}| = 8$ and that

- (I) the knowledge of three neighboring edge bits gives full information about the three complementary bits;
- (II) no information about any other single bit can be obtained by the knowledge of one particular bit.

Furthermore, two neighboring edge bits never reveal information about bits next to them and in general two bits can at most give one other bit with certainty.

After this more general discussion, we give an explicit example of a set of strings that fulfils the above properties. It is given by

$$\mathfrak{S} = \{000000, 001111, 010110, 011001, 100101, 101010, 110011, 111100\}, \quad (4.31)$$

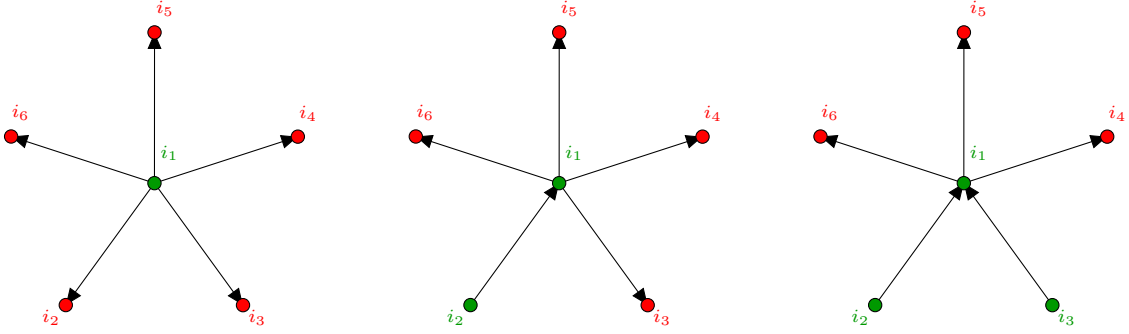


Figure 4.5: The set $\mathfrak{S} = \{s_i\}$ of strings s_i of bits i_n generates the (probabilistic) mappings. Here, we display from the left to the right the mappings: $1 \rightarrow 5$, $2 \rightarrow 4$, and $3 \rightarrow 3$. Each dot represents one bit, where the one in the center, i_1 , is the bulk input and the remaining ones are edge input (green) and outputs (red). The probability distribution of the outputs is obtained via the conditional probabilities $p_{\text{out}}(s_{\text{out}} | s_{\text{in}})$, where s_{in} denotes the string of inputs and s_{out} is the string of outputs.

with the probability distribution $p(s_i \in \mathfrak{S}) = \frac{1}{8}$. In consequence, the $1 \rightarrow 5$ mapping is given by

$$\begin{aligned} \tilde{0} &\rightarrow p(00000) = p(01111) = p(10110) = p(11001) = \frac{1}{4}, \\ \tilde{1} &\rightarrow p(11100) = p(10011) = p(00101) = p(01010) = \frac{1}{4}, \end{aligned} \quad (4.32)$$

where here and in the following the tilde indicates the bulk input and $p(X_1 X_2 X_3 X_4 X_5)$ denotes the probability of the output $X_1 X_2 X_3 X_4 X_5$ ($X_i \in \{0, 1\}$). Unfortunately, the mapping breaks the pentagon symmetry of the network. This is because the central bulk bit can be reconstructed with the knowledge of the second and fifth or the third and fourth output bit but not with the knowledge of any other two bits. Therefore these bits are distinguished. All sets \mathfrak{S} give rise to $1 \rightarrow 5$ mappings that break the symmetry in a similar way. However, this does not spoil the desired property for the full network.

For $2 \rightarrow 4$ we obtain

$$\begin{aligned} \tilde{0}0_e &\rightarrow p(0000) = p(1111) = \frac{1}{2}, & \tilde{1}0_e &\rightarrow p(0101) = p(1010) = \frac{1}{2}, \\ \tilde{0}1_e &\rightarrow p(0110) = p(1001) = \frac{1}{2}, & \tilde{1}1_e &\rightarrow p(1100) = p(0011) = \frac{1}{2}, \end{aligned} \quad (4.33)$$

where the subscript e indicates the edge input from the previous layer. Finally, the $3 \rightarrow 3$

map deduced from the set (4.31) is given by

$$\begin{aligned} \tilde{0}0_{e_1}0_{e_2} &\rightarrow 000, & \tilde{0}0_{e_1}1_{e_2} &\rightarrow 111, & \tilde{1}0_{e_1}0_{e_2} &\rightarrow 101, & \tilde{1}0_{e_1}1_{e_2} &\rightarrow 010, \\ \tilde{0}1_{e_1}0_{e_2} &\rightarrow 110, & \tilde{0}1_{e_1}1_{e_2} &\rightarrow 001, & \tilde{1}1_{e_1}0_{e_2} &\rightarrow 011, & \tilde{1}1_{e_1}1_{e_2} &\rightarrow 100, \end{aligned} \tag{4.34}$$

where e_1, e_2 denote the bits of the incoming edges.

In the following, we show that a map from the bulk to the boundary induced by a set with the outlined properties – and in particular the specific example (4.31) – together with the geometric structure of the network inherit the above mentioned features. For that reason, we call them *classical holographic codes*. In particular, the properties we demand on \mathfrak{S} are sufficient to obtain the results of the next section.

The above approach is a generic way to construct codes on a hyperbolic space that give rise to the features we show in the following section. However, there are many more possible probabilistic codes that work, too. One can *e.g.* define each individual map by a different set that fulfils the above property of maximal mutual information. This does not alter any property we study in section 4.4. One can also consider the situation where the maximally correlated set that defines the mapping is random at each vertex. In this case the classical version of the RT formula still holds.⁹ This establishes a similarity with the random tensor networks considered in [56].

In particular, we emphasize that, in contrast with the simple example of section 4.3.1, the classical codes introduced in this section cannot be obtained by simple decoherence of the boundary. That is, decoherence of the output of a quantum code, like *e.g.* the one considered in section 4.2.2, does lead to a different probability distribution. In particular, it is not at all clear why the system that results from decoherence should possess any special properties. In general, that is surely not the case.

4.4 Features of classical holographic codes

In this section, we investigate to what extend classical probabilistic codes defined by a network on AdS produce properties similar to those of quantum error-correcting codes. As we find, classical holographic codes possess several interesting properties that are analogous

⁹A reconstruction of the bulk degrees of freedom is no longer possible, as for this task the knowledge of the mapping at each vertex is required. For fixed (and therefore known) mappings at each vertex that are obtained by sampling from some probability distribution, however, all properties we obtain in 4.4 still hold.

to properties of QECC and, in particular, AdS/CFT.

4.4.1 Ryu-Takayanagi formula

A relation analogous to the Ryu-Takayanagi formula (4.16) holds for the quantum error-correcting codes considered in [54, 55]. Considering a so-called holographic state – that is a boundary state of a tensor network of perfect tensors with a graph of non-positive curvature – then measured in units of $\log(2)$ the entanglement entropy of any connected region A on the boundary equals the length of the shortest cut¹⁰ γ_A through the network whose boundary matches that of A

$$E_A = |\gamma_A|. \quad (4.35)$$

That is, for these tensor networks, the *lattice RT formula* holds.

Interestingly, in the case of a classical holographic code a very similar statement is true. Of course, the concept of entanglement entropy does not exist in classical systems. In particular, there is no quantum entanglement. However, if we interpret this quantity not only as a measure of quantum entanglement but of correlations, or even more abstract as a measure of joint information between two subsystems, then there is a classical analogue namely the mutual information I_{cl} . It can formally be defined in the same way for both classical and quantum theories

$$I_{qu/cl}(A, B) = S(A) + S(B) - S(A, B), \quad (4.36)$$

where A and B denote two subsystems and the subscripts *qu* and *cl* specify the quantum mutual information I_{qu} , defined in terms of von Neumann entropies, and the classical mutual information I_{cl} , defined in terms of Shannon entropies. In a quantum theory, $S(A)$ and $S(B)$ are the von Neumann entropies of the respective reduced density matrices of subsystems A and B . $S(A, B)$ denotes in this case the von Neumann entropy of the union of A and B . For a bipartition of a system in a pure state into A and $B = A^c$, the total entanglement entropy vanishes and the two partitions show equal entropy, $S(A) = S(B) \equiv E_A$, such that

$$I_{qu}(A, A^c) = 2E_A. \quad (4.37)$$

¹⁰A cut is a path through the network that separates it into two disjoint sets of vertices and the length of the cut is given by the number of edges it crosses.

In a classical system $S(\cdot) \equiv S_S(\cdot)$ denotes the Shannon (or marginal) entropy of the system inside the bracket. As in the quantum case, the mutual information measures the joint information of the two subsystems A and B . However, for classical systems, the mutual information is solely due to classical correlations between subsystems.

Above considerations lead us to the conclusion that the mutual information is the natural candidate to quantify classical correlations between distinct parts of the classical system of interest. Further motivation to single it out as the measure of correlations in the present work is provided by its close relation to the entanglement entropy for pure states given in (4.37). Therefore, in what follows we formulate and prove a formula in terms of the mutual information that shows the same behaviour as the lattice version of the RT formula for QECCs. The intuition behind this formula is that it establishes a duality between a geometric quantity in the bulk – namely the length of the minimal cut – and classical correlations, as measured by the mutual information, on the boundary. This is closely analogous to the RT formula in AdS/CFT, where, for pure boundary states, the statement is that the entanglement entropy given by half of the mutual information is proportional to the area of a minimal surface in the bulk.

A version of the RT formula for classical holographic codes: For an arbitrary but fixed bulk input, the classical mutual information between a (connected) subregion A on the boundary and its complement A^c is given by the length of the minimal cut γ_A through the network, whose boundary matches that of A ,

$$I_{cl}(A, A^c) = |\gamma_A|. \quad (4.38)$$

Therefore, a version of the RT formula holds for these classical systems. The length of the minimal cut equals classical correlations on the boundary.¹¹

The proof of (4.38) that we give in appendix C.2 proceeds along the following steps. First, we argue that the length of any cut dividing the network into two parts provides an upper bound for the mutual information. Therefore, it is clear that the minimal cut γ_A gives the smallest upper bound. Subsequently, we complete the proof by showing that the edges that are crossed by the cut are uncorrelated. From that, it follows that the bound is saturated and, thus, (4.38) holds.

¹¹Note that the lattice RT formula (4.35), that was proven for holographic quantum error-correcting codes, can, for pure boundary states, be written in terms of the mutual information, as $I_{qu}(A, A^c) = 2|\gamma_A|$. Thus, it is evident that for quantum codes the mutual information is twice the classical one.

4.4.2 Bulk and operator reconstruction

As also discussed in 4.1.4, the information required to reconstruct some region of the bulk is contained in a boundary region if its entanglement wedge contains this region of the bulk [144] (see also figure 4.1). Here, in the classical case, we argue that the relevant wedge is the *correlation wedge* $C(A)$ that is defined as the region bounded by the minimal cut. It is therefore very similar to entanglement wedge reconstruction. In the following, we demonstrate the possibility of bulk reconstruction in the correlation wedge of a region of the boundary. Furthermore, we address the issue of operator reconstruction and show that – in our case – classical operations, like bit flips, on bulk degrees of freedom contained in the correlation wedge of some boundary region A can be performed by acting (non-locally) on the boundary degrees of freedom in A .

Let us assume A is connected and the minimal cut γ_A is unique, then we can reconstruct every bulk input bit in $C(A)$. This is evident by considering the algorithm for constructing the minimal cut as described in appendix C.2. In every step, it crosses three neighboring edges that allow to reconstruct all the other bits, including the bulk input of the vertex it jumps over – due to property (I).

Most bulk inputs in the complement of $C(A)$ cannot be reconstructed with some exceptions. These occur when the minimal cut crosses two neighboring bits from a vertex outside of the correlation wedge. Then the conditions we demand for the code allow that, for example, these two edge bits are maximally correlated with the respective bulk input and, hence, it can be reconstructed. This is visible in our explicit example and is most evident if we consider the $2 \rightarrow 4$ mapping given in (4.33). If the minimal cut crosses the second and third output, their knowledge immediately allows to reconstruct the bulk input. Besides these cases, that only allow to reconstruct inputs directly behind the minimal cut, no other bulk inputs in the complement of $C(A)$ can be reconstructed. We do not consider the exceptions as a crucial problem, as in the limit of large networks, *i.e.* where the number of bulk inputs goes to infinity, this effect is negligible.

Next, we consider the reconstruction of bulk operations.¹² Assuming a connected boundary region A , all bit flip operations O on vertices in the bulk region $C(A)$ can be represented as multiple bit flips in A . The reason for this is the following. From the algorithm to construct the minimal cut as given in appendix C.2 it follows that any vertex in region $C(A)$ has at least three neighboring edges that are contained in $C(A)$ and go in the direction of A ; see figure 4.6. Solely flipping some of these bits cannot affect bits in the complement

¹²Note that in a classical code the “bit flip operator” O is the only non-trivial operation.

of A . Therefore, degrees of freedom in A are sufficient to reconstruct operations in $C(A)$. Consider now the action of an operation O on a vertex in $C(A)$. Then it is possible to successively modify the edge bits in $C(A)$ until we reach the boundary region A . Obviously, no edge bit leaving $C(A)$ is touched by this procedure. Therefore the operation O on any bulk bit in $C(A)$ can be reconstructed by flipping the respective subset in A that was flipped by the above procedure. This is, in general, not possible for bit flips on vertices in the complement of $C(A)$.

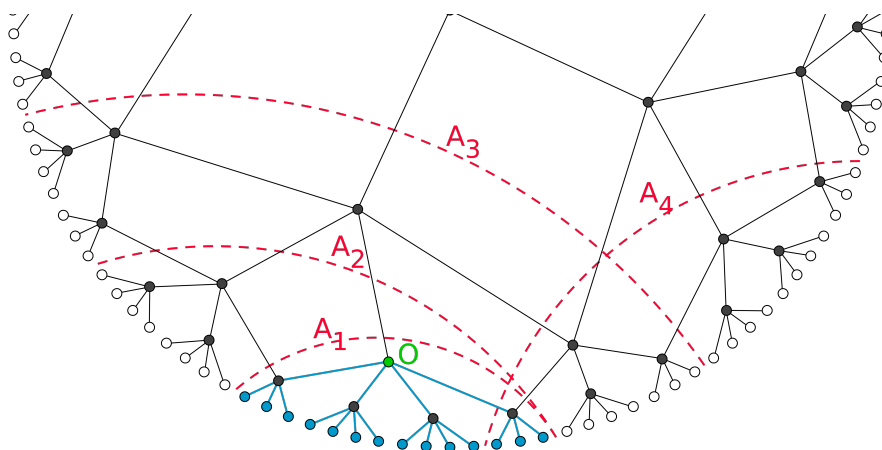


Figure 4.6: Representing bulk operations. The action of an operation O on one of the bulk bits, bit I , can be definitely represented on a boundary region A_i if I is contained in $C(A)$. Here, we show one particular example and marked the edges and vertices blue that can be affected by the operation on the green vertex. Here, $C(A_{1,2,3})$ contain the bit I and hence the bit flip O can be realized on these boundary regions. A_4 is an example that does not allow to reconstruct O .

Another question arising is whether the operations on the boundary region that realize a specific bit flip in the bulk depend on the configuration of the boundary bits. For the example given in (4.32), (4.33), and (4.34) this is not the case. This becomes evident if we look at the individual mappings. Flipping some inputs in a specific way always leads to the same possible flips in the output, independent of the actual values of the bits. For example, flipping the bulk input in the $3 \rightarrow 3$ map always flips the first and third output bit, or solely changing the edge input in the $2 \rightarrow 4$ mapping can always be realized by changing the second and third output. It never depends on the actual value of the bits. This holds for any mapping in the network, so in total it holds for the entire network. Therefore, the boundary realization of a bit flip operation on some bulk bit does not depend on the

boundary configuration. However, it is in general not unique. For a flip operation on one of the inputs, the $1 \rightarrow 5$ and the $2 \rightarrow 4$ mappings allow different realizations on the output. In our example in (4.33), a bulk input flip can be realized by flipping the first and third output or by flipping the second and fourth output. In general, a flip in the bulk has more representations on the boundary the deeper in the bulk it is located.

Subregion duality: The so-called subregion duality in AdS/CFT states that operators in the bulk can, in general, be represented on different subregions of the boundary, see figure 4.1. In [53], the toy model we reviewed in section 4.2.1 was suggested to capture essential features of this duality. Also in more elaborate tensor network models based on quantum error-correcting codes, it was shown to hold [54]. Here, we show that also in the classical network, we introduced, there is a notion of subregion duality. Indeed, it immediately follows from the fact that an operation O on any bulk input I can be represented on a boundary region A_i if $I \in C(A_i)$, as we have shown above; also see figure 4.6. Therefore, all representations of O on each of the A_i 's are dual to each other. This establishes a notion of subregion duality for classical holographic codes.

Black holes: A naive picture of asymptotically AdS spacetimes containing black holes is to describe these configurations by “cutting out” some region of the network [54]. The microstates of black holes are then described by the edge bits crossed by the horizon that function as inputs for the remaining network. In consequence, the black hole has a non-vanishing entropy that scales like the number of edges crossed by the horizon, *i.e.* it scales like the area of the black hole. Interestingly, this behavior is only expected in the semi-classical approach [151, 133] and should not appear at the classical level. However, we emphasize that this picture of black holes is very naive.

4.4.3 Secret sharing

Finally, we insert a brief discussion of the secret sharing property of classical holographic codes. The fact that these codes possess this property provides further motivation for their construction beyond the holographic interpretation. Secret sharing codes are characterized by the fact that there is a secret information (some string of bits) – or secret for short – that is distributed amongst several parties such that each party individually has no access to the secret. If, however, a sufficient number of parties collaborate they can gain access to the secret [152, 153].

Let us start the discussion by showing that the simple trit example that we introduced in section 4.3.1 falls into the class of secret sharing codes. In this example, we view the input trit as the secret. What the probabilistic code (4.25) does is that distributes the secret amongst three parties such that each party gets exactly one trit. Since the Shannon entropy of each of the three trits is maximal, $S_S = \log(3)$, an individual party has no information about the secret. However, as soon as two arbitrary parties collaborate and share their trits, they obtain full information about the secret. Thus, the code (4.25) is a $(n = 3, t = 2)$ -threshold scheme, where n denotes the number of parties and t denotes the threshold of parties that is necessary to obtain the secret.

As we argue next, also classical holographic codes belong to the class of secret sharing codes. To see this, we interpret the bulk inputs as the secret to be shared. Imagine now that each party is in possession of one of the boundary bits.¹³ Then, individually, each party has no chance to learn about any of the bulk inputs. However, by collaborating, *i.e.* by sharing their knowledge of their respective boundary bits, a team (a set of parties) can learn (part) of the bulk inputs (part of the secret). An illustrative example is the setting in which all bulk inputs are publicly known, except for the one in the center. We refer to the center bit as the secret. In this case, once a sufficient number of parties¹⁴ team up they can reveal the secret, while the remaining ones obtain no knowledge at all about the secret. Therefore, classical holographic codes are secret sharing codes.

4.5 On a possible physical interpretation

While so far we discussed classical holographic codes and their properties in a rather abstract way, in this section, we give a possible physical interpretation of these. In particular, we focus on the radial space-like direction and connect it to coarse graining in phase space, where the main idea is to interpret the additional bulk direction as parameter for an effective description of the boundary. This is similar to the interpretation of the radial direction in AdS as geometrizing the renormalization group flow of the dual CFT (see *e.g.* [136, 154] and section 4.1.1).

In our case, we interpret the boundary degrees of freedom/code subspace as the microstates of a classical statistical system characterized by a probability distribution in a dis-

¹³Of course, it does not have to be exactly one of the boundary bits per party, but also larger fractions of the boundary bits can be in possession of each party. However, for the sake of clarity and simplicity, let us assume that situation.

¹⁴Here, a team of roughly more than 50% of the parties is sufficient.

cretized phase space. To simplify the following considerations, but without loss of generality, we assume the probability distribution to be uniform within its support in phase space. Then the discretization is such that the region of phase space that supports the probability distribution is tiled with tiles of equal volume. It is the bulk inputs in the layer next to the boundary that dictate the support of the distribution, *i.e.* each bulk input corresponds to the location of one of the tiles in phase space.

Then each step in the radial direction, *i.e.* considering the network with one reduced layer, corresponds to joining¹⁵ neighbouring tiles and, therefore, by going deeper into the bulk, a more and more coarse grained description of the system is obtained. In terms of bulk inputs, moving inward for one layer of the graph means that the number of bulk inputs in this layer is strictly smaller than the one in the previous layer. The same is true for the number of boundary degrees of freedom. This number also decreases with each step. Therefore, coarse graining naturally emerges, see figure 4.7.

Thus, we interpret the bulk direction as a coarse graining parameter for an effective description of the boundary. It interpolates between the microscopic description at the boundary of AdS and the macroscopic, *i.e.* thermodynamic, description in the center of AdS, while both are connected by coarse graining phase space. From these considerations, the analogy to the renormalization group flow on the CFT side of AdS/CFT becomes apparent. In AdS/CFT the radial direction can be thought of as a geometric manifestation of the renormalization group flow from the UV to the IR fix point.

To illustrate the idea, consider the micro-canonical description of a free gas. The probability density $\rho(X, P)$, where $X = \{x_i\}$ and $P = \{p_i\}$ denote the collection of positions and momenta of the particles, has support only in the close vicinity to the sphere characterized by $E = \sum_i \frac{m_i}{2} |p_i|^2$ in phase space, where E is the total energy and m_i is the mass of particle i . We denote the sphere by S_E . Then, macroscopically, the system is completely characterized by one (macroscopic) variable, the total energy E . In phase space, this can be viewed as maximally ignorant description (in our language, a completely coarse grained description), where one only cares about the fact that the underlying microscopic state of the system actually is described by an arbitrary point in S_E . In case of classical networks, this is the description in the center of the bulk. Let us now consider a more fine grained description, for example, by dividing S_E in k ($k \in \mathbb{N}, k > 1$) patches of equal volume. Physically, the more fine grained description is due to some additional knowledge. For

¹⁵In general, the coarse graining does not necessarily require to join tiles pairwise. In principle, any constant number k of tiles can be joined in each step. k depends on the structure of the underlying graph defined by the classical holographic code.

example, one might for some reason be able to distinguish the micro-state of the actual configuration to a precision characterized by the volume of the patches. Going to this more fine grained description of the system corresponds to proceeding in the radial direction in the bulk. Finally, a completely fine grained (microscopic) description corresponds to the boundary. That is, the number of bulk inputs in each layer of the network counts the information about the system. This number increases in the radial direction and interpolates between the macroscopic and the microscopic description.

In this picture, for a black hole in the center of AdS, coarse graining has to terminate, when the horizon of the black hole is reached. Therefore, not all patches can be joined and a non-vanishing (coarse grained) entropy emerges.

4.5 On a possible physical interpretation

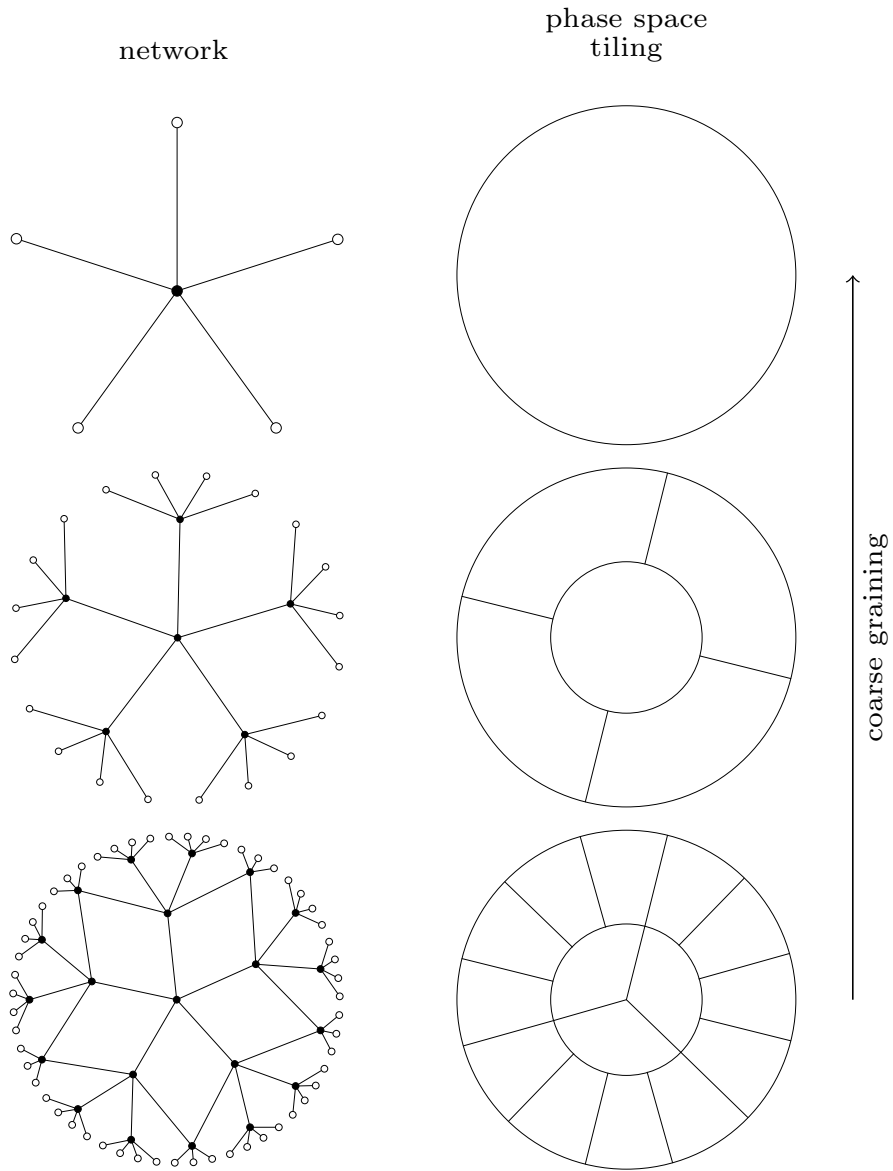


Figure 4.7: The bulk direction is interpreted as a coarse graining parameter for an effective description of the boundary. It interpolates between the microscopic description at the boundary of AdS and the macroscopic description in the center of AdS, while both are connected by coarse graining phase space.

Conclusion and Outlook

In this work we discussed the entanglement entropy in two-dimensional conformal field theories with interfaces and introduced *classical holographic codes*, where both was done to shed more light on the correlation structure in different physical situations.

Entanglement entropy through topological defects: In this part our focus has been on unitary CFTs with a discrete spectrum. We trace out one side of the interface, *i.e.* half of the space, which results in a reduced density matrix with (3.13) giving the probability of finding the reduced system in a thermal state in the representation (i, \bar{i}) . The final result for the entanglement entropy through a topological defect is (3.16). The universal term from no defect insertion proportional to $\log L$ is not affected, because correlation functions do not depend on the position or shape of the interface insertion. However, to subleading order the topological interface contributes a universal term to the entanglement entropy. It is the negative of the relative entropy (Kullback-Leibler divergence) of the distribution associated to the interface, compared with the situation when there was no interface to start with.

We are also able to derive the left/right entanglement entropy at a boundary (3.51) proceeding analogously as before after unfolding a theory with a boundary to a chiral theory with a topological defect. However, in this situation we lose the interpretation of the entanglement entropy in terms of a relative entropy although the resulting formulas have a similar structure.

The Kullback-Leibler divergence has many appealing features. In the present work, we have interpreted some of them in the context of interfaces. In particular, we have given a meaning to its positivity: a topological interface will never increase entanglement. We have also connected a vanishing Kullback-Leibler divergence to interfaces with properties that do not lead to any information loss.

One particular issue that we did not investigate further in this work is that the Kullback-Leibler divergence measures the difference between probability distributions, and in this sense shares some properties with a distance. We only obtained Kullback-Leibler di-

Conclusion and Outlook

vergences of interfaces with respect to the identity defect. In order to explore the distance property further, it would be interesting to study concrete physical realizations for Kullback-Leibler divergences with respect to arbitrary interfaces as reference points.

The Kullback-Leibler divergence is obviously not symmetric, and even after a symmetrization fails to satisfy the triangle inequality. The distance measure it might yield for topological defects would hence share the same features.

Interfaces have been used to define distances before. In particular, in [155] the interface entropy $\log g$ of deformation interfaces¹⁶ was identified with Calabi's Diastasis function. Ultimately, the proposal was that the g -factor between interfaces can be used to define a distance between different CFTs. However, also in this case they found that the triangle inequality is not satisfied.

A further observation for the $\log g$ distance is that it gives rise to a metric at the infinitesimal level, which coincides with the Zamolodchikov metric on the moduli space. This is again similar in the case of the Kullback-Leibler divergence, where the infinitesimal limit yields the Fisher information metric. At the moment this property is rather formal, as the interfaces we have studied here are generally labeled by discrete numbers.

Finally, let us comment on $\mathcal{N}=2$ supersymmetric theories. Such theories can be topologically twisted, and one can define boundary as well as interface gluing conditions that are compatible with these topological twists. On the level of the topological theory, all interfaces can be moved freely. It would be interesting to consider entanglement entropy through topological interfaces in the supersymmetric situation, where entanglement should have a topological interpretation. For results on the supersymmetric case without interfaces see [156].

Entanglement entropy through conformal defects of the Ising model: We have discussed the entanglement entropy through general conformal interfaces in the critical Ising model – *i.e.* a GSO projected free fermion theory – and for supersymmetric systems. We have computed the prefactor $\sigma(\mathcal{T})$ given in (3.139) which dresses the leading order term in the entanglement entropy and seen explicitly how it arises purely from the contribution of higher oscillator modes. These largely cancel against bosonic modes in the model with supersymmetry. We could also show that the constant shift which was also computed in the case of only topological interfaces stays the same withing their class of conformal defects given by marginal deformations.

¹⁶Deformation interfaces relate different CFTs in the same moduli space in a minimal way.

It would be very interesting to generalize these findings further. It is suggestive that also in more general systems topological data of the defect will enter in a constant sub-leading shift of the entanglement entropy, whereas oscillator data enters the prefactor of leading order term.

The defects we investigated in this paper can be regarded as marginal perturbations of the topological defects of the Ising model. The latter are labeled by the primaries of the theory [27], in the case at hand $1, \sigma, \epsilon$. The perturbing operator is a marginal defect perturbation, living only on the defect. It would be interesting to consider more generally the entanglement entropy for initially topological defects perturbed by marginal and possibly also relevant defect operators (see *e.g.* [157]).

Another form of perturbation appears for the interfaces in the free boson theory considered in [30] and in section 3.2.6 above. They come in several classes characterized by topological data k_1, k_2 , which cannot be changed under perturbations. However, for k_1, k_2 fixed, there are again interfaces related by perturbations, but this time marginal bulk perturbations deforming the CFT at one side of the defect.¹⁷ It would be very interesting to generalize this to other systems related by RG domain walls [23, 24, 158, 159] (where the free boson “RG domain walls” are obtained for $k_1 = k_2 = 1$ in the above discussion) and to compute the entanglement entropy for them, *e.g.* in perturbation theory, similar to the discussion of the defect entropy in [158].

Apart from being interesting from the point of view of the physics of impurities, this program might also be interesting from the point of view of the physics of defects. In the discussion of defects, well-known quantities are the g -factor and the reflectivity/transmissivity. The entanglement entropy might provide another useful characteristic of an interface, where the transmissivity enters the prefactor of the logarithmic part whereas topological features enter separately, namely in the constant part. This is different for the g -factor, where both topological data and oscillator data enter in one factor.

Classical Holographic Codes: We introduced *classical holographic codes* and analyzed their properties. They are defined via a network originating from a uniform tiling of a constant time slice of AdS_3 . Interpreting the input of the codes as the bulk degrees of freedom and its output as the boundary degrees of freedom, a classical holographic code establishes a map between these. A main feature of the codes is that a classical version of the Ryu-Takayanagi formula holds: the mutual information between a connected region A

¹⁷There are also marginal defect perturbations for the free boson, which however change neither transmissivity nor entanglement entropy.

Conclusion and Outlook

on the boundary and its complement A^c is given by the length of the minimal cut γ_A connecting the ends of the region A . We have called the bulk region that is enclosed between γ_A and the boundary region the correlation wedge $C(A)$ of A . We have shown that the bulk inputs contained in $C(A)$ can always be reconstructed from the data in A but never by the data in the complement A^c . Furthermore, we have shown that a (bit flip) operation O , acting on any bulk input contained in $C(A)$, can be represented by multiple bit flips in the boundary region. These feature naturally establish a notion of subregion duality. That is, we have shown that any operation O acting on some input in the bulk can be represented in any boundary region A that possesses a respective correlation wedge $C(A)$ such that the bulk input is contained in it. Finally, the additional bulk dimension can be interpreted as a coarse graining parameter that interpolates between the microscopic description at the boundary of AdS and the macroscopic description in the center of AdS.

We did not intend to construct a purely classical toy model for the AdS/CFT correspondence. However, interestingly, all the features we described above are to be expected from AdS/CFT. Furthermore, these are the features that are modeled by quantum error-correcting codes, such as the ones in [53, 54]. Of course, there is the obvious caveat that the boundary theory is purely classical and by no means can approximate a quantum CFT. In particular, the entanglement structure of a quantum CFT is completely absent. Another shortcoming of the classical code is that bulk and boundary operations (bit flips) are rather simple compared to general operators appearing in a CFT. Finally, in our particular example, the center vertex has some shortcomings, as we described. However, especially in the limit of large networks, the center vertex should not cause serious problems.

Even so there are these shortcomings in the construction, it is interesting to note that, by starting from a purely classical code, one can obtain all the AdS/CFT-like features, we outlined above. This shows that, given the geometric structure of the network, the scaling of the mutual information, *i.e.*, a version of the RT formula, and important bulk and operator reconstruction properties are due to the “correlation structure” and can exist even classically in the absence of quantum correlations, like entanglement.

For the future, it would be interesting to generalize the bulk-to-boundary mappings of this work. In particular, it is an open question, whether suitable random networks could possess properties similar to the ones of classical holographic codes. Recently, for random tensor networks, this was shown to be true [56]. Furthermore, it might be worthwhile to see whether classical analogs of the Witten-like diagrams introduced in [57] could be found for classical holographic codes. Another interesting project would be to find a

connection between classical holographic codes and existing probabilistic codes used for error correction that, *e.g.*, can be related to spin glasses models [160].

Danksagung

Abschließend möchte ich allen danken, die mir in verschiedenster Weise bei der Entstehung dieser Arbeit geholfen haben.

Im Besonderen möchte ich mich bei Ilka Brunner bedanken. Sie hat mich hervorragend betreut und mir ausgezeichnete Projekte vorgeschlagen. Es hat immer Spaß gemacht mit ihr über Physik und die Arbeit zu diskutieren. Auch kann man sich mit ihr wunderbar über ganz verschiedene Themen abseits der Physik unterhalten. Ich freue mich sehr, dass sie mich als Doktorand aufgenommen hat.

Weiteren besonderen Dank möchte ich Cornelius Schmidt-Colinet und Daniel Jaud widmen. Wir drei zusammen bilden das Fußvolk der CFT-Community hier in München. Die Arbeit an der gemeinsamen Veröffentlichungen und natürlich weit darüber hinaus hat immer Spaß gemacht und ich bin froh, dass ich Teil einer so angenehmen und vor allem sympathischen Gruppe war.

Den dritten ganz besonderen Dank möchte ich Benedikt Richter aussprechen. Die Arbeit mit ihm an unserer gemeinsamen Veröffentlichung hätte besser kaum sein können. Auch als Nebensitzer im Büro kann ich mir kaum jemand Besseren vorstellen – sowohl im menschlichen als auch im professionellen Sinne.

Weiteren Dank möchte ich meinen anderen Nebensitzern im Büro Artem, Eric und Marc widmen. Durch sie war die Atmosphäre im Büro immer angenehm und freundlich, was einem guten Gelingen der Doktorarbeit nur zu Gute steht.

Zum Schluss möchte ich noch meiner Freundin Kim danken, die sich immer tapfer meine Physik anhört und mich stets unterstützt.

Appendix A

Special Objects

A.1 Important functions in CFT

In the following we use $q = e^{2\pi i\tau}$.

The Dedekind η -function

The Dedekind η -function is defined as

$$\eta(\tau) = q^{\frac{1}{24}} \prod_{n=1}^{\infty} (1 - q^n) . \quad (\text{A.1})$$

It behaves under T - and S -transformations as

$$\eta(\tau + 1) = e^{\frac{\pi i}{12}} \eta(\tau), \quad \eta\left(-\frac{1}{\tau}\right) = \sqrt{-i\tau} \eta(\tau) . \quad (\text{A.2})$$

The Θ -functions

An important class of functions that appear in Virasoro characters are the so-called generalized Θ -functions. They are defined by

$$\Theta_{m,k}(\tau) = \sum_{n \in \mathbb{Z} + \frac{m}{2k}} q^{kn^2} . \quad (\text{A.3})$$

Appendix A Special Objects

The T -transformation of the Θ -functions is given by

$$\Theta_{m,k}(\tau + 1) = e^{\pi i \frac{m^2}{2k}} \Theta_{m,k}(\theta), \quad (\text{A.4})$$

where the S -transformation of the Θ -functions takes the following form:

$$\Theta_{m,k} \left(-\frac{1}{\tau} \right) = \sqrt{-i\tau} \sum_{m'=-k+1}^k S_{m,m'} \Theta_{m',k}(\tau), \quad (\text{A.5})$$

with the modular S -matrix elements given by

$$S_{m,m'} = \frac{1}{\sqrt{2k}} e^{-\pi i \frac{m m'}{k}}. \quad (\text{A.6})$$

The θ -functions

The general form of the θ -functions is

$$\begin{aligned} \theta[\alpha, \beta](\tau, z) &= \sum_{n \in \mathbb{Z}} q^{\frac{1}{2}(n+\alpha)^2} e^{2\pi i(n+\alpha)(z+\beta)} \\ &= \eta(\tau) e^{2\pi i\alpha(z+\beta)} q^{\frac{\alpha^2}{2} - \frac{1}{24}} \prod_{n=1}^{\infty} \left(1 + q^{n+\alpha-\frac{1}{2}} e^{2\pi i(z+\beta)} \right) \left(1 + q^{n-\alpha-\frac{1}{2}} e^{-2\pi i(z+\beta)} \right). \end{aligned} \quad (\text{A.7})$$

Important special cases are

$$\begin{aligned} \theta_1(\tau) &= \theta\left[\frac{1}{2}, \frac{1}{2}\right](\tau, 0) = \sum_{n \in \mathbb{Z}} (-1)^n q^{\frac{1}{2}(n+\frac{1}{2})^2} = \frac{1}{2} \eta(\tau) q^{\frac{1}{12}} \prod_{n=0}^{\infty} (1 - q^n)^2 \equiv 0, \\ \theta_2(\tau) &= \theta\left[\frac{1}{2}, 0\right](\tau, 0) = \sum_{n \in \mathbb{Z}} q^{\frac{1}{2}(n+\frac{1}{2})^2} = \frac{1}{2} \eta(\tau) q^{\frac{1}{12}} \prod_{n=0}^{\infty} (1 + q^n)^2, \\ \theta_3(\tau) &= \theta[0, 0](\tau, 0) = \sum_{n \in \mathbb{Z}} q^{\frac{n^2}{2}} = \eta(\tau) q^{-\frac{1}{24}} \prod_{n=0}^{\infty} (1 + q^{n+\frac{1}{2}})^2, \\ \theta_4(\tau) &= \theta\left[0, \frac{1}{2}\right](\tau, 0) = \sum_{n \in \mathbb{Z}} (-1)^n q^{\frac{n^2}{2}} = \eta(\tau) q^{-\frac{1}{24}} \prod_{n=0}^{\infty} (1 - q^{n+\frac{1}{2}})^2. \end{aligned}$$

The modular transformations for the general θ -function is given by

$$\begin{aligned}\theta[\alpha, \beta](\tau + 1, z) &= e^{-i\pi\alpha(\alpha-1)}\theta[\alpha, \alpha + \beta - \frac{1}{2}](\tau, z), \\ \theta[\alpha, \beta](-\frac{1}{\tau}, \frac{z}{\tau}) &= \sqrt{-i\tau}e^{2\pi i\alpha\beta + i\pi\frac{z^2}{\tau}}\theta[\beta, -\alpha](\tau, z)\end{aligned}\tag{A.8}$$

from which we find

$$\begin{aligned}\theta_1(\tau + 1) &= e^{\frac{\pi i}{4}}\theta_1(\tau), & \theta_1(-\frac{1}{\tau}) &= e^{\frac{\pi i}{2}}\sqrt{-i\tau}\theta_1(\tau), \\ \theta_2(\tau + 1) &= e^{\frac{\pi i}{4}}\theta_2(\tau), & \theta_2(-\frac{1}{\tau}) &= \sqrt{-i\tau}\theta_4(\tau), \\ \theta_3(\tau + 1) &= \theta_4(\tau), & \theta_3(-\frac{1}{\tau}) &= \sqrt{-i\tau}\theta_3(\tau), \\ \theta_4(\tau + 1) &= \theta_3(\tau), & \theta_4(-\frac{1}{\tau}) &= \sqrt{-i\tau}\theta_2(\tau).\end{aligned}$$

A.2 Bernoulli polynomials and numbers

The Bernoulli polynomials $B_n(x)$ are defined by

$$\frac{te^{xt}}{e^t - 1} = \sum_{n=0}^{\infty} B_n(x) \frac{t^n}{n!} \quad \text{with } |t| < 2\pi.\tag{A.9}$$

The Bernoulli numbers B_n are given by the polynomials evaluated at $x = 0$, namely $B_n = B_n(0)$. Odd Bernoulli numbers vanish.

The sums of m th powers of integers can be expressed by the use of Bernoulli polynomials and numbers as

$$\sum_{k=1}^N k^m = \frac{B_{m+1}(N+1) - B_{m+1}}{m+1}\tag{A.10}$$

Using the facts that $B'_n(x) = nB_{n+1}(x)$ and $B_n(1) = B_n$ for $n \neq 1$ and $B_1(1) = 1/2$ together with the integral representation

$$B_{2n} = 4n(-1)^n \int_0^{\infty} \frac{t^{2n-1}}{1 - e^{2\pi t}} dt,\tag{A.11}$$

it follows that

$$\frac{1}{n+1} \partial_x B_{n+1}(x)|_{x \rightarrow 1} = \delta_{n,0} + \frac{1}{2} \delta_{n,1} + (i^n - (-i)^n) \int_0^{\infty} \frac{nt^{n-1}}{1 - e^{2\pi t}} dt.\tag{A.12}$$

Appendix B

Entanglement through Interfaces

The following calculations are directly adapted from [29] and [26].

B.1 Entanglement entropy of a fusion product

In this appendix we show that the pattern (3.45) holds. This follows from the fact that in the large k limit, the contribution

$$-2 \int_0^1 \frac{\sin^2(\pi(a+1)x) \sin^2(\pi(b+1)x)}{\min(a+1, b+1) \cdot \sin^2(\pi x)} \log \left(\frac{\sin^2(\pi(a+1)x) \sin^2(\pi(b+1)x)}{\sin^4(\pi x)} \right) dx \quad (\text{B.1})$$

is a rational number. In order to see this, the basic integral that has to be evaluated is

$$-\frac{1}{\pi} \int_0^\pi \frac{\sin^2((a+1)x) \sin^2((b+1)x)}{\sin^2(x)} \log(\sin^2((l+1)x)) dx. \quad (\text{B.2})$$

By the two representations of Clausen's function Cl_1 we can express the logarithmic factor in terms of the sum

$$\log(\sin^2(y)) = -\log 4 - \sum_{k=1}^{\infty} \frac{2 \cos(2ky)}{k}. \quad (\text{B.3})$$

We note that the $\log 2$ terms cancel out in (B.1), so it is enough to keep only the sum over cosines from the right-hand side of (B.3) for further calculations. One might be concerned that while the individual terms in the summation over k give rational results, resummation may yet yield something non-rational. In order to see that this is not the case we eliminate the sine functions in the denominator of (B.2) by writing the remaining sine functions in

Appendix B Entanglement through Interfaces

the numerator in terms of spread polynomials [161]

$$\sin^2(nx) = \sum_{p=0}^{n-1} \frac{n}{n-p} \binom{2n-1-p}{p} (-4)^{n-1-p} \sin^{2(n-p)}(x) =: \sum_{\{p\}} \sin^{2p}(x). \quad (\text{B.4})$$

Since we are not interested in the precise value of the finite result, the only relevant property for us is that the spread polynomials have rational coefficients and finite order. We define the summation symbol on the right-hand side to indicate a finite sum of trigonometric functions with rational coefficients. We reduce the right-hand side further by the identity

$$\sin^{2p}(x) = \frac{1}{2^{2p}} \binom{2p}{p} + \frac{2}{2^{2p}} \sum_{r=0}^{p-1} (-1)^{p-r} \binom{2p}{r} \cos(2(n-r)x) =: \sum_{\{r\}} \cos(2rx). \quad (\text{B.5})$$

The purpose of writing (B.4) and (B.5) is to demonstrate that (B.1) can indeed be written in the form

$$\frac{1}{\pi} \int_0^\pi \sum_{\{s\}} \cos(2sx) \sum_{k=1}^{\infty} \cos(2k(l+1)x) \frac{1}{k} dx. \quad (\text{B.6})$$

By the integral identity $\int_0^\pi \cos(nx) \cos(mx) dx = \frac{\pi}{2} \delta_{n,m}$, the finite sum over s reduces the infinite sum over k to a rational result, and we obtain (3.45) as proposed.

B.2 Odd is enough

The following calculation shows that for the derivation of the EE through a defect in the free fermion theory or the Ising model it suffices to consider the formula for odd K .

$$Z(K) \stackrel{(a)}{=} \prod_{n>0} (p^+)^K + (p^-)^K + 2 (\sin(2\phi) e^{-n\delta})^{2K} \equiv \prod_{n>0} F_n(K) \quad (\text{B.7})$$

$$\begin{aligned} &\stackrel{(b)}{=} \prod_{n>0} \left[I(K) 4 (\sin(2\phi) e^{-n\delta})^{2K} + \prod_{k=1}^K 2e^{-2n\delta} (2 \cos^2(\nu_k) - 1 + \cosh(2n\delta)) \right] \\ &\equiv \prod_{n>0} G_n(K) + H_n(K), \end{aligned} \quad (\text{B.8})$$

where $I(K)$ is an analytic function interpolating between the values for odd and even K with

$$I(K) = \begin{cases} 0 & \text{for odd } K \\ 1 & \text{for even } K \end{cases}. \quad (\text{B.9})$$

In particular we have $G_n(1) = 0$ and $F_n(1) = G_n(1)$. The EE is then given by

$$S = (1 - \partial_K) \log Z(K)|_{K \rightarrow 1} \quad (\text{B.10})$$

$$\stackrel{(a)}{=} \sum_{n>0} \left(\log F_n(1) - \frac{1}{F_n(1)} F'_n(1) \right) \quad (\text{B.11})$$

$$\stackrel{(b)}{=} \sum_{n>0} \left(\log(G_n(1) + H_n(1)) - \frac{1}{G_n(1) + H_n(1)} (G'_n(1) + H'_n(1)) \right) \quad (\text{B.12})$$

$$= \sum_{n>0} \left(\log F_n(1) - \frac{1}{F_n(1)} (G'_n(1) + H'_n(1)) \right). \quad (\text{B.13})$$

We want to assume that the natural analytical continuation for (a) gives the right result for the entanglement entropy. Then the last line shows that if $G'_n(1)$ equals $F'_n(1)$ we need $H'_n(1)$ to vanish (and thus also $I'(1)$) and in particular it suffices to consider $G_n(K)$ in $Z(K)$ to derive the EE. The hard part here is to derive the derivative of $G_n(K)$. We start with rewriting

$$\begin{aligned} G_n(K) &= \prod_{k=1}^K 2e^{-2n\delta} \left(1 + \cosh(2n\delta) - \sin^2 \left(\pi \frac{k}{K} \right) \sin^2(2\phi) \right) \\ &= \exp \left(\sum_{k=1}^K \log \left[2e^{-2n\delta} \left(1 + \cosh(2n\delta) - \sin^2 \left(\pi \frac{k}{K} \right) \sin^2(2\phi) \right) \right] \right) \quad (\text{B.14}) \\ &\equiv \exp \left(\sum_{k=1}^K g_n(k/K) \right), \end{aligned}$$

where $g_n(x) \equiv \log [2e^{-2n\delta} (1 + \cosh(2n\delta) - \sin^2(\pi x) \sin^2(2\phi))]$ can be expanded around $x = k/K = 0$, so that

$$\begin{aligned} G_n(K) &= \exp \left(\sum_{m \geq 0} \frac{g_{nm}}{K^m} \sum_{k=1}^K k^m \right) \\ &= \exp \left(\sum_{m \geq 0} \frac{g_{nm}}{K^m} \frac{B_{m+1}(K+1) - B_{m+1}}{m+1} \right). \quad (\text{B.15}) \end{aligned}$$

Appendix B Entanglement through Interfaces

$B_N(u)$ and B_N are the Bernoulli polynomials and numbers, respectively, as defined in A.2. Proceeding similar as in (3.136) and the following one can calculate

$$\begin{aligned}
G'_n(K) &= \exp\left(\sum_{m \geq 0} \frac{g_{nm}}{K^m} \frac{B_{m+1}(K+1) - B_{m+1}}{m+1}\right) \cdot \left(\sum_{m \geq 0} \frac{g_{nm}}{m+1} \partial_K B_{m+1}(K)\right) \\
&\xrightarrow{K \rightarrow 1} \exp(g_n(1)) \cdot \left(g_n(0) + \frac{1}{2}g'_n(0) + \int_0^\infty \frac{ig'_n(it) - ig(-it)}{1 - e^{2\pi t}} dt\right) \\
&= 2e^{-2n\delta} (1 + \cosh(2n\delta)) \left(\log[2e^{-2n\delta} (1 + \cosh(2n\delta))] - \right. \\
&\quad \left. - \int_0^\infty \frac{2\pi(\coth(\pi t) - 1) \sin(2\phi) \sinh(2\pi t)}{1 + \cosh(2n\delta) + 2\sin^2(2\phi) \sinh^2(\pi t)} dt\right) \\
&= \sqrt{2} \operatorname{arctanh}\left(\frac{\sqrt{\cos(4\phi) + \cosh(2n\delta)}}{\sqrt{2} \cosh(n\delta)}\right) \frac{\sqrt{\cos(4\phi) + \cosh(2n\delta)}}{\cosh(n\delta)} + \log(\sin^2(2\phi)) - \log(4 \cosh^2(n\delta))
\end{aligned}$$

At this point one only needs tedious algebraic deformations to show that the latter is equal to

$$F'_n(1) = e^{-2n\delta} (\log(e^{-2n\delta} p^+) p^+ + \log(e^{-2n\delta} p^-) p^- + 2 \log(e^{-2n\delta} \sin^2(2\phi)) \sin^2(2\phi)) , \tag{B.16}$$

with p^\pm given as in the main text.

Appendix C

Classical Holographic Codes

C.1 Some properties of \mathfrak{S}

In this appendix, we discuss some of the properties of the set \mathfrak{S} that we use in section 4.3.2. First we consider bipartitions into substrings of length three that are maximally correlated. The maximal possible value for the mutual information is, in this case, $3 \log(2)$ which also is the maximal possible Shannon entropy of three bits. Look, for example, at the bipartition into input and output bits of the $3 \rightarrow 3$ mapping, *i.e.* $s_{\text{in}} = i_1 i_2 i_3$ and $s_{\text{out}} = i_4 i_5 i_6$, where i_n is the n th bit in the full strings. We require $S_S(s_{\text{in}}) = 3 \log(2)$, such that

$$0 = S_S(s_{\text{out}}) - S_S(\mathfrak{S}). \quad (\text{C.1})$$

Since $S_S(s_{\text{out}}) \leq 3 \log(2)$ and $S_S(\mathfrak{S}) \geq 3 \log(2)$, condition (C.1) can only be satisfied if $S_S(s_{\text{out}}) = 3 \log(2) = S_S(\mathfrak{S})$. It follows that $|\mathfrak{S}| = N = e^{S_S(\mathfrak{S})} = 2^3 = 8$ and the $3 \rightarrow 3$ map is bijective. In general, it is true that

- (I) the knowledge of three neighboring edge bits gives full information about the three complementary bits.

Let us next consider bipartitions into a single bit and the remaining five bits. The maximal possible mutual information is $\log(2)$. Since we already know that the Shannon entropy of the set \mathfrak{S} is $3 \log(2)$, we can conclude that the entropy of any single bit must be $\log(2)$ and that of any substring of five bits has to be $3 \log(2)$. From the latter it follows that no two substrings of length five can be the same. One can also show that no two single bits i_A and i_B in \mathfrak{S} can be correlated by deriving their mutual information which

Appendix C Classical Holographic Codes

can be expressed in terms of the maximal mutual information of the bipartitions as

$$\begin{aligned} I_{\text{cl.}}(i_A, i_B) &= S_S(i_A) + S_S(i_B) - S_S(i_A \cup i_B) \\ &= \log(2) + \log(2) - 2\log(2) = 0. \end{aligned} \tag{C.2}$$

As a consequence,

- (II) no information about any other single bit can be obtained by the knowledge of one particular bit.

Finally, we consider the case of bipartitions into strings of length two and their complement. In this case, the maximal value for the mutual information is $2\log(2)$. As before, one can show that the Shannon entropy of two bits is always $2\log(2)$ (we already used this in (C.2)) and the entropy of four bits has to equal $3\log(2)$, such that any two substrings of length four have to be different. The mutual information between two bits and a third bit vanishes if their union or their complement contains only neighboring bits. In particular, it follows that two neighboring edge bits never reveal information about bits next to them and in general two bits can at most give one other bit with certainty.

A further consequence of demanding that any bipartition of \mathfrak{S} into substrings of non-equal size is maximally correlated, is that the tripartite information $I_3(A, B, C)$ that is defined as

$$I_3(A, B, C) = S_S(A) + S_S(B) + S_S(C) - S_S(AB) - S_S(AC) - S_S(BC) + S_S(ABC), \tag{C.3}$$

where A, B, C denote arbitrary subsets of neighboring bits, is non-positive, $I_3(A, B, C) \leq 0$. For all cases except for $|A| = |B| = |C| = 2$, this can be shown using the upper bound $I_3(A, B, C) \leq \min\{I_{\text{cl.}}(A, B), I_{\text{cl.}}(B, C), I_{\text{cl.}}(A, C)\}$ that was obtained *e.g.* in [162]. In the special case of a split in three sets of equal cardinality with $|A| = |B| = |C| = 2$, it follows from the fact that $I_3(A, B, C) = I_{\text{cl.}}(A, B) + I_{\text{cl.}}(A, C) - S(A) = 0$. The physical interpretation of $I_3(A, B, C) \leq 0$ is that the mutual information between any pair of subsets A, B , and C increases once the other random variable is known. Interestingly, it was shown that, for boundary regions A, B , and C , $I_3(A, B, C) \leq 0$ holds in AdS/CFT [39].

C.2 Proof of a version of the RT formula for classical holographic codes

In this appendix, we prove a version of the RT formula (4.38) for classical holographic codes. Therefore, we first argue that the mutual information of a connected region A and its complement is bounded from above by the length of the minimal cut γ_A , *i.e.*,

$$I_{cl}(A, A^c) \leq |\gamma_A|. \quad (\text{C.4})$$

It is evident that all correlations in the system must be generated in the interior of the bulk and are transported by the network to the boundary. If we consider an arbitrary cut through the network whose ends coincide with the boundary of the interval, then all correlations between regions A and A^c are transmitted through the edges that are crossed by the cut. Of course, that is also true for the minimal cut γ_A and, since every edge can at most transfer one bit of information, the amount of correlation (or shared information) is bounded from above by the length of this cut. Therefore, bound (C.4) holds.

In the case of classical holographic codes, the upper bound (C.4) for the mutual information is saturated, as we show next. The general idea of the proof is that any of the bits that are transferred through an edge crossed by the minimal cut γ_A can be reconstructed with certainty from either side. Furthermore, there is no correlation between the edge bits crossed by γ_A . Then each of the bits has to carry one bit of shared information and hence contribute to the mutual information by one. In consequence, the mutual information is given by the length of the minimal cut γ_A and the version of the RT formula (4.38) holds.

One can convince oneself that this statement is true by considering an algorithm for constructing the minimal cut that was also presented in [54]. Given some connected region of the boundary, the algorithm starts with the cut that crosses all open edges at the boundary. The algorithm then proceeds in the following way: It lets the cut jump over a vertex if at least three edges of one vertex are crossed by the cut. After the jump it crosses all the edges of the vertex that were not crossed before. Then, given the new cut, it starts again. The algorithm stops when the cut is minimal, cf. figure C.1. From that it is clear that each bit flowing through any edge crossed by a cut constructed in this way can be reconstructed from the bits of the boundary region it starts from. This directly follows by applying property (I) in every step of the algorithm.

In most cases the minimal surface constructed from a connected region A on the bound-

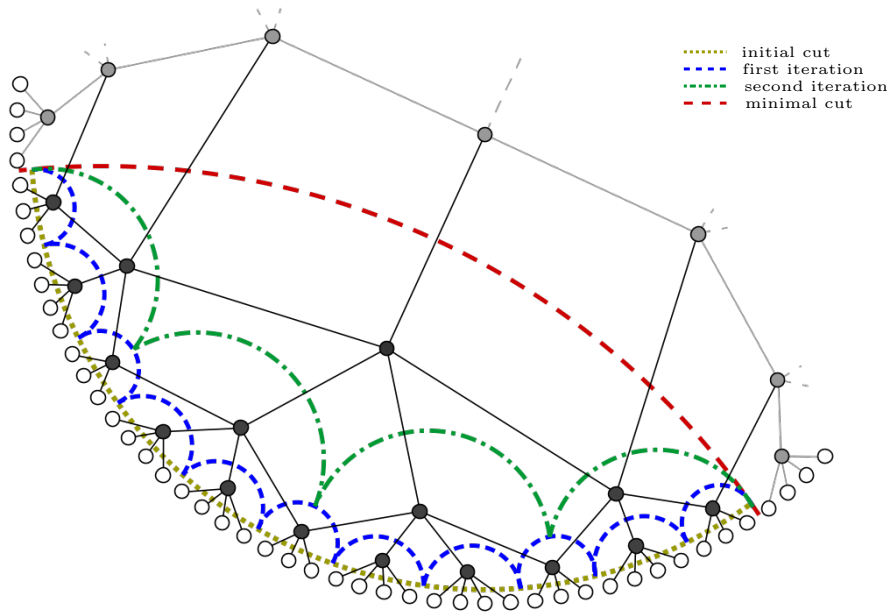


Figure C.1: Visualization of the algorithm that constructs the minimal cut (red) for a boundary region. The algorithm starts from a cut that divides the bits in that boundary region from the remaining system (initial cut). Then, for each vertex, it evaluates how many edges belonging to the vertex are crossed by this cut. If this number is larger or equal to three, the cut is moved across the vertex such that it cuts all edges of this vertex that have previously not been crossed (in the first iteration that results in the blue cut). Subsequently, it takes the new cut as starting point. The algorithm terminates, when the cut is minimal (red cut).

ary and the one from its complement coincide. However, as also mentioned in [54], there is the possibility that these do not coincide. If the minimal cut is unique, we certainly can construct its edge from both boundary regions.

Next, we argue that the edge bits that are crossed by a **unique** minimal cut cannot be correlated. Therefore, we show that no information about an edge bit can be obtained by the knowledge of any subset of the remaining edge bits.

First, let us assume the contrary, *i.e.*, one can obtain information about a crossed edge bit e from the knowledge of other crossed edge bits. In figure C.2, which illustrates our proof, this is the green edge. Now fix the vertex v from which one assumes to get information about e . Edges at that vertex that point “deeper into the bulk”, and hence away from the minimal cut, cannot carry information about any other leg crossed by the minimal cut

C.2 Proof of a version of the RT formula for classical holographic codes

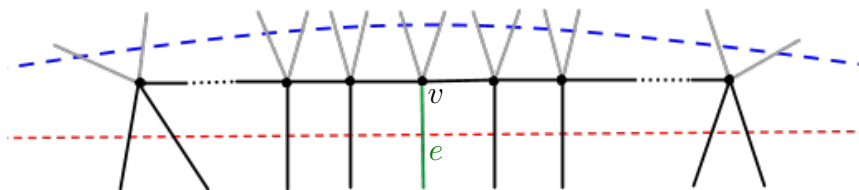


Figure C.2: Illustration of the reasoning about the correlation of crossed edge bits. We assume the green edge bit through the red minimal cut can be constructed. The black edges are needed to gather information about the green one. The grey edges are pointing away from the minimal cut and can give no information. The blue cut is the minimal cut constructed – using algorithm illustrated in figure C.1 – from the complementary boundary. The two minimal cuts do not coincide. Hence, if we assume some bits are correlated the minimal cut cannot be unique.

simply because their distance through the network to them is too large. In figure C.2, these are the gray edges. Now there are two possibilities: either one of the two neighboring edges also crosses the minimal cut and the other edge goes parallel to it, or both neighboring edges go parallel to it, where the latter is shown in figure C.2. In both cases we need the knowledge of at least one edge going parallel to the minimal cut, because property (II) tells us that we need at least two bits to reconstruct a third one. Lets focus on this parallel edge and ask how to obtain the bit associated to it. Again because of property (II) we need to know at least two edge bits from the other vertex it is connected to, and again there are two possibilities: either there are two edges crossing the minimal cut, or we have one edge crossing the minimal cut and another one going parallel to it. As before, we can get no information from edges pointing deeper into the bulk. We can conclude that one requires the knowledge from another parallel edge if there are not two known and necessarily neighboring edge bits crossed by the minimal cut.

This logic stays true for any parallel edge bit and, hence, if we assume that we can reconstruct e then there need to be two neighboring edge bits crossed by the minimal cut before we reach the boundary in both directions (which includes the possibility that e itself is one of these bits). If not, then we would need a parallel edge at the boundary that by requirement is not known. This is also shown in figure C.2: to construct e one needs to know all the (black) crossed edge bits to construct the (black) parallel edge bits, where finally the two parallel edge bits next to e are needed to construct e itself. In summery, we need a “chain” of parallel edges, where the chain ends in both directions with two

Appendix C Classical Holographic Codes

neighboring crossed edges.

The crucial caveat is that the minimal cut **cannot** be unique in the above situations! Simply consider the minimal cut whose construction started at the boundary in the direction of the parallel edges. This cut cannot jump over the vertices that are connected to the previously considered parallel edges, because there are always less than three edges pointing in the direction of the boundary. This is in particular the case at the two ends of the above “chain”. This is also shown in figure C.2, where the blue cut can only cross the gray legs. It cannot jump over the vertices to finally coincide with the red minimal cut. This now shows that the edges of a **unique** minimal cut cannot be constructed from the knowledge of any subset of other crossed edges and, hence, they none of them can be correlated. Together with the fact that each edge crossed by the minimal cut can be reconstructed from either side, this finishes the proof of the RT formula (4.38).

□

Note that there are still the cases left, where the minimal surface is not unique. From the argumentation above it becomes clear that for those the mutual information is smaller than the length of the minimal cut.

All these results are supported by numerical checks up to the fourth layer of the network.¹

¹The numerical results also suggest that in the case of two different minimal cuts coming from A and A^c , the mutual information is given by the length of the smaller cut minus the number of connected regions between the two cuts.

Bibliography

- [1] A. Einstein, B. Podolsky and N. Rosen, *Can quantum-mechanical description of physical reality be considered complete?*, *Phys. Rev.* **47** (May, 1935) 777–780.
- [2] A. Aspect, P. Grangier and G. Roger, *Experimental tests of realistic local theories via bell's theorem*, *Phys. Rev. Lett.* **47** (Aug, 1981) 460–463.
- [3] J. Barrett, *Information processing in generalized probabilistic theories*, eprint *arXiv:quant-ph/0508211* (Aug., 2005) , [quant-ph/0508211].
- [4] S. Pironio, *Randomness vs. non-locality in a no-signalling world*, *Journal of Physics: Conference Series* **67** (2007) 012017.
- [5] M. Müller, *Quantum correlations and generalized probabilistic theories: an introduction*, 2014.
- [6] M. A. Nielsen and I. L. Chuang, *Frontmatter*, pp. i–viii. Cambridge University Press, 2010.
- [7] L. K. Grover, *A Fast quantum mechanical algorithm for database search*, *quant-ph/9605043*.
- [8] J. Eisert, *Entanglement and tensor network states*, in *Autumn School on Correlated Electrons: Emergent Phenomena in Correlated Matter Jülich, Germany, 23-27. September 2013*, 2013. 1308.3318.
- [9] G. Evenbly and G. Vidal, *Algorithms for entanglement renormalization*, *Phys. Rev. B* **79** (Apr, 2009) 144108.
- [10] K. G. Wilson, *The Renormalization Group: Critical Phenomena and the Kondo Problem*, *Rev. Mod. Phys.* **47** (1975) 773.

Bibliography

- [11] J. Schnakenberg, *A. z. patashinskii, v. l. pokrovskii: Fluctuation theory of phase transitions*. pergamon press, oxford, new york, toronto, sydney, paris, frankfurt 1979. 321 seiten, *Berichte der Bunsengesellschaft für physikalische Chemie* **84** (1980) 709–709.
- [12] M. Green, J. Schwarz and E. Witten, *Superstring Theory: Volume 1, Introduction*. Cambridge Monographs on Mathematical Physics. Cambridge University Press, 1988.
- [13] J. Polchinski, *String Theory: Volume 1, An Introduction to the Bosonic String*. Cambridge Monographs on Mathematical Physics. Cambridge University Press, 1998.
- [14] K. Becker, M. Becker and J. Schwarz, *String Theory and M-Theory: A Modern Introduction*. Cambridge University Press, 2006.
- [15] M. B. Plenio and S. Virmani, *An Introduction to entanglement measures*, *Quant. Inf. Comput.* **7** (2007) 1–51, [quant-ph/0504163].
- [16] P. Calabrese and J. Cardy, *Entanglement entropy and conformal field theory*, *J.Phys.* **A42** (2009) 504005, [0905.4013].
- [17] C. Bachas, J. de Boer, R. Dijkgraaf and H. Ooguri, *Permeable conformal walls and holography*, *JHEP* **06** (2002) 027, [hep-th/0111210].
- [18] T. Quella, I. Runkel and G. M. Watts, *Reflection and transmission for conformal defects*, *JHEP* **0704** (2007) 095, [hep-th/0611296].
- [19] M. Henkel, A. Patkós and M. Schlottmann, *The Ising quantum chain with defects (I). The exact solution*, *Nuclear Physics B* **314** (Mar., 1989) 609–624.
- [20] M. Oshikawa and I. Affleck, *Defect lines in the Ising model and boundary states on orbifolds*, *Phys.Rev.Lett.* **77** (1996) 2604–2607, [hep-th/9606177].
- [21] C. P. Bachas, *On the Symmetries of Classical String Theory*, in *Quantum Mechanics of Fundamental Systems: The Quest for Beauty and Simplicity: Claudio Bunster Festschrift*, pp. 17–26, 2009. 0808.2777. DOI.

- [22] J. Fröhlich, J. Fuchs, I. Runkel and C. Schweigert, *Kramers-Wannier Duality from Conformal Defects*, *Physical Review Letters* **93** (Aug., 2004) 070601, [[cond-mat/0404051](#)].
- [23] I. Brunner and D. Roggenkamp, *Defects and bulk perturbations of boundary Landau-Ginzburg orbifolds*, *JHEP* **04** (2008) 001, [[0712.0188](#)].
- [24] D. Gaiotto, *Domain Walls for Two-Dimensional Renormalization Group Flows*, *JHEP* **12** (2012) 103, [[1201.0767](#)].
- [25] K. Graham and G. M. T. Watts, *Defect lines and boundary flows*, *JHEP* **04** (2004) 019, [[hep-th/0306167](#)].
- [26] E. M. Brehm, I. Brunner, D. Jaud and C. Schmidt-Colinet, *Entanglement and topological interfaces*, *Fortsch. Phys.* **64** (2016) 516–535, [[1512.05945](#)].
- [27] V. Petkova and J. Zuber, *Generalized twisted partition functions*, *Phys.Lett.* **B504** (2001) 157–164, [[hep-th/0011021](#)].
- [28] D. Das and S. Datta, *Universal features of left-right entanglement entropy*, *Phys. Rev. Lett.* **115** (2015) 131602, [[1504.02475](#)].
- [29] E. M. Brehm and I. Brunner, *Entanglement entropy through conformal interfaces in the 2D Ising model*, *JHEP* **09** (2015) 080, [[1505.02647](#)].
- [30] K. Sakai and Y. Satoh, *Entanglement through conformal interfaces*, *JHEP* **0812** (2008) 001, [[0809.4548](#)].
- [31] G. 't Hooft, *Dimensional reduction in quantum gravity*, in *Salamfest 1993:0284-296*, pp. 0284–296, 1993. [[gr-qc/9310026](#)].
- [32] L. Susskind, *The World as a hologram*, *J. Math. Phys.* **36** (1995) 6377–6396, [[hep-th/9409089](#)].
- [33] J. M. Maldacena, *The Large N limit of superconformal field theories and supergravity*, *Int. J. Theor. Phys.* **38** (1999) 1113–1133, [[hep-th/9711200](#)].
- [34] S. Ryu and T. Takayanagi, *Holographic derivation of entanglement entropy from AdS/CFT*, *Phys. Rev. Lett.* **96** (2006) 181602, [[hep-th/0603001](#)].

Bibliography

- [35] S. Ryu and T. Takayanagi, *Aspects of Holographic Entanglement Entropy*, *JHEP* **08** (2006) 045, [[hep-th/0605073](#)].
- [36] B. Swingle, *Entanglement Renormalization and Holography*, *Phys. Rev. D* **86** (2012) 065007, [[0905.1317](#)].
- [37] M. Van Raamsdonk, *Building up spacetime with quantum entanglement*, *Gen. Rel. Grav.* **42** (2010) 2323–2329, [[1005.3035](#)].
- [38] J. Maldacena and L. Susskind, *Cool horizons for entangled black holes*, *Fortsch. Phys.* **61** (2013) 781–811, [[1306.0533](#)].
- [39] P. Hayden, M. Headrick and A. Maloney, *Holographic Mutual Information is Monogamous*, *Phys. Rev. D* **87** (2013) 046003, [[1107.2940](#)].
- [40] N. Lashkari, M. B. McDermott and M. Van Raamsdonk, *Gravitational dynamics from entanglement ‘thermodynamics’*, *JHEP* **04** (2014) 195, [[1308.3716](#)].
- [41] A. R. Brown, D. A. Roberts, L. Susskind, B. Swingle and Y. Zhao, *Holographic Complexity Equals Bulk Action?*, *Phys. Rev. Lett.* **116** (2016) 191301, [[1509.07876](#)].
- [42] M. Freedman and M. Headrick, *Bit threads and holographic entanglement*, [1604.00354](#).
- [43] P. Hayden and J. Preskill, *Black holes as mirrors: Quantum information in random subsystems*, *JHEP* **09** (2007) 120, [[0708.4025](#)].
- [44] S. L. Braunstein, S. Pirandola and K. Życzkowski, *Better Late than Never: Information Retrieval from Black Holes*, *Phys. Rev. Lett.* **110** (2013) 101301, [[0907.1190](#)].
- [45] A. Almheiri, D. Marolf, J. Polchinski and J. Sully, *Black Holes: Complementarity or Firewalls?*, *JHEP* **02** (2013) 062, [[1207.3123](#)].
- [46] D. Harlow and P. Hayden, *Quantum Computation vs. Firewalls*, *JHEP* **06** (2013) 085, [[1301.4504](#)].
- [47] G. Dvali and M. Panchenko, *Black Hole Based Quantum Computing in Labs and in the Sky*, *Fortsch. Phys.* **64** (2016) 569–580, [[1601.01329](#)].

- [48] X. Dong, *The Gravity Dual of Renyi Entropy*, *Nature Commun.* **7** (2016) 12472, [1601.06788].
- [49] G. Dvali, C. Gomez, D. Lust, Y. Omar and B. Richter, *Universality of Black Hole Quantum Computing*, *Fortsch. Phys.* **65** (2017) 46–65, [1605.01407].
- [50] G. Vidal, *Entanglement Renormalization*, *Phys. Rev. Lett.* **99** (2007) 220405, [cond-mat/0512165].
- [51] X.-L. Qi, *Exact holographic mapping and emergent space-time geometry*, 1309.6282.
- [52] B. Swingle, *Constructing holographic spacetimes using entanglement renormalization*, 1209.3304.
- [53] A. Almheiri, X. Dong and D. Harlow, *Bulk Locality and Quantum Error Correction in AdS/CFT*, *JHEP* **04** (2015) 163, [1411.7041].
- [54] F. Pastawski, B. Yoshida, D. Harlow and J. Preskill, *Holographic quantum error-correcting codes: Toy models for the bulk/boundary correspondence*, *JHEP* **06** (2015) 149, [1503.06237].
- [55] D. Harlow, *The Ryu–Takayanagi Formula from Quantum Error Correction*, *Commun. Math. Phys.* **354** (2017) 865–912, [1607.03901].
- [56] P. Hayden, S. Nezami, X.-L. Qi, N. Thomas, M. Walter and Z. Yang, *Holographic duality from random tensor networks*, *JHEP* **11** (2016) 009, [1601.01694].
- [57] A. Bhattacharyya, Z.-S. Gao, L.-Y. Hung and S.-N. Liu, *Exploring the Tensor Networks/AdS Correspondence*, *JHEP* **08** (2016) 086, [1606.00621].
- [58] Z. Yang, P. Hayden and X.-L. Qi, *Bidirectional holographic codes and sub-AdS locality*, *JHEP* **01** (2016) 175, [1510.03784].
- [59] E. Mintun, J. Polchinski and V. Rosenhaus, *Bulk-Boundary Duality, Gauge Invariance, and Quantum Error Corrections*, *Phys. Rev. Lett.* **115** (2015) 151601, [1501.06577].
- [60] E. M. Brehm and B. Richter, *Classical Holographic Codes*, 1609.03560.
- [61] P. Francesco, P. Mathieu and D. Senechal, *Conformal Field Theory*. Graduate Texts in Contemporary Physics. Springer-Verlag New York, 1997.

Bibliography

- [62] P. H. Ginsparg, *APPLIED CONFORMAL FIELD THEORY*, in *Les Houches Summer School in Theoretical Physics: Fields, Strings, Critical Phenomena Les Houches, France, June 28-August 5, 1988*, pp. 1–168, 1988. [hep-th/9108028](#).
- [63] R. Blumenhagen and E. Plauschinn, *Introduction to Conformal Field Theory*. Lecture Notes in Physics. Springer-Verlag Berlin Heidelberg, 2009.
- [64] M. R. Gaberdiel, *An Introduction to conformal field theory*, *Rept. Prog. Phys.* **63** (2000) 607–667, [[hep-th/9910156](#)].
- [65] A. N. Schellekens, *Conformal field theory*, 1995–2016.
- [66] G. Moore and N. Seiberg, *Classical and quantum conformal field theory*, *Communications in Mathematical Physics* **123** (1989) 177–254.
- [67] A. A. Belavin, A. M. Polyakov and A. B. Zamolodchikov, *Infinite conformal symmetry in two-dimensional quantum field theory*, *Nucl. Phys.* **B241** (1984) 333–380.
- [68] D. Friedan and S. Shenker, *The analytic geometry of two-dimensional conformal field theory*, *Nuclear Physics B* **281** (1987) 509 – 545.
- [69] G. B. Segal, *The Definition of Conformal Field Theory*, pp. 165–171. Springer Netherlands, Dordrecht, 1988. [10.1007/978-94-015-7809-7_9](#).
- [70] E. Witten, *Quantum field theory and the jones polynomial*, *Comm. Math. Phys.* **121** (1989) 351–399.
- [71] J. Fröhlich and C. King, *Two-Dimensional Conformal Field Theory and Three-Dimensional Topology*, pp. 121–199. Springer US, Boston, MA, 1990. [10.1007/978-1-4684-5838-1_6](#).
- [72] J. Fuchs, I. Runkel and C. Schweigert, *TFT construction of RCFT correlators 1. Partition functions*, *Nucl. Phys.* **B646** (2002) 353–497, [[hep-th/0204148](#)].
- [73] R. E. Borcherds, *Vertex algebras, kac-moody algebras, and the monster*, .
- [74] A. Giveon and D. Kutasov, *Brane dynamics and gauge theory*, *Rev. Mod. Phys.* **71** (1999) 983–1084, [[hep-th/9802067](#)].

- [75] A. Strominger and C. Vafa, *Microscopic origin of the Bekenstein-Hawking entropy*, *Phys. Lett.* **B379** (1996) 99–104, [[hep-th/9601029](#)].
- [76] N. Ishibashi, *The Boundary and Crosscap States in Conformal Field Theories*, *Modern Physics Letters A* **4** (1989) 251–264.
- [77] P. Fendley, M. P. A. Fisher and C. Nayak, *Boundary conformal field theory and tunneling of edge quasiparticles in non-Abelian topological states*, *Annals of Physics* **324** (July, 2009) 1547–1572, [[0902.0998](#)].
- [78] J. Frohlich, J. Fuchs, I. Runkel and C. Schweigert, *Duality and defects in rational conformal field theory*, *Nucl. Phys.* **B763** (2007) 354–430, [[hep-th/0607247](#)].
- [79] A. Recknagel, *Permutation branes*, *JHEP* **04** (2003) 041, [[hep-th/0208119](#)].
- [80] C. Bachas, I. Brunner and D. Roggenkamp, *Fusion of Critical Defect Lines in the 2D Ising Model*, *J.Stat.Mech.* **2013** (2013) P08008, [[1303.3616](#)].
- [81] D. Deutsch and R. Jozsa, *Rapid Solution of Problems by Quantum Computation*, *Proceedings of the Royal Society of London Series A* **439** (Dec., 1992) 553–558.
- [82] P. W. Shor, *Polynomial time algorithms for prime factorization and discrete logarithms on a quantum computer*, *SIAM J. Sci. Statist. Comput.* **26** (1997) 1484, [[quant-ph/9508027](#)].
- [83] A. B. Zamolodchikov, *Irreversibility of the Flux of the Renormalization Group in a 2D Field Theory*, *JETP Lett.* **43** (1986) 730–732.
- [84] I. Affleck and A. W. W. Ludwig, *Universal noninteger “ground-state degeneracy” in critical quantum systems*, *Phys. Rev. Lett.* **67** (Jul, 1991) 161–164.
- [85] H. Casini and M. Huerta, *A c-theorem for the entanglement entropy*, *J. Phys.* **A40** (2007) 7031–7036, [[cond-mat/0610375](#)].
- [86] H. Casini, I. S. Landea and G. Torroba, *The g-theorem and quantum information theory*, *JHEP* **10** (2016) 140, [[1607.00390](#)].
- [87] M. Cadoni and M. Melis, *Holographic entanglement entropy of the BTZ black hole*, *Found. Phys.* **40** (2010) 638–657, [[0907.1559](#)].

Bibliography

- [88] M. A. Nielsen, *Conditions for a Class of Entanglement Transformations*, *Physical Review Letters* **83** (July, 1999) 436–439, [quant-ph/9811053].
- [89] C. H. Bennett, H. J. Bernstein, S. Popescu and B. Schumacher, *Concentrating partial entanglement by local operations*, *Phys. Rev.* **A53** (1996) 2046–2052, [quant-ph/9511030].
- [90] V. Vedral, M. B. Plenio, M. A. Rippin and P. L. Knight, *Quantifying entanglement*, *Phys. Rev. Lett.* **78** (1997) 2275–2279, [quant-ph/9702027].
- [91] R. F. Werner, *Quantum states with einstein-podolsky-rosen correlations admitting a hidden-variable model*, *Phys. Rev. A* **40** (Oct, 1989) 4277–4281.
- [92] E. M. Rains, *Entanglement purification via separable superoperators*, quant-ph/9707002.
- [93] P. M. Hayden, M. Horodecki and B. M. Terhal, *The asymptotic entanglement cost of preparing a quantum state*, *Journal of Physics A Mathematical General* **34** (Sept., 2001) 6891–6898, [quant-ph/0008134].
- [94] W. K. Wootters, *Entanglement of formation of an arbitrary state of two qubits*, *Phys. Rev. Lett.* **80** (1998) 2245–2248, [quant-ph/9709029].
- [95] F. Verstraete, J. Dehaene, B. de Moor and H. Verschelde, *Four qubits can be entangled in nine different ways*, *pra* **65** (May, 2002) 052112, [quant-ph/0109033].
- [96] P. Calabrese and J. L. Cardy, *Entanglement entropy and quantum field theory*, *J.Stat.Mech.* **0406** (2004) P06002, [hep-th/0405152].
- [97] J. Eisert, M. Cramer and M. B. Plenio, *Area laws for the entanglement entropy - a review*, *Rev. Mod. Phys.* **82** (2010) 277–306, [0808.3773].
- [98] M. B. Hastings, *An area law for one-dimensional quantum systems*, *Journal of Statistical Mechanics: Theory and Experiment* **8** (Aug., 2007) 08024, [0705.2024].
- [99] E. H. Lieb and D. W. Robinson, *The Finite Group Velocity of Quantum Spin Systems*, pp. 425–431. Springer Berlin Heidelberg, Berlin, Heidelberg, 2004. 10.1007/978-3-662-10018-9 25.

- [100] A. I. Lvovsky, *Iterative maximum-likelihood reconstruction in quantum homodyne tomography*, *Journal of Optics B: Quantum and Semiclassical Optics* **6** (June, 2004) S556–S559, [quant-ph/0311097].
- [101] G. M. D’Ariano, M. D. Laurentis, M. G. A. Paris, A. Porzio and S. Solimeno, *Quantum tomography as a tool for the characterization of optical devices*, *Journal of Optics B: Quantum and Semiclassical Optics* **4** (2002) S127.
- [102] G. Tóth, W. Wieczorek, D. Gross, R. Krischek, C. Schwemmer and H. Weinfurter, *Permutationally invariant quantum tomography*, *Phys. Rev. Lett.* **105** (Dec, 2010) 250403.
- [103] D. A. Abanin and E. Demler, *Measuring Entanglement Entropy of a Generic Many-Body System with a Quantum Switch*, *Physical Review Letters* **109** (July, 2012) 020504, [1204.2819].
- [104] R. Islam, R. Ma, P. M. Preiss, M. Eric Tai, A. Lukin, M. Rispoli et al., *Measuring entanglement entropy in a quantum many-body system*, *Nature* **528** (Dec., 2015) 77–83.
- [105] J. A. Harvey, S. Kachru, G. W. Moore and E. Silverstein, *Tension is dimension*, *JHEP* **03** (2000) 001, [hep-th/9909072].
- [106] T. Azeyanagi, A. Karch, T. Takayanagi and E. G. Thompson, *Holographic calculation of boundary entropy*, *JHEP* **03** (2008) 054–054, [0712.1850].
- [107] T. Takayanagi, *Holographic boundary entropy and janus solutions*, *Prog. Theor. Phys. Suppl.* **177** (2009) 191–202.
- [108] J. Estes, K. Jensen, A. O’Bannon, E. Tsatis and T. Wrase, *On holographic defect entropy*, *JHEP* **05** (2014) 084, [1403.6475].
- [109] L. A. Pando Zayas and N. Quiroz, *Left-Right Entanglement Entropy of Boundary States*, *JHEP* **1501** (2015) 110, [1407.7057].
- [110] M. Gutperle and J. D. Miller, *Entanglement entropy at holographic interfaces*, *Phys. Rev.* **D93** (2016) 026006, [1511.08955].

Bibliography

- [111] X.-L. Qi, H. Katsura and A. W. W. Ludwig, *General Relationship between the Entanglement Spectrum and the Edge State Spectrum of Topological Quantum States*, *Physical Review Letters* **108** (May, 2012) 196402, [1103.5437].
- [112] S. Kullback and R. Leibler, *On information and sufficiency*, *Annals of Mathematical Statistics* **22** (1951) 79–86.
- [113] A. Yu. Alekseev and V. Schomerus, *D-branes in the WZW model*, *Phys. Rev.* **D60** (1999) 061901, [hep-th/9812193].
- [114] C. Bachas, M. R. Douglas and C. Schweigert, *Flux stabilization of D-branes*, *JHEP* **05** (2000) 048, [hep-th/0003037].
- [115] J. M. Figueroa-O’Farrill and S. Stanciu, *D-branes in $AdS_3 \times S^3 \times S^3 \times S^1$* , *JHEP* **04** (2000) 005, [hep-th/0001199].
- [116] I. Affleck, N. Laflorencie and E. S. Sørensen, *Entanglement entropy in quantum impurity systems and systems with boundaries*, *Journal of Physics A: Mathematical and Theoretical* **42** (2009) 504009.
- [117] C. Bachas, I. Brunner and D. Roggenkamp, *A worldsheet extension of $O(d,d;Z)$* , *JHEP* **1210** (2012) 039, [1205.4647].
- [118] C. Bachas and I. Brunner, *Fusion of conformal interfaces*, *JHEP* **0802** (2008) 085, [0712.0076].
- [119] R. Blumenhagen, D. Lüüst and S. Theisen, *Basic Concepts of String Theory*. Theoretical and Mathematical Physics. Springer Berlin Heidelberg, Berlin, Heidelberg, 2013.
- [120] D. B. Abraham, L. F. Ko and N. M. Švrakić, *Transfer matrix spectrum for the finite-width Ising model with adjustable boundary conditions: Exact solution*, *Journal of Statistical Physics* **56** (Sept., 1989) 563–587.
- [121] M. Oshikawa and I. Affleck, *Boundary conformal field theory approach to the critical two-dimensional Ising model with a defect line*, *Nucl.Phys.* **B495** (1997) 533–582, [cond-mat/9612187].
- [122] F. Iglói, Z. Szatmári and Y.-C. Lin, *Entanglement entropy with localized and extended interface defects*, *Phys. Rev. B* **80** (July, 2009) 024405, [0903.3740].

- [123] V. Eisler and I. Peschel, *Solution of the fermionic entanglement problem with interface defects*, *ArXiv e-prints* (May, 2010) , [1005.2144].
- [124] P. Calabrese, M. Mintchev and E. Vicari, *Entanglement entropy of quantum wire junctions*, *Journal of Physics A Mathematical General* **45** (Mar., 2012) 105206, [1110.5713].
- [125] I. Peschel and V. Eisler, *Exact results for the entanglement across defects in critical chains*, *Journal of Physics A Mathematical General* **45** (Apr., 2012) 155301, [1201.4104].
- [126] V. Eisler and I. Peschel, *On entanglement evolution across defects in critical chains*, *EPL (Europhysics Letters)* **99** (July, 2012) 20001, [1205.4331].
- [127] M. Collura and P. Calabrese, *Entanglement evolution across defects in critical anisotropic Heisenberg chains*, *Journal of Physics A Mathematical General* **46** (May, 2013) 175001, [1302.4274].
- [128] V. Eisler, M.-C. Chung and I. Peschel, *Entanglement in composite free-fermion systems*, *ArXiv e-prints* (Mar., 2015) , [1503.09116].
- [129] G. Delfino, G. Mussardo and P. Simonetti, *Scattering theory and correlation functions in statistical models with a line of defect*, *Nucl.Phys.* **B432** (1994) 518–550, [hep-th/9409076].
- [130] J. L. Cardy, *Boundary conditions, fusion rules and the Verlinde formula*, *Nuclear Physics B* **324** (Oct., 1989) 581–596.
- [131] J. Maldacena and D. Stanford, *Remarks on the Sachdev-Ye-Kitaev model*, *Phys. Rev.* **D94** (2016) 106002, [1604.07818].
- [132] S. Giombi and X. Yin, *The Higher Spin/Vector Model Duality*, *J. Phys.* **A46** (2013) 214003, [1208.4036].
- [133] J. D. Bekenstein, *Black holes and entropy*, *Phys. Rev.* **D 7** (1973) 2333–2346.
- [134] S. W. Hawking, *Breakdown of predictability in gravitational collapse*, *Phys. Rev. D* **14** (Nov, 1976) 2460–2473.

Bibliography

- [135] S. Lloyd, *Computational capacity of the universe*, *Phys. Rev. Lett.* **88** (2002) 237901, [quant-ph/0110141].
- [136] J. Casalderrey-Solana, H. Liu, D. Mateos, K. Rajagopal and U. A. Wiedemann, *Gauge/String Duality, Hot QCD and Heavy Ion Collisions*, 1101.0618.
- [137] G. 't Hooft, *A planar diagram theory for strong interactions*, *Nuclear Physics B* **72** (1974) 461 – 473.
- [138] E. Witten, *Baryons in the 1n expansion*, *Nuclear Physics B* **160** (1979) 57 – 115.
- [139] A. V. Manohar, *Large N QCD*, in *Probing the standard model of particle interactions. Proceedings, Summer School in Theoretical Physics, NATO Advanced Study Institute, 68th session, Les Houches, France, July 28-September 5, 1997. Pt. 1, 2*, pp. 1091–1169, 1998. hep-ph/9802419.
- [140] T. Banks, M. R. Douglas, G. T. Horowitz and E. J. Martinec, *AdS dynamics from conformal field theory*, hep-th/9808016.
- [141] A. Hamilton, D. N. Kabat, G. Lifschytz and D. A. Lowe, *Holographic representation of local bulk operators*, *Phys. Rev.* **D74** (2006) 066009, [hep-th/0606141].
- [142] D. Harlow and D. Stanford, *Operator Dictionaries and Wave Functions in AdS/CFT and dS/CFT*, 1104.2621.
- [143] V. E. Hubeny and M. Rangamani, *Causal Holographic Information*, *JHEP* **06** (2012) 114, [1204.1698].
- [144] X. Dong, D. Harlow and A. C. Wall, *Reconstruction of Bulk Operators within the Entanglement Wedge in Gauge-Gravity Duality*, *Phys. Rev. Lett.* **117** (2016) 021601, [1601.05416].
- [145] R. Cleve, D. Gottesman and H.-K. Lo, *How to share a quantum secret*, *Phys. Rev. Lett.* **83** (1999) 648–651, [quant-ph/9901025].
- [146] W. Helwig, W. Cui, A. Riera, J. I. Latorre and H.-K. Lo, *Absolute Maximal Entanglement and Quantum Secret Sharing*, *Phys. Rev.* **A86** (2012) 052335, [1204.2289].

- [147] D. Goyeneche, D. Alsina, J. I. Latorre, A. Riera and K. Życzkowski, *Absolutely maximally entangled states, combinatorial designs, and multiunitary matrices*, *Phys. Rev.* **A92** (2015) 032316, [1506.08857].
- [148] R. Laflamme, C. Miquel, J. P. Paz and W. H. Zurek, *Perfect quantum error correction code*, [quant-ph/9602019](#).
- [149] R. G. Gallager, *Low-density parity-check codes*, *IRE Trans. Information Theory* **8** (1962) 21–28.
- [150] C. Berrou, *Error-correction coding method with at least two systematic convolutional codings in parallel, corresponding iterative decoding method, decoding module and decoder*, Aug. 29, 1995.
- [151] S. W. Hawking, *Particle Creation by Black Holes*, *Commun. Math. Phys.* **43** (1975) 199–220.
- [152] A. Shamir, *How to share a secret*, *Commun. ACM* **22** (Nov., 1979) 612–613.
- [153] G. R. Blakley, *Safeguarding cryptographic keys*, *Managing Requirements Knowledge, International Workshop on* **00** (1899) 313.
- [154] L. Susskind and E. Witten, *The Holographic bound in anti-de Sitter space*, [hep-th/9805114](#).
- [155] C. P. Bachas, I. Brunner, M. R. Douglas and L. Rastelli, *Calabi’s diastasis as interface entropy*, *Phys. Rev.* **D90** (2014) 045004, [1311.2202].
- [156] A. Giveon and D. Kutasov, *Supersymmetric Renyi entropy in CFT_2 and AdS_3* , *JHEP* **01** (2016) 042, [1510.08872].
- [157] M. Kormos, I. Runkel and G. M. T. Watts, *Defect flows in minimal models*, *Journal of High Energy Physics* **2009** (Nov., 2009) 057–057.
- [158] A. Konechny and C. Schmidt-Colinet, *Entropy of conformal perturbation defects*, *J.Phys.* **A47** (2014) 485401, [1407.6444].
- [159] G. Poghosyan and H. Poghosyan, *RG domain wall for the $N=1$ minimal superconformal models*, *JHEP* **05** (2015) 043, [1412.6710].

- [160] N. Surlas, *Spin-glass models as error-correcting codes*, *Nature* **339** (June, 1989) 693–695.
- [161] S. Goh, *Chebyshev polynomials and spread polynomials*, *Honours Thesis, School of Mathematics and Statistics, UNSW* (2005) .
- [162] R. W. Yeung, *A new outlook on shannon's information measures*, *IEEE Transactions on Information Theory* **37** (May, 1991) 466–474.

Curriculum Vitae

Enrico M. Brehm

St.-Cajetan-Str. 5, 81669 Munich, Germany;
Nationality: german; Born: Dec. 16th 1989, Stuttgart;

Education

University of Heidelberg	Heidelberg, Germany
Master of Science, Physics	Oct 2012 - Oct 2014
University of Stuttgart	Stuttgart, Germany
Bachelor of Science, Physics	Oct 2009 - Sep 2012
High Schools	Stuttgart and Villingen-Schwenningen, Germany
Abitur	Aug 2000 - July 2008

Publications

Classical Holographic Codes

E.M. Brehm, B. Richter Sep 2016
arXiv: 1609.03460

Entanglement and topological interfaces

E.M. Brehm, I. Brunner, D. Jaud, C. Schmidt-Colinet Dec 2015
arXiv: 1512.05945

Entanglement entropy through conformal interfaces in the 2D Ising model

E.M. Brehm, I. Brunner May 2015
arXiv: 1505.02647

Skills

Programming Mathematica, C++, Delphi, LaTeX
Languages German (native), English (fluent)